Stability of Steady States and Steady-State Limit of Elastoplastic Trusses under Quasi-Static Cyclic Loading(Dissertation_全文)

AUTHOR(S):

Araki, Yoshikazu

STABILITY OF STEADY STATES AND STEADY-STATE LIMIT OF ELASTOPLASTIC TRUSSES UNDER QUASI-STATIC CYCLIC LOADING

By

Yoshikazu Araki

December 1997

STABILITY OF STEADY STATES AND STEADY-STATE LIMIT OF ELASTOPLASTIC TRUSSES UNDER QUASI-STATIC CYCLIC LOADING

By

Yoshikazu Araki

December 1997

Acknowledgments

I would especially like to acknowledge Professor Koji Uetani. In the development of this work, I have benefited from his guidance of interesting research topics, and from advises, suggestions, and discussions. The topic of "steady-state limit of elastoplastic structures" was originally developed by Professor Koji Uetani for cantilever beam-columns. And he has guided me the topic throughout my graduate study. His energetic attitude towards research has been encouraged me to do further research.

I am grateful of Prof. B. Tsuji and Prof. H. Kunieda for reading this manuscript. I express sincere appreciation to Dr. I. Takewaki and Dr. M. Ohsaki for providing valuable advises on my research and for reading a part of this thesis. I thank to Mr. T. Masui and Mr. H. Tagawa for their positive comments. I wish to acknowledge Dr. T. Nakamura for his valuable suggestions at the early stage of this work. Thanks are due to Miss. T. Yorifuji who supported a part of numerical analyses.

It has been a pleasure to work with the students in master and undergraduate courses. Discussions with them have been stimulated me to find and remember the problems that would have been missed without their honest comments. I acknowledge the financial support provided by JSPS Research Fellowships for Young Scientists for these two years. Finally, I am truly grateful of all of the help and encouragement I have received in the development of this work.

Finally, I am greatly indebted to my mother Natsue Araki for her tireless support and patience.

Contents

Chapter 1

Introduction

1.1 BACKGROUND

In current and common seismic design of building structures, the buildings are designed so that the following requirements are satisfied: (1) In moderate earthquakes, which occur frequently, no plastic deformation takes place; and (2) In strong earthquakes, which happen rarely, plastifications of their structural elements are allowed but total collapse should be avoided. Namely, plastic deformations are allowed in case of strong earthquakes. In addition to this fact, there is a tendency to use deliberately the energy absorption due to the plastic deformations in order to control the displacements and accelerations caused by earthquakes.

To clarify the fundamental properties of the structural response with plastic deformations, extensive research has been done on the elastoplastic response of structures subjected to quasi-static loads (see, e.g. [1, 2, 3, 4, 5, 6]). According to whether the loading condition is monotonic or cyclic, the research is classified into eight categories shown in Table 1.1. The

Table 1.1: Classification of elastoplastic analysis.

Monotonic Loading	Cyclic Loading
Tracing All Loading History	Tracing All Loading History
Limit Analysis	Shakedown Theory
Plastic Buckling Theory	Symmetry Limit Theory,
	Steady-State Limit Theory
Stability of Equilibrium States	Stability of Steady States

main objectives of the research are: (1) to clarify how structures behave under the quasi-static loads; and (2) to find the critical loading condition beyond which unstable responses occur.

The plastic buckling and the plastic collapse have been mainly considered in the research. In addition to these types of instability, it is known that, plastic deformations of structures under cyclic loads may accumulate proportionally or exponentially with respect to the number of the cycles. The accumulation may lead to the degradation of load capacity and stiffness. Obviously, no stable energy dissipation can be expected in this case. This phenomena is considered to be a type of instability and is the main subject of this thesis. By the way, although fractures are frequently observed in strong earthquakes [7, 8], our discussion is limited to the case where neither ductile nor brittle cracking occurs.

Under both monotonic and cyclic loads, a direct but elaborating approaches for investigating the elastoplastic response is to trace the all loading history of structures. Experimental, analytical, and numerical methods are available for this purpose. By tracing the all loading history, we can observe the whole process of the deformations and find the loading conditions below which structures behave in a stable manner. Nonetheless, generally, analytical methods can be applied only to very simple models. Experimental and numerical approaches require a number of parametric analyses to bound the stable response. Moreover, it is very difficult to derive the theoretical condition similar to that for the Euler buckling load from the results of the parametric analyses.

For the stability of elastoplastic structures subjected to monotonic loads, theoretical foundation seems to be established. As a theory of stability, the limit analysis [9] is well known and widely used in structural design. In the limit analysis, both collapse loads and collapse modes are obtained based on the upper bound or the lower bound theorem. The limit analysis is originally developed for the structures with perfectly plastic material. And the effect of geometrical nonlinearity is completely neglected in the theory of the limit analysis. Another well-known theory on stability is the plastic buckling theory [10]. Plastic buckling is predicted as the fist bifurcation or limit points of equilibrium paths, which represents the variation of equilibrium states under the monotonic loads. In addition, based on the definition of stability due to Liapunov [11], a general criterion on the stability of an equilibrium state was derived by Hill [12] for elastoplastic structures.

On the other hand, the stability of elastoplastic structures under quasi-static cyclic loads appears to remain as research subjects. As a theoretical approach, the shakedown theory [13] is well known. In the shakedown theory, we can find the domain of the cyclic loads within

which a structure converges to a shakedown response regardless of loading histories based on the upper bound or lower bound theorem. Similar to the limit analysis, the classical shakedown theory was developed for the structures composed of perfectly plastic materials without taking into account geometrical nonlinearity. Several papers extended in recent years the shakedown theory taking the geometrical nonlinearity into consideration, (see e.g. [14, 15, 16, 17]). But the path-independent shakedown theories have inherent difficulties when geometrical nonlinearity plays crucial role. This is because the responses are path-dependent in this case [1].

In such situations, Uetani and Nakamura [18, 19, 20] proposed the symmetry limit theory and the steady-state limit theory for cantilever beam-columns subjected to cyclic bending in the presence of a compressive axial force. With these two theories, though under a specified loading history, we can find the limit that bounds convergence and divergence of plastic deformations as a mathematical critical point even if geometrical nonlinearity has strong effect on structural responses. In the two theories, a steady state and variation of the steady state generated under the idealized cyclic loading with continuously increasing amplitude are regarded as a point and a continuous path, respectively. In analogy with an equilibrium state and an equilibrium path, the continuous path is called steady-state path. The symmetry limit and the steady-state limit are predicted as the first branching and limit points of the steady-state path, respectively.

For a few classes of structures, the symmetry limit theory and the steady-state limit theory have been applied. Severe degradation of load capacity and stiffness were observed if the deflection amplitude was in excess of the symmetry limit or the steady-state limit [19, 21, 20]. In those studies, however, only the simple structures, e.g. a cantilever beam-column or a unit frame, were treated for which analytical solutions can be derived. Hence, to investigate the limit states of more complex and practical structures, which generally do not have symmetry limits if they do not have symmetric shapes, it is necessary to establish a method for predicting the steady-state limit using appropriate finite element methods. In addition, it is desirable from theoretical view, by analogy with the stability of equilibrium state, to introduce the concept of stability of steady states or closed orbits and to characterize the steady-state limit as the steady state at which the stability of the steady states is lost [19, 20]. This concept of the stability of closed orbits is well known for the elastic structures subjected to dynamic loads (see, for instance [22, 23, 24]). But, to the best of author's knowledge, no clear stability criterion has been given for elastoplastic structures subjected to dynamic or quasi-static cyclic loads.

1.2 SCOPE

This research has two purposes. One is to generalize the steady-state limit theory, originally developed for cantilever beam-columns, so as to find the steady-state limits of elastoplastic trusses subjected to cyclic, quasi-static and proportional loading in the presence of constant loads. The other is to introduce the concept of stability of steady states into the quasi-static problem of elastoplastic structures under cyclic loads.

This research is part of the project that aims to develop the theories and methods for predicting the critical loading conditions that bound convergence and divergence of deformations of elastoplastic structures with arbitrary shapes and materials. For this purpose, appropriate discretization schemes, such as finite element methods, seem to be promising. We treat only trusses in this research for simplicity. But the theories presented in this thesis can be easily extended to the elastoplastic structures with arbitrary shapes whose behavior is described by uni-axial stress-strain relations. In fact, one of the present methods has been successfully applied to moment-resisting frames with a fiber element [25]. In addition, another theory presented in this thesis is expected to be directly applicable to three dimensional continua with almost no restriction.

Toward the ends stated above, the specific subjects of this study are described as follows:

1. To formulate incremental relations for the variation of the steady states of trusses with respect to the variation of the amplitude of cyclic loading.
2. To relax and exclude the basic assumption on strain reversals employed in the previous steady-state limit theory for cantilever beam-columns.
3. To derive the stability criterion of steady states and to characterize the steady-state limit as the critical steady state at which the stability is lost.

The relations between these subjects and the composition of this thesis are written in the following paragraphs. All chapters are written to be as self-consistent as possible. Throughout this thesis, validity of the hypothesis and the results of the proposed methods are shown in numerical examples.

In chapter 2 a method is presented for finding the steady-state limits that bound convergence to elastic shakedown and divergence of plastic deformations. The method is a simple extension of the steady-state limit theory for cantilever beam-columns. But a chapter is assigned to this method because it provide the backbone of the methods presented in the later chapters. In the present method, a steady state is uniquely described by the state

variables at load reversals by assuming that strain reversals in steady states occur only at load reversals. By differentiating all the state variables representing a steady state and by using the Taylor series expansion, new incremental relations are formulated for tracing a steady-state path, which represents variation of a steady state under the idealized cyclic loading program with continuously increasing amplitude. The steady-state limit is found as the first limit point of the steady-state path.

Chapter 3 presents a theory and method for finding the steady-state limit that bounds divergence of plastic deformations and convergence to plastic shakedown. When plastic shakedown occurs, strain reversals may take place not only at load reversals but also at the yielding of the elements exhibiting the plastic shakedown. The previous approach cannot be applied to such cases because the assumption on strain reversals in the previous method is not valid in such a case. This difficulty is overcome by relaxing the assumption so that the strain reversals due to the yielding is taken into account. Based on the relaxed assumption, a steady state is described by the state variables not only at load reversals but also at yielding points of the elements exhibiting plastic shakedown. This is the key extension from the methods presented in the previous chapter. Once a steady state is represented by a set of equilibrium states, similar to the previous method, incremental relations are formulated by differentiating the state variables, steady-state path is traced incrementally, and the steady-state limit is found as the first limit point of the steady-state path.

In chapter 4, an alternative method is presented for tracing the steady-state paths, and a theory is developed for finding the steady-state limit as the critical steady state at which loss of the stability of steady states occurs. In this method, first, a steady state is expressed by discretizing its equilibrium path with respect to an equilibrium path parameter. Second, deviation from the steady state due to the change of the amplitude of cyclic loading is expressed using the recurrence equation that relates two consecutive periodic instants. The recurrence equation is formulated in terms of the plastic strain increments with respect to the change of the amplitude of cyclic loads. Then the stability of the steady state is rigorously defined and the stability criterion is given in terms of the eigenvalue of the coefficient matrix in the recurrence equation. The steady-state path is traced using the recurrence equation, and the steady-state limit is found as the critical steady state at which the stability of steady states is lost.

Finally, concluding remarks are made in section 5. Advantages and drawbacks are written for the methods proposed in this thesis. Subjects of future research are summarized.

1.3 LIMITATIONS

The assumptions and limitations made in this research are listed below:

- Analytical models are pin-jointed space trusses.
- Buckling of the element is ruled out. But buckling of a global type is taken into account.
- Only quasi-static loads are applied. In other words, dynamic effects are neglected.
- For both constant and cyclic loads, only proportional loading is considered.
- Stresses and strains are measured using the Total Lagrangian formulation.
- Assumptions of large displacements-small strains are employed.
- As a uni-axial constitutive law, bi-linear kinematic hardening rule is employed. Thermal effect is neglected. Cyclic hardening and cyclic softening is neglected.
- Neither brittle nor ductile cracking is considered.

1.4 TERMINOLOGY

The terminology used in this paper is briefly summarized. More rigorous definition of these terms are given in the following chapters.

- *Steady State*: When elastoplastic structures are subjected to quasi-static cyclic loads, its response may converge to a cyclic response. The cyclic response is called a steady state.
- *Elastic Shakedown, Classical Shakedown, Shakedown*: A cyclic and fully elastic structural response after some histories of plastic deformations.
- *Plastic Shakedown, Alternating Plasticity*: The steady state in which plastic deformations are included.
- *Cyclic Instability, Incremental Collapse, Ratchetting*: The state in which deformation grows proportionally or exponentially with respect to the number of the cycles.
- *Idealized Cyclic Loading Program*: The loading program where the amplitude of the load factor of proportional loads is continuously increased. At each level of the amplitude, the loading cycle is repeated as many times as necessary for convergence.
- *Steady-State Path*: Under the idealized cyclic loading program, variation of a steady state can be regarded as a path. This path is called a steady-state path.
- *Symmetric Steady State, Asymmetric Steady State*: A steady state is called a symmetric steady state if a pair of the deflected configurations at load reversals is symmetric with

respect to the initial symmetric axis. Otherwise, the steady sate is called asymmetric steady state.

- *Symmetry Limit*: The symmetry limit is the critical steady state at which transition from the symmetric steady state to the asymmetric steady state can occur under the idealized cyclic loading program.
- *Steady-State Limit*: The steady-state limit is the critical steady state beyond which structures will no longer exhibit any convergent behavior under the idealized cyclic loading program.
- *Stability of Steady States*: A steady state is said to be stable if a small change in the amplitude of cyclic loading leads to a small change in the responses. Otherwise, the steady state is said to be unstable.

References

[1] J. A. König. *Shakedown of Elastic-Plastic Structures.* Elsevier, Amsterdam, 1987.

[2] W. F. Chen and D. J. Han. *Plasticity for Structural Engineering.* Springer-Verlag, New York, 1988.

[3] P. Z. Bazant and L. Cedolin. *Stability of Structures.* Oxford University Press, New York, 1991.

[4] AIJ. *Unstable Behavior and Limit State of Structures*, volume 1. Maruzen, 1994. (in Japanese).

[5] AIJ. *Recommendations for Stability Design of Steel Structures.* Maruzen, 1996. (in Japanese).

[6] AIJ. *Collapse Analysis of Structures*, volume 1. Maruzen, 1997. (in Japanese).

[7] V. V. Bertero, J. C. Anderson, and H. Krawinkler. Performance of steel building structure during the northlidge earthquake. Technical Report UCB/EERC-94/09, Earthquake Research Center, 1994.

[8] Building Research Institute. *A survey report for building damages due to the 1995 Hyogo-ken Nanbu earthquake.* Building Research Institute, Ministry of Construction, 1996.

[9] D. C. Drucker, W. Prager, and H. J. Greenberg. Extended limit design theorems for continuous media. *Quartry of Applied Mathematics*, 9:381–389, 1952.

[10] F. R. Shanley. Inelastic column theory. *Journal of Aeronautical Sciences*, 14:261–268, 1947.

[11] A. M. Liapunov. *The General Problem of the Stability of Motion.* Taylor & Francis, London, 1992. Translated and edited by A. T. Fuller.

[12] R. Hill. A general theory of uniqueness and stability in elastic-plastic solids. *Journal of the Mechanics and Physics of Solids*, 6:236–249, 1958.

[13] W. T. Koiter. General theorems for elastic-plastic structures. In J. N. Sneddon and R. Hill, editors, *Progress in Solid Mechanics*, volume 1, pages 167–221, North Holland, Amsterdam, 1960.

[14] G. Maier. A shakedown matrix theory allowing for workhardening and second-order geometric effects. In A. Sawczuk, editor, *Foundations of plasticity*, volume 1, pages 417–433, Noordhoff, Leyden, 1972.

[15] Q. S. Nguyen, G. Gary, and G. Baylac. Interaction buckling-progressive deformation. *Nuclear Engineering and Design*, 75:235–243, 1983.

[16] Z. Mroz, D. Weichert, and S. Dorosz, editors. *Inelastic Behavior of Structures under Variable Loads.* Kluwer Academic Publishers, Netherlands, 1995.

[17] C. Polizzotto and G. Borio. Shakedown and steady-state responses of elastic-plastic solids in large displacements. *International Journal of Solids and Structures*, 33:3415–3437, 1996.

[18] K. Uetani and T. Nakamura. Symmetry limit theory for cantilever beam-columns subjected to cyclic reversed bending. *Journal of the Mechanics and Physics of Solids*, 31(6):449–484, 1983.

[19] K. Uetani. *Symmetry Limit Theory and Steady-State Limit Theory for Elastic-Plastic Beam-Columns Subjected to Repeated Alternating Bending.* PhD thesis, Kyoto University, 1984. (in Japanese).

[20] K. Uetani and T. Nakamura. Steady-state limit theory for cantilever beam-columns subjected to cyclic reversed bending. *Journal of Structural and Construction Engineering, AIJ*, (438):105–115, 1992.

[21] K. Uetani. Cyclic plastic collapse of steel planar frames. In Y. Fukumoto and Lee G, editors, *Stability and Ductility of Steel Structures under Cyclic loading*, pages 261–271. CRC press, 1992.

[22] J. Guckenheimer and P. Holmes. *Nonlinear Oscillations, Dynamical Systems, and Bifurcations of Vector Fields.* Springer, New York, 1983.

[23] J. M. T. Thompson and H. B. Stewart. *Nonlinear Dynamics and Chaos.* John Wiley & Sons Ltd., 1986.

[24] S. Wiggins. *Introduction to Applied Nonlinear Dynamical Systems and Chaos.* Springer, New York, 1990.

[25] K. Uetani and Y. Araki. A method for symmetry limit analysis of planar frames subjected to cyclic horizontal loading. *Journal of Structural and Construction Engineering, AIJ*, (490):149–158, Dec. 1996.

Chapter 2

Steady-State Limit for Elastic Shakedown Region

2.1 INTRODUCTION

Under cyclic bending with stepwisely increasing amplitude in the presence of a certain compressive axial force, it is known through experiments [1, 2] that a cantilever beam-column exhibits the following consecutive three classes of behavior as shown in Fig. 2.1: (1) Convergent behavior to a *symmetric steady-state*, in which a pair of deflected configurations at load reversals is symmetric with respect to the initial member axis; (2) Convergent behavior to an *asymmetric steady-state*, where the deflected shapes involve a certain anti-symmetric mode; (3) Divergent behavior, which is referred to as *cyclic instability* in this paper, where deformation grows proportionally or exponentially with respect to the number of the cycles. The concepts, called the *symmetry limit* and the *steady-state limit*, were introduced as the

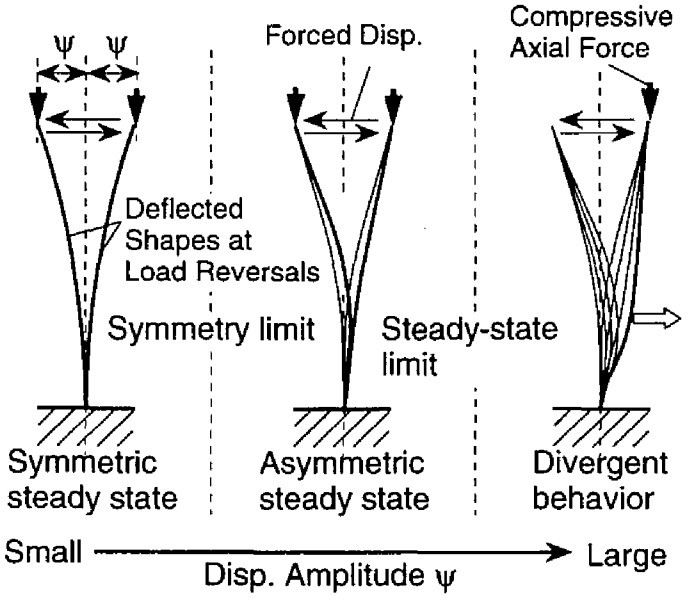

Figure 2.1: The Symmetry limit and the steady-state limit of a cantilever beam-column.

critical steady states that bound these three classes of behavior. The symmetry limit is the critical steady state at which transition from the symmetric steady state to the asymmetric steady state occurs. The steady-state limit is the critical steady state beyond which the beam-column will no longer exhibit any convergent behavior. To predict the symmetry limit and the steady-state limit, the *symmetry limit theory* and the *steady-state limit theory* were developed, respectively [1, 2, 3].

It might be thought that the symmetry limit and the steady-state limit can be found by applying previously established theories. Nevertheless, none of them are directly applicable for the following reasons: (1) *Plastic buckling theory* [4, 5]: The symmetry limit and the steady-state limit are phenomenologically and conceptually different from the critical points, such as a branching point and a limit point, of the equilibrium path. In other words, cyclic instability may take place without passing the critical equilibrium points; (2) *Shakedown theory* and its extensions: The symmetry limit and the steady-state limit are generally observed under the strong effect of geometrical nonlinearity. In the *classical shakedown theory* [6, 7], however, geometrical nonlinearity is completely neglected. Though several papers [8, 9, 10, 11, 12, 13, 14, 15, 16] extended the classical shakedown theory by taking geometrical nonlinearity into account, the extended shakedown theories are not valid when compressive stresses and/or large deformations have strong influence on the structural response, where

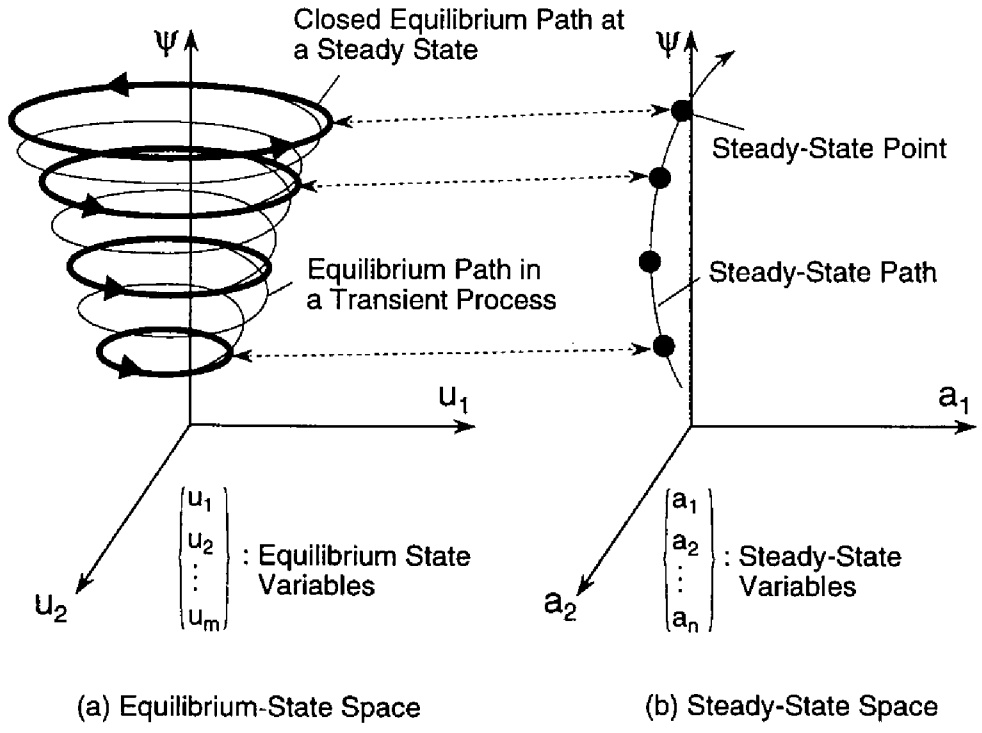

Figure 2.2: The equilibrium-state space and the steady-state space.

structural responses are path-dependent; (3) *Numerical methods for response analysis*: It is possible to bound convergence and divergence of plastic deformations (see e.g. [17, 18]) under specified loading histories. But a number of parametric analyses are required for bounding the structural responses. Moreover, the parametric analyses will never lead to any theoretical condition similar to that for the Euler load.

On the other hand, the symmetry limit and the steady-state limit can be found theoretically, though under a specified loading history, in the symmetry limit theory and the steady-state limit theory. The limits are found based on the following concepts. First, a steady state is considered as a point in a special space schematically illustrated in Fig. 2.2. Second, the sequence of these points, generated under an idealized cyclic loading program with continuously increasing amplitude, is regarded as a continuous path. This path is called the *steady-state path*. Third, the symmetry limit and the steady-state limit are found respectively as the first branching point and the first limit point of the steady-state path as shown in Fig. 2.3. Since only the sequence of the steady states is traced, there is no need for tracing the transient process between any pair of two adjacent steady states. Furthermore, no parametric analysis is needed to detect the two limits because they are predicted as the critical points of the steady-state path.

For a few classes of structures, the symmetry limit theory and the steady-state limit theory have been applied. It was shown that severe cyclic instability is induced when the deflection amplitude is in excess of the symmetry limit or the steady-state limit [2, 19]. In those studies, however, only the simple structures, e.g. a cantilever beam-column or a unit

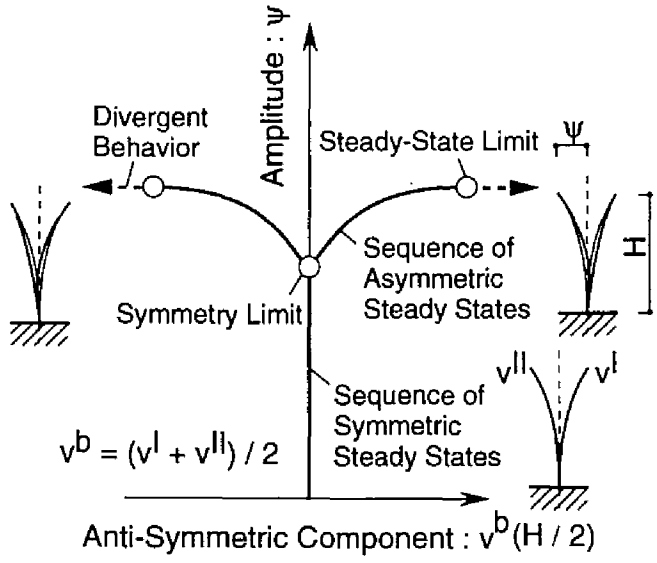

Figure 2.3: The symmetry limit and the steady-state limit in a steady-state plane.

frame, were treated for which analytical solutions can be derived. Hence, to investigate the limit states of more complex and practical structures, which generally do not have a symmetry limit if they do not have a symmetric shape, it is necessary to establish a method for predicting the steady-state limit using appropriate finite element methods.

The purpose of this chapter is to present a new method for finding the steady-state limit of elastoplastic trusses, which are one of the simplest finite dimensional structures, subjected to initial constant loads and subsequent cyclic loads. In the following sections, governing equations are described first. Then the fundamental concepts of the steady-state limit theory are shown. Next, using the Taylor-series expansion, a new incremental theory is formulated for tracing the steady-state path. Finally, validity of the proposed method is demonstrated through numerical examples. The effects of the difference of loading histories on structural responses are also shown in the numerical examples.

For simplicity, our consideration is restricted to the case in which dynamic and thermal effects can be neglected. In addition, the scope of this chapter is limited to an *elastic shakedown* region because the problem becomes much more complicated when *plastic shakedown* occurs in the trusses. Throughout this chapter, as referred in recent papers (see e.g. [9, 18]), elastic shakedown or classic shakedown means a cyclic and fully elastic structural response after some history of plastic deformations. And plastic shakedown is so called *alternating plasticity* in which plastic deformations are included in steady cycles.

2.2 GOVERNING EQUATIONS

2.2.1 Analytical Model

Consider a space truss with M elements and N nodes. Compatibility conditions, equilibrium conditions and constitutive relations are given for an element shown in Fig. 2.4. By assembling the equilibrium equations for the element, we have those for the total system. Buckling of the element is ruled out. But buckling of a global type is taken into account using a nonlinear strain-displacement relation.

We measure stresses and strains using the Total Lagrangian formulation (see e.g. [20, 21, 22, 23]). Assumptions of large displacements-small strains are employed. Green-Lagrangian strain ε is expressed as

$$\varepsilon = \frac{L^2 - L_0^2}{2L_0^2} \tag{2.1}$$

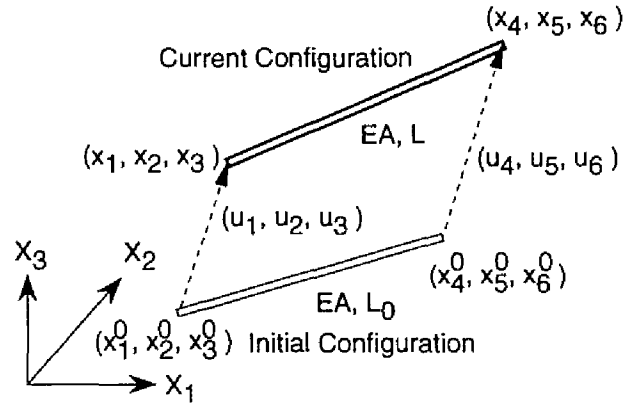

Figure 2.4: A space truss element.

where L and L_0 are the current length and the initial length of the element, respectively. The relations between the current length L and the nodal displacements u_i are written as

$$L^2 = (x_4 - x_1)^2 + (x_5 - x_2)^2 + (x_6 - x_3)^2 \tag{2.2}$$

$$x_i = x_i^0 + u_i; \qquad i = 1, \cdots, 6 \tag{2.3}$$

in which x_i and x_i^0 indicate the current position and the initial position of the nodes at the two ends, respectively, as illustrated in Fig. 2.4.

The principle of virtual work for the element is given by

$$f_i \delta u_i = \int_V \sigma \delta \varepsilon dV = AL_0 \sigma \frac{\partial\, \varepsilon}{\partial\, u_i} \delta u_i \tag{2.4}$$

where f_i is the nodal forces, δu_i is the virtual nodal displacements, V is the initial volume, σ is the second Piola-Kirchhoff stress, $\delta\varepsilon$ is the virtual strain, and A is the initial cross sectional area. Note that summation convention is used only for subscripts i and j throughout this chapter. Since the virtual work equation (2.4) should be satisfied for any δu_i, we obtain the equilibrium equation

$$f_i = AL_0 \sigma \frac{\partial\, \varepsilon}{\partial\, u_i}. \tag{2.5}$$

As a uni-axial constitutive relation for the truss element, we use a bi-linear kinematic hardening rule shown in Fig. 2.5. In terms of Young's modulus E, the tangent modulus after yielding E_t, the initial tensile yield stress σ_y, and the plastic strain ε_p, the constitutive law is expressed as follows:

$$\sigma = E(\varepsilon - \varepsilon_p) \qquad \text{in the elastic and unloading ranges,} \tag{2.6}$$

$$\sigma = E_t \varepsilon + \bar{\sigma}_y \qquad \text{for the plastic loading in tension,} \tag{2.7}$$

$$\sigma = E_t \varepsilon - \bar{\sigma}_y \qquad \text{for the plastic loading in compression.} \tag{2.8}$$

where $\bar{\sigma}_y = (1 - E_t/E)\sigma_y$.

2.2.2 Cyclic Responses

For later formulation of the steady-state limit theory, we must examine all possible types of the cyclic responses in the stress-strain plane. Possible cyclic responses are classified into four different types E, C, T and P as shown in Fig. 2.6, where the superscripts t and c indicate the state variables, such as stresses, strains, and displacements, at strain reversals in tension and compression, respectively. In terms of $(\varepsilon^t, \sigma^t)$ and $(\varepsilon^c, \sigma^c)$, the cyclic responses can be uniquely described as:

$$\sigma^t = E(\varepsilon^t - \varepsilon_p^t), \tag{2.9}$$

$$\sigma^c = E(\varepsilon^c - \varepsilon_p^c) \tag{2.10}$$

for type E, which represents a purely elastic response or an elastic shakedown state.

$$\sigma^t = E_t\varepsilon^t + \bar{\sigma}_y, \tag{2.11}$$

$$\sigma^c = (E_t - E)\varepsilon^t + E\varepsilon^c + \bar{\sigma}_y \tag{2.12}$$

for type T, which is the elastic shakedown state whose maximum stress reaches the tensile yield stress.

$$\sigma^t = E\varepsilon^t - (E - E_t)\varepsilon^c + \bar{\sigma}_y, \tag{2.13}$$

$$\sigma^c = E_t\varepsilon^c - \bar{\sigma}_y \tag{2.14}$$

for type C, which represents the elastic shakedown state that starts from and reaches the compressive strain hardening line. Though all the possible types are shown in Fig. 2.6, type

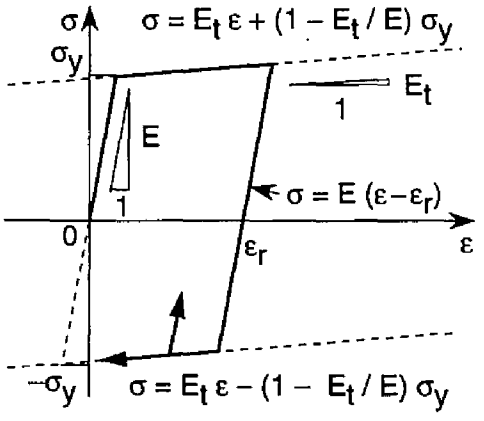

Figure 2.5: A bi-linear kinematic hardening rule.

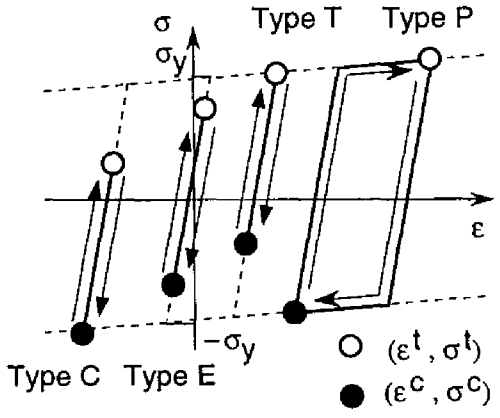

Figure 2.6: Possible types of cyclic responses.

P is not considered in this chapter because the discussion is limited to the elastic shakedown region as mentioned in the introduction.

Note that the plastic strain ε_p is eliminated in Eqs. (2.12) and (2.13). For type T, σ^t is expressed in two ways using Eqs. (2.6) and (2.7), while σ^c is written using only Eq. (2.6). The plastic strains at the strain reversals is eliminated using these three expressions and the following relation

$$\varepsilon_p^t = \varepsilon_p^c. \tag{2.15}$$

For type C, the plastic strain can be eliminated similarly.

2.3 FUNDAMENTAL CONCEPTS

2.3.1 Loading Conditions

The truss is subjected to initial constant loads $\lambda_0\bar{\mathbf{P}}_0$ and subsequent cyclic loads $\lambda_c\bar{\mathbf{P}}_c$. Here, λ and $\bar{\mathbf{P}}$ denote the load factor and the constant vector, respectively. The subscripts 0 and c indicate that the variables refer to the constant loads and to the cyclic loads, respectively. External forces and/or forced displacements are applied as the external loads. In other words, nodal forces and/or nodal displacements are included in $\bar{\mathbf{P}}$. The load factor λ_c is varied between the maximum value $\lambda_c^{\mathrm{I}} = \psi$ and the minimum value $\lambda_c^{\mathrm{II}} = -\psi$ in a cycle, where ψ denotes the amplitude of λ_c. The equilibrium states at which $\lambda_c = \lambda_c^{\mathrm{I}}$ and $\lambda_c = \lambda_c^{\mathrm{II}}$ are called Γ^{I} state and Γ^{II} state, respectively. The superscripts I and II indicate that the state variables refer to those for the Γ^{I} and Γ^{II} states, respectively.

As a preliminary program, consider a cyclic loading program shown in Fig. 2.7 (a). In the program, the loading cycle is repeated as many times as necessary for the truss to converge

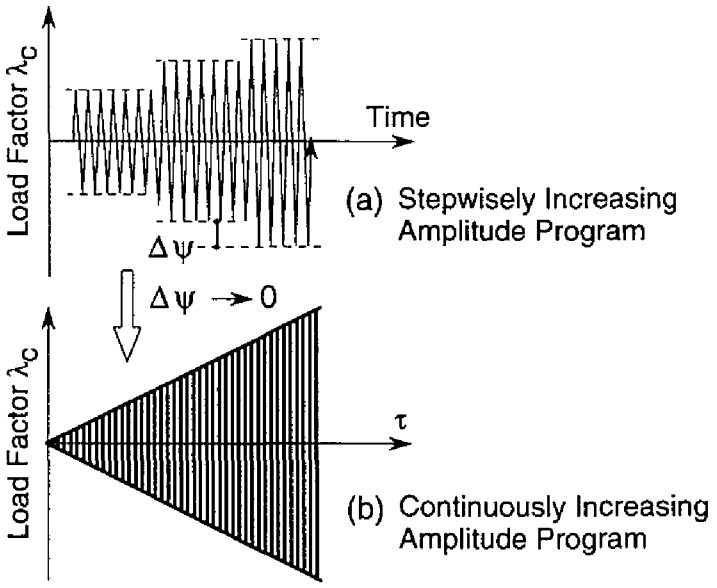

Figure 2.7: The idealized cyclic loading program.

to a steady state. After convergence, a small increment $\Delta\psi$ is added. A sequence of the steady states is generated under the cyclic loading program as shown in Fig. 2.2.

By taking the limit $\Delta\psi \to 0$ as illustrated in Fig. 2.7 (b), the sequence of the points can be considered as a continuous path. The continuous path is called *steady-state path*. The steady-state path is defined by a monotonically increasing parameter τ, called *steady-state path parameter*. The steady-state limit is characterized as the first limit point of the steady-state path as shown in Fig. 2.3.

2.3.2 Hypotheses

To formulate the sequence of the steady states in terms of the state variables for Γ^{I} and Γ^{II}, the following hypotheses are introduced:

Hypothesis 2.1 All the state variables for Γ^{I} and Γ^{II} are continuous and piecewise differentiable functions of τ.

Hypothesis 2.2 For all elements, strain reversals occur only at Γ^{I} or Γ^{II}.

These hypotheses are the alternative statements of the hypotheses (H2) and (H3), respectively, introduced by Uetani and Nakamura [1, 2]. Note that hypothesis 2.2 is applied not for the transient response between the consecutive steady states but for the steady state response after convergence.

2.3.3 Outline

Based on these hypotheses, the procedures for finding the steady-state limit are outlined as follows:

1. A steady-state is uniquely described by a set of the state variables that belong to the equilibrium states Γ^{I} and Γ^{II}.
2. The steady-state path is traced incrementally, where incremental relations are obtained by differentiating the state variables for Γ^{I} and Γ^{II} with respect to τ.
3. The steady-state limit is found as the first limit point of the steady-state path.

2.4 FORMULATION

2.4.1 Incremental Relations for Variation of Steady State

When all the state variables are known for the current steady states at $\tau = \tau_h$, the problem is then to determine those for a neighboring steady state at $\tau = \tau_{h+1}$. Let $\Delta\tau = \tau_{h+1} - \tau_h$ be an increment of the steady-state path parameter τ. Then, on the basis of hypothesis 2.1, the state variables for Γ^{I} at $\tau = \tau_{h+1}$ are expressed using Taylor-series expansion as:

$$\mathbf{U}^{\mathrm{I}}(\tau_{h+1}) = \mathbf{U}^{\mathrm{I}}(\tau_h) + \dot{\mathbf{U}}^{\mathrm{I}}(\tau_h)\Delta\tau + \frac{1}{2}\ddot{\mathbf{U}}^{\mathrm{I}}(\tau_h)\Delta\tau^2 + \cdots, \tag{2.16}$$

$$\mathbf{F}^{\mathrm{I}}(\tau_{h+1}) = \mathbf{F}^{\mathrm{I}}(\tau_h) + \dot{\mathbf{F}}^{\mathrm{I}}(\tau_h)\Delta\tau + \frac{1}{2}\ddot{\mathbf{F}}^{\mathrm{I}}(\tau_h)\Delta\tau^2 + \cdots, \tag{2.17}$$

$$\mathbf{E}^{\mathrm{I}}(\tau_{h+1}) = \mathbf{E}^{\mathrm{I}}(\tau_h) + \dot{\mathbf{E}}^{\mathrm{I}}(\tau_h)\Delta\tau + \frac{1}{2}\ddot{\mathbf{E}}^{\mathrm{I}}(\tau_h)\Delta\tau^2 + \cdots, \tag{2.18}$$

$$\mathbf{E}_p^{\mathrm{I}}(\tau_{h+1}) = \mathbf{E}_p^{\mathrm{I}}(\tau_h) + \dot{\mathbf{E}}_p^{\mathrm{I}}(\tau_h)\Delta\tau + \frac{1}{2}\ddot{\mathbf{E}}_p^{\mathrm{I}}(\tau_h)\Delta\tau^2 + \cdots, \tag{2.19}$$

$$\mathbf{S}^{\mathrm{I}}(\tau_{h+1}) = \mathbf{S}^{\mathrm{I}}(\tau_h) + \dot{\mathbf{S}}^{\mathrm{I}}(\tau_h)\Delta\tau + \frac{1}{2}\ddot{\mathbf{S}}^{\mathrm{I}}(\tau_h)\Delta\tau^2 + \cdots \tag{2.20}$$

where $\mathbf{F}$ and $\mathbf{U}$ are the nodal force vector and the nodal displacements vector, respectively, with $3N$ components, and $\mathbf{E}$, $\mathbf{E}_p$ and $\mathbf{S}$ denote the strain vector, the plastic strain vector, and the stress vector, respectively, with M components. The super dot indicates differentiation with respect to τ. The variables for Γ^{II} are expressed by replacing the superscript I with II.

For simple presentation of the incremental theory, only the formulation is shown here in which the terms higher than or equal to the second order are neglected. However, since it is desirable to use a more accurate solution method for this highly nonlinear system, the formulation including the higher-order derivatives is presented in Appendix A.

2.4.2 Rate Forms of Governing Equations

By differentiating all the governing equations for Γ^{I} and Γ^{II} with respect to the steady-state parameter τ, we derive the rate form of the governing equations. The rate forms of the governing equations are simply called *rate equations* in this chapter. Differentiation of the compatibility conditions (2.1)-(2.3) yields

$$\dot{\varepsilon}^{\mathrm{I}} = \frac{\partial\, \varepsilon^{\mathrm{I}}}{\partial\, u_i^{\mathrm{I}}} \dot{u}_i^{\mathrm{I}}, \tag{2.21}$$

$$\dot{\varepsilon}^{\mathrm{II}} = \frac{\partial\, \varepsilon^{\mathrm{II}}}{\partial\, u_i^{\mathrm{II}}} \dot{u}_i^{\mathrm{II}}. \tag{2.22}$$

Recall that summation convention is used only for the subscripts i, j and k which are varied from 1 to 6. Rate forms of the equilibrium conditions are given by

$$\dot{f}_i^{\mathrm{I}} = AL_0 \left(\dot{\sigma}^{\mathrm{I}} \frac{\partial\, \varepsilon^{\mathrm{I}}}{\partial\, u_i^{\mathrm{I}}} + \sigma^{\mathrm{I}} \frac{\partial^2\, \varepsilon^{\mathrm{I}}}{\partial\, u_i^{\mathrm{I}}\, \partial\, u_j^{\mathrm{I}}} \dot{u}_j^{\mathrm{I}} \right), \tag{2.23}$$

$$\dot{f}_i^{\mathrm{II}} = AL_0 \left(\dot{\sigma}^{\mathrm{II}} \frac{\partial\, \varepsilon^{\mathrm{II}}}{\partial\, u_i^{\mathrm{II}}} + \sigma^{\mathrm{II}} \frac{\partial^2\, \varepsilon^{\mathrm{II}}}{\partial\, u_i^{\mathrm{II}}\, \partial\, u_j^{\mathrm{II}}} \dot{u}_j^{\mathrm{II}} \right). \tag{2.24}$$

Differentiating the stress-strain relations (2.9)-(2.12), the stress rate-strain rate relations can be expressed for the strain-reversal points in the form of

$$\dot{\sigma}^t = C^{tt}\dot{\varepsilon}^t + C^{tc}\dot{\varepsilon}^c, \tag{2.25}$$

$$\dot{\sigma}^c = C^{ct}\dot{\varepsilon}^t + C^{cc}\dot{\varepsilon}^c \tag{2.26}$$

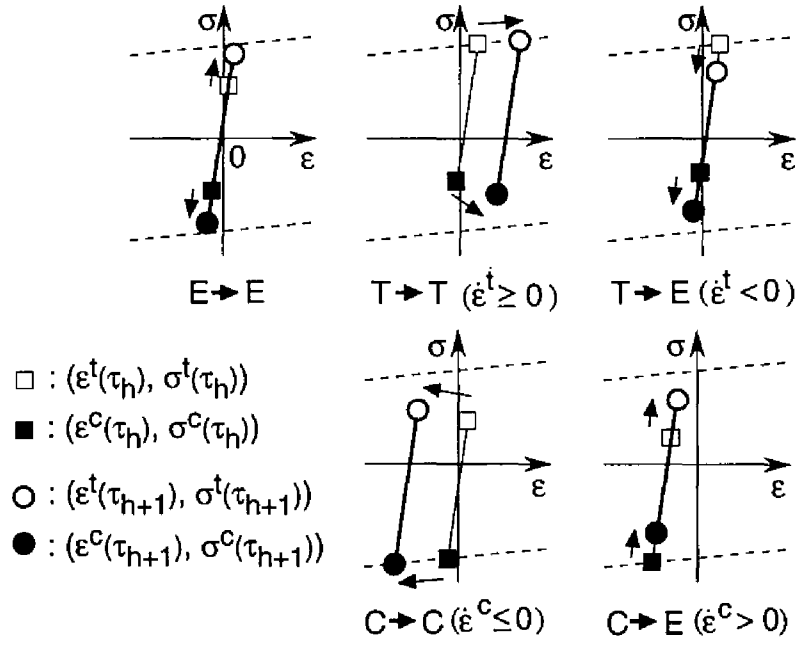

Figure 2.8: Possible types of the variation of cyclic responses.

where C^{cc}, C^{ct}, C^{tc} and C^{tt} are coefficients that should be chosen according to the current type of the cyclic response and the signs of the strain rates as schematically illustrated in Table 2.1 and Fig. 2.8. It may be worth noting that the stress rate-strain rare relations are derived by differentiating Eqs. (2.9)-(2.14) in the proposed method for steady-state limit analysis. In contrast, they are obtained by differentiating Eqs. (2.6)-(2.8) in the conventional methods for response analysis.

To derive the rate equations for Γ^{I} and Γ^{II}, Eqs. (2.25) and (2.26) for the strain-reversal points are transformed into those for the load-reversal points by replacing their superscripts on the basis of hypothesis 2.2. The superscripts c and t are replaced by I and II, respectively, or they are replaced with II and I, respectively. After replacing the superscripts, we have

$$\dot{\sigma}^{\mathrm{I}} = C^{\mathrm{II}}\dot{\varepsilon}^{\mathrm{I}} + C^{\mathrm{III}}\dot{\varepsilon}^{\mathrm{II}}, \tag{2.27}$$

$$\dot{\sigma}^{\mathrm{II}} = C^{\mathrm{III}}\dot{\varepsilon}^{\mathrm{I}} + C^{\mathrm{III}}\dot{\varepsilon}^{\mathrm{II}}. \tag{2.28}$$

Substituting Eqs. (2.21), (2.22), (2.27) and (2.28) into Eqs. (2.23) and (2.24), we have the rate equations for each element

$$\dot{f}_i^{\mathrm{I}} = k_{ij}^{\mathrm{II}}\dot{u}_j^{\mathrm{I}} + k_{ij}^{\mathrm{III}}\dot{u}_j^{\mathrm{II}}, \tag{2.29}$$

$$\dot{f}_i^{\mathrm{II}} = k_{ij}^{\mathrm{III}}\dot{u}_j^{\mathrm{I}} + k_{ij}^{\mathrm{III}}\dot{u}_j^{\mathrm{II}} \tag{2.30}$$

Table 2.1: Stress rate-strain rate relations for the strain-reversal points.

Type	Strain Rate	C^{tt}	C^{tc}	C^{ct}	C^{cc}
E		E	0	0	E
T	$\dot{\varepsilon}^t \geq 0$	E_t	0	$E_t - E$	E
T	$\dot{\varepsilon}^t < 0$	E	0	0	E
C	$\dot{\varepsilon}^c \leq 0$	E	$E_t - E$	0	E_t
C	$\dot{\varepsilon}^c > 0$	E	0	0	E

where

$$k_{ij}^{\mathrm{II}} = AL_0\left(C^{\mathrm{II}}\frac{\partial\,\varepsilon^{\mathrm{I}}}{\partial\,u_i^{\mathrm{I}}}\frac{\partial\,\varepsilon^{\mathrm{I}}}{\partial\,u_j^{\mathrm{I}}} + \sigma^{\mathrm{I}}\frac{\partial^2\,\varepsilon^{\mathrm{I}}}{\partial\,u_i^{\mathrm{I}}\,\partial\,u_j^{\mathrm{I}}}\right), \tag{2.31}$$

$$k_{ij}^{\mathrm{III}} = AL_0C^{\mathrm{III}}\frac{\partial\,\varepsilon^{\mathrm{I}}}{\partial\,u_i^{\mathrm{I}}}\frac{\partial\,\varepsilon^{\mathrm{II}}}{\partial\,u_j^{\mathrm{II}}}, \tag{2.32}$$

$$k_{ij}^{\mathrm{II\,I}} = AL_0C^{\mathrm{III}}\frac{\partial\,\varepsilon^{\mathrm{II}}}{\partial\,u_i^{\mathrm{II}}}\frac{\partial\,\varepsilon^{\mathrm{I}}}{\partial\,u_j^{\mathrm{I}}}, \tag{2.33}$$

$$k_{ij}^{\mathrm{III}} = AL_0\left(C^{\mathrm{III}}\frac{\partial\,\varepsilon^{\mathrm{II}}}{\partial\,u_i^{\mathrm{II}}}\frac{\partial\,\varepsilon^{\mathrm{II}}}{\partial\,u_j^{\mathrm{II}}} + \sigma^{\mathrm{II}}\frac{\partial^2\,\varepsilon^{\mathrm{II}}}{\partial\,u_i^{\mathrm{II}}\,\partial\,u_j^{\mathrm{II}}}\right). \tag{2.34}$$

By assembling Eqs. (2.29) and (2.30) throughout the whole structure, the following rate equations are derived for the total system:

$$\dot{\mathbf{F}}^{\mathrm{I}} = \mathbf{K}^{\mathrm{II}}\dot{\mathbf{U}}^{\mathrm{I}} + \mathbf{K}^{\mathrm{III}}\dot{\mathbf{U}}^{\mathrm{II}}, \tag{2.35}$$

$$\dot{\mathbf{F}}^{\mathrm{II}} = \mathbf{K}^{\mathrm{II\,I}}\dot{\mathbf{U}}^{\mathrm{I}} + \mathbf{K}^{\mathrm{III}}\dot{\mathbf{U}}^{\mathrm{II}} \tag{2.36}$$

where $\mathbf{K}^{\mathrm{II}}$, $\mathbf{K}^{\mathrm{III}}$, $\mathbf{K}^{\mathrm{II\,I}}$ and $\mathbf{K}^{\mathrm{III}}$ are the coefficient matrices of the nodal displacement rates. By specifying $\dot{\psi}$ and by using the boundary conditions, we have a system of $2\times 3N$ simultaneous linear equations.

2.4.3 Consistent Set of Stress Rate-Strain Rate Relations

When an element exhibits type T or type C behavior, the coefficients of the strain rates should be chosen according to the signs of the strain rates as shown in Table 2.1 and Fig. 2.8. Therefore, for all the elements exhibiting the type T or the type C behavior, we should choose a set of the coefficients that are consistent with the signs of the resulting strain rates. Note that the term *consistent* used here has no relation with the one used in integration algorithms for the numerical response analysis of elastoplastic solids or structures (see e.g. [24, 25]).

To find the consistent set of the coefficients, we employ a trial and error approach, which is also used in the conventional response analysis [26]. In the trial and error approach, first, the signs of the strain rates $\dot{\mathbf{E}}^{\mathrm{I}}$ and $\dot{\mathbf{E}}^{\mathrm{II}}$ are assumed to be equal to those in the last step. Then, the coefficients C^{cc}, C^{ct}, C^{tc} and C^{tt} are determined according to the assumptions, and the rate equations are constructed. After the rate equations are solved and $\dot{\mathbf{E}}^{\mathrm{I}}$ and $\dot{\mathbf{E}}^{\mathrm{II}}$ are calculated, the consistency is checked between the assumed signs of the strain rates and the resulting ones for all the elements exhibiting the type T or the type C behavior. If the signs are not consistent, the assumed signs are reversed. This procedure is continued until all the resulting signs of the strain rates are consistent with the assumed ones.

2.4.4 Termination Conditions for Incremental Step

When the type of the stress-strain cyclic response changes, a different type of stress rate-strain rate relation should be used in Eqs. (2.27) and (2.28). Step length $\Delta\tau$ is therefore determined considering the conditions for the transition of the type of the stress-strain cyclic response. Let σ_{yt} and σ_{yc} denote the subsequent yield stresses in tension and compression, respectively. Then, for every element, $\Delta\tau$ is calculated using the following conditions:

$$\sigma^t(\tau_{h+1}) = \sigma_{yt}, \tag{2.37}$$

$$\sigma^c(\tau_{h+1}) = \sigma_{yc}, \tag{2.38}$$

$$\sigma^t(\tau_{h+1}) - \sigma^c(\tau_{h+1}) = \sigma_{yt} - \sigma_{yc} = 2\sigma_y \tag{2.39}$$

where $\sigma^t(\tau_{h+1}) = \sigma^t(\tau_h) + \dot{\sigma}^t(\tau_h)\Delta\tau$ and $\sigma^c(\tau_{h+1}) = \sigma^c(\tau_h) + \dot{\sigma}^c(\tau_h)\Delta\tau$ in the linear approximation. Here, the Eqs. (2.37)-(2.39) describe the conditions for the transition of the cyclic response for E $\rightarrow$ T, E $\rightarrow$ C, and E, C or T $\rightarrow$ P, respectively. Examples of the transition are given in Fig. 2.9. Note that the subsequent yield stresses are expressed in terms of the plastic strain at the current steady state as follows:

$$\sigma_{yt} = \frac{EE_t}{E - E_t}\varepsilon_p(\tau_h) + \sigma_y, \tag{2.40}$$

$$\sigma_{yc} = \frac{EE_t}{E - E_t}\varepsilon_p(\tau_h) - \sigma_y. \tag{2.41}$$

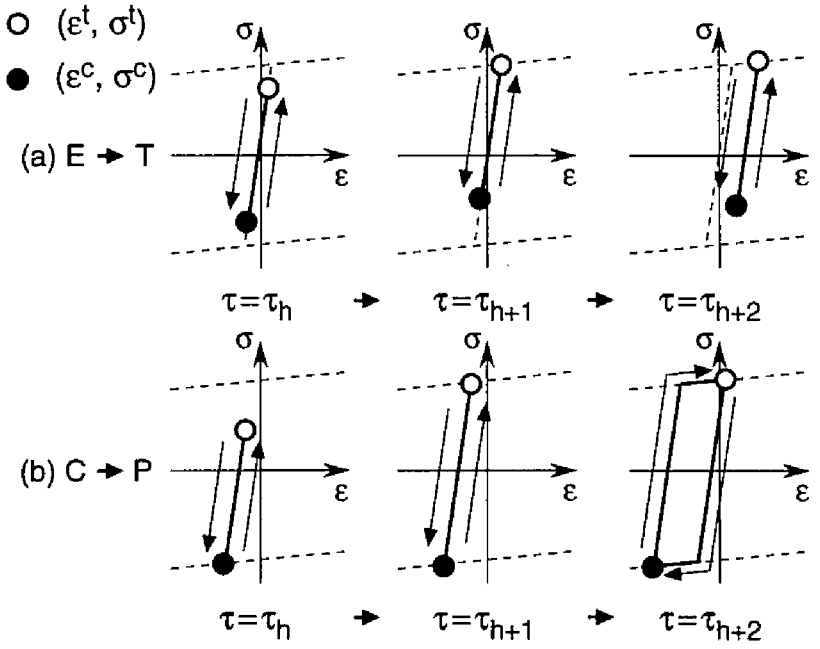

Figure 2.9: Examples of transition of cyclic responses: (a) E $\rightarrow$ T and (b) C $\rightarrow$ P.

Besides the conditions above, the step length $\Delta\tau$ should be kept small enough to prevent excessive accumulation of truncation errors. Hence the step length $\Delta\tau$ is selected as the smallest value among the values calculated from the conditions (2.37)-(2.39) and the specified maximum allowable value $\Delta\bar{\tau}_{max}$. When $\Delta\tau$ is determined by (2.37) or (2.38), the stress rate-strain rate relations are changed in the next step. When (2.39) is used to determine $\Delta\tau$, the incremental analysis is terminated.

2.4.5 Steady-State Limit Condition

Now, all the first-order derivatives and the step length $\Delta\tau$ have been obtained. Substituting $\Delta\tau$ and the first-order derivatives into Eqs. (2.16)-(2.20), we have all the state variables at $\tau = \tau_{h+1}$. Repeating these procedures, the steady-state path is traced incrementally.

As mentioned before, the steady-state limit is defined as the first limit point of the steady-state path as shown in Fig. 2.3. The steady-state limit condition is given as

$$\dot{\psi} \leq 0 \tag{2.42}$$

Note that, to find the limit point and to trace the steady-state path after the limit point, an procedure should be employed similar to displacement control schemes [26, 22].

2.5 NUMERICAL EXAMPLES

The proposed method has been developed on the basis of the two hypotheses. Moreover the steady-state limit is predicted regardless of the transient process between the two consecutive steady states. Hence validity of the two hypotheses and the steady-state limit should be examined. For this purpose, both steady-state limit analysis and conventional response analysis, in which the entire history is traced, are carried out for a two-bar arch truss and a ten-bar cantilever truss. And the results of the analyses are compared. In addition, the effect of the differences of the loading histories are discussed through these numerical examples.

2.5.1 Steady-State Limit Analysis

Initial shape, boundary conditions and loading conditions of both plane trusses are illustrated in Fig. 2.10. The initial constant forces and the subsequent cyclic forced displacements are denoted by $\lambda_0\bar{F}_0$ and $\lambda_c\bar{U}_c$, respectively. Here, $\bar{F}_0 = 9.807 \times 10^3$N and $\bar{U}_c = 1$cm. The cross-sectional areas of the two-bar truss are $A_{(1)} = 1$ cm^2 and $A_{(2)} = 2$ cm^2, and those of the ten-bar truss are as follows: $A_{(1)} = A_{(4)} = A_{(5)} = 11$ cm^2, $A_{(2)} = A_{(3)} = 1.1$ cm^2,

$A_{(6)} = A_{(9)} = A_{(10)} = 10$ cm^2, and $A_{(7)} = A_{(8)} = 1$ cm^2. Both trusses obey a bi-linear kinematic hardening rule with $E = 1.961 \times 10^2$GPa, $E_t = 0.01E$, and $\sigma_y = 2.942 \times 10^2$MPa. Throughout the steady-state limit analysis, higher-order terms up to the second order are incorporated (see Appendix A), and the maximum allowable step lengths are set to $\Delta\bar{\tau}_{max} = 0.05$ and $\Delta\bar{\tau}_{max} = 0.2$ for the two-bar truss and the ten-bar truss, respectively.

Let $\lambda_y\bar{F}_0$ and $\lambda_b\bar{F}_0$ denote the initial yield load and the initial buckling load, respectively, for the trusses subjected to only $\lambda_0\bar{F}_0$. As the results of the conventional response analysis, we have $\lambda_y = \lambda_b = 0.7477$ for the two-bar truss, and $\lambda_y = 30.96$ and $\lambda_b = 40.38$ for the ten-bar truss. Note that the term *buckling* means that the lowest eigenvalue of the tangent stiffness matrix for the Hill's linear comparison solid [5, 27] becomes non-positive in tracing the equilibrium path. In Hill's linear comparison solid, any yielding element is assumed to behave with their tangent stiffness for plastic loading even if its strain changes in an unloading direction.

Figures 2.11 and 2.12 illustrate the results of the steady-state limit analysis performed under different initial constant loads. The normalized load factor λ_0/λ_b is parametrically changed between 0 and 1 with increments of 0.005 and 0.01 for the two-bar truss and the ten-bar truss, respectively. The solid line represents the steady-state limit ψ_{ssl} and the dashed line shows the boundary between the elastic shakedown region and the plastic shakedown region.

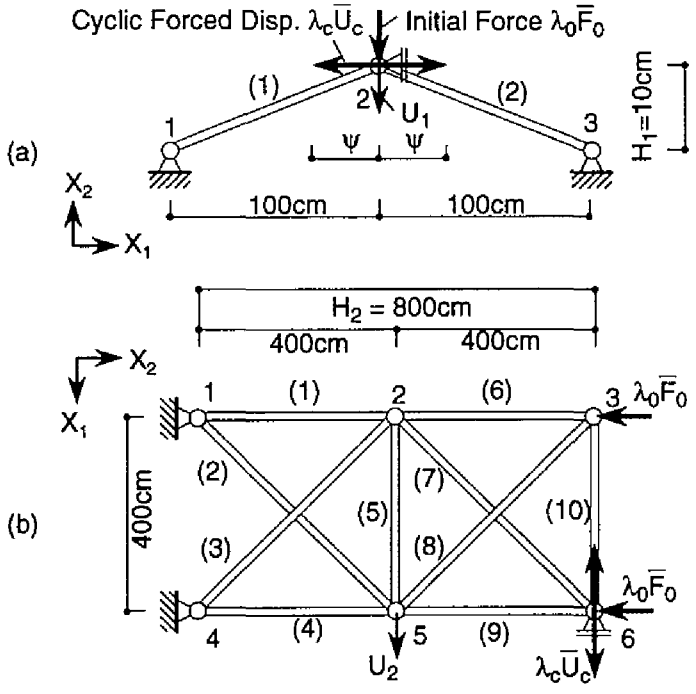

Figure 2.10: The geometry of (a) a two-bar truss and (b) a ten-bar truss.

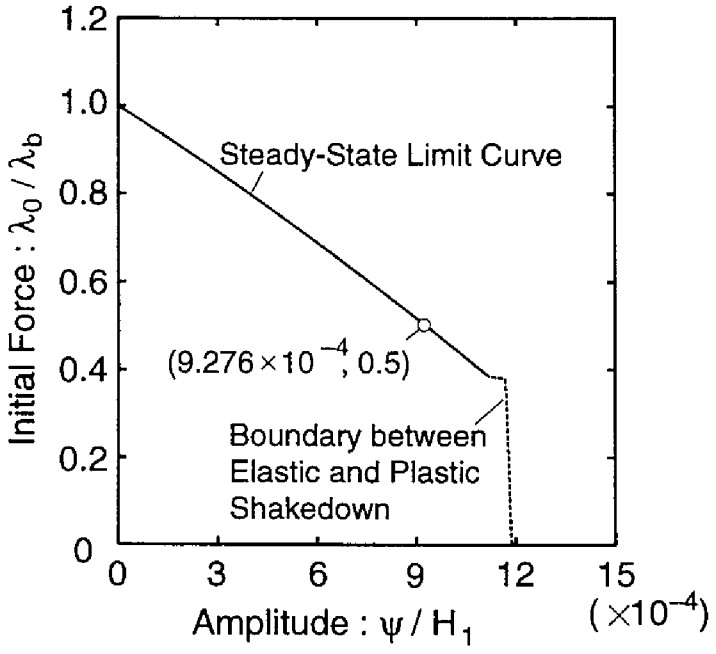

Figure 2.11: The elastic shakedown boundaries for the two-bar truss.

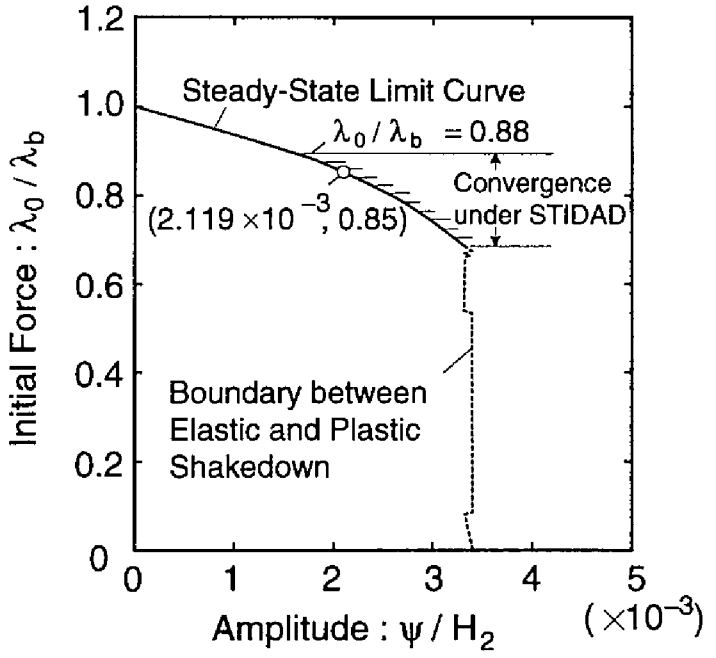

Figure 2.12: The elastic shakedown boundaries for the ten-bar truss.

2.5.2 Response Analysis

It is very difficult to realize the idealized cyclic loading program employed in steady-state limit analysis. For the verification, therefore, we use the following two realistic loading programs shown in Fig. 2.13: (1) STIDAC program. The amplitude ψ of the forced displacement is increased every half cycle with an increment $\Delta\bar{\psi}$ from zero to a specified value $\bar{\psi}_{max}$, then ψ is kept constant in the following cycles; (2) STIDAD program. Throughout all cycles, ψ is kept a constant value $\bar{\psi}$. The value of $\bar{\psi}_{max}$ is set so as to be just below and above that of ψ_{ssl}. The value of $\bar{\psi}$ is set similarly. Consequently, the response analysis is performed four times for each value of ψ_{ssl}. Formulation for the response analysis and criteria for convergence and divergence are shown in Appendix B.

For both of the trusses, the steady-state limit predicted by the proposed method is in good agreement with the results of the response analysis performed under the STIDAC program with $\bar{\psi}_{max} = (1 \pm 0.001)\psi_{ssl}$ and $\Delta\bar{\psi} = 0.001\psi_{ssl}$. Namely, convergence is observed if $\bar{\psi}_{max} < \psi_{ssl}$ and, otherwise, divergence is obtained. Obviously, the program STIDAC become closer to the idealized program employed in the steady-state limit analysis as $\Delta\psi$ is made smaller. It may be therefore concluded that the steady state limit obtained by the proposed method is directly verified.

On the other hand, under the STIDAD program with $\bar{\psi} = (1 \pm 0.001)\psi_{ssl}$, the ten-bar truss converges to elastic shakedown state in the hatched range in Fig. 2.12 regardless of $\bar{\psi} > \psi_{ssl}$. However, such inconsistent results are obtained only when $\bar{\psi} > \psi_{ssl}$. From these results, it is observed that the value of the steady-state limit ψ_{ssl}, defined for the idealized cyclic loading program, is smaller than the limiting value of $\bar{\psi}$ that bounds convergence and divergence under the STIDAD program.

In Fig. 2.14, the relation between the vertical displacement U_1^1 and the number of the cycles is plotted for the two-bar truss subjected to the STIDAD program with the four constant amplitudes $\bar{\psi}/\psi_{ssl} = 0.80$, 0.99, 1.01 and 1.05 under the initial loads $\lambda_0/\lambda_b = 0.5$.

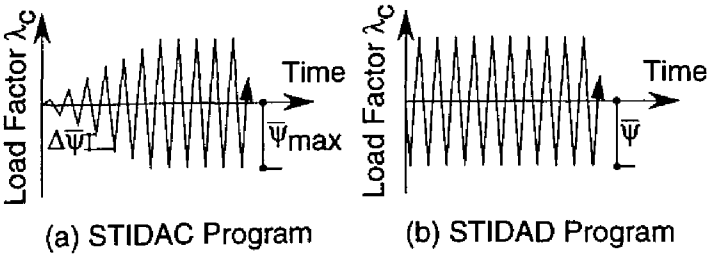

Figure 2.13: The cyclic loading programs: (a) STIDAC and (b) STIDAD.

It can be observed from Fig. 2.14 that cyclic instability occurs if the amplitude ψ is above the predicted value of ψ_{ssl}, whereas U_1^I converges otherwise.

Figure 2.15 illustrates comparison of the results for the ten-bar truss obtained by the steady-state limit analysis and the response analyses performed under various cyclic loading programs under the initial constant load $\lambda_0/\lambda_b = 0.85$. This figure shows the path-

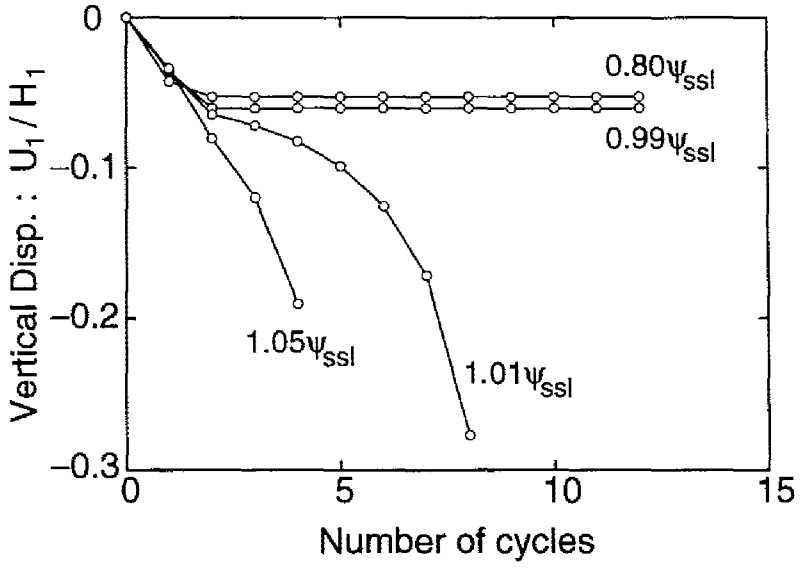

Figure 2.14: Convergence and divergence of U_1 for the two-bar truss ($\lambda/\lambda_b = 0.5$).

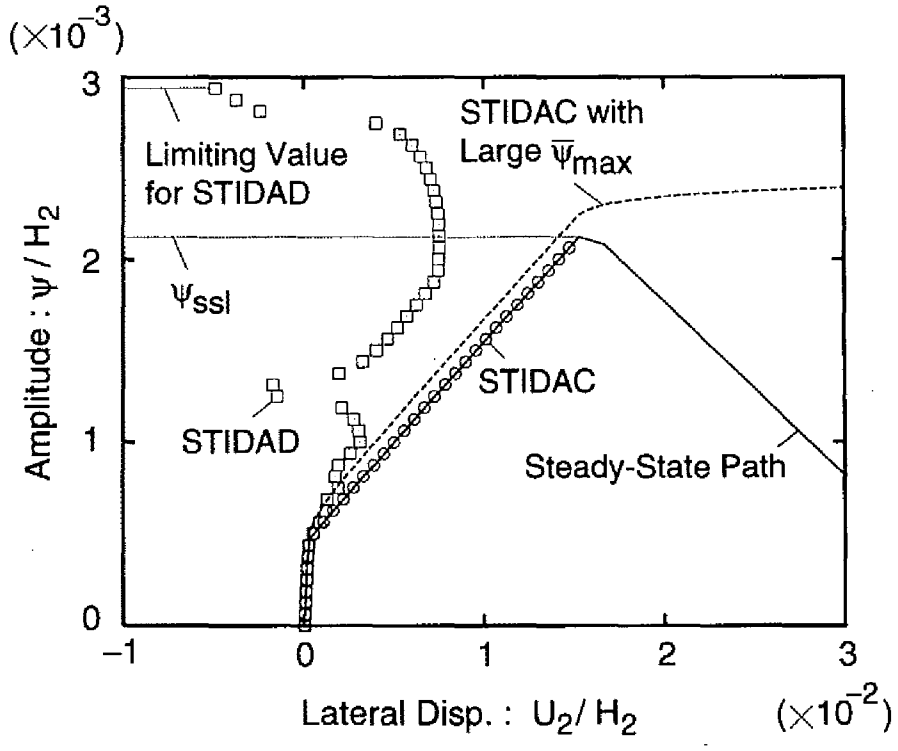

Figure 2.15: Path dependence of U_1^I on loading history for the ten-bar trusses ($\lambda/\lambda_b = 0.85$).

dependence on loading history of the limiting value that bounds convergence and divergence. In the figure, U_2 is the displacement of node 5 for X_1 direction. The solid line indicates the steady-state path. The dashed line shows the variation of U_2^{I} with respect to ψ under STIDAC program with $\Delta\bar{\psi} = 0.001\psi_{ssl}$ and a sufficiently large value of $\bar{\psi}_{max}$. The circular symbols plot U_2^{I} in the steady states under the STIDAC programs with $\Delta\bar{\psi} = 0.001\psi_{ssl}$ and various values of $\bar{\psi}_{max}$. The square symbols indicate U_2^{I} after convergence under the STIDAD programs with the values of $\bar{\psi}$ corresponding to the values of $\bar{\psi}_{max}$. Good agreement between the steady-state path and the circular points demonstrates the validity of the hypotheses (H2*) and (H3*).

2.6 CONCLUSIONS

A new method has been presented for predicting the steady-state limit of elastoplastic trusses subjected to quasi-static cyclic loads in the presence of constant loads. By applying the proposed method, we can find the steady-state limit of arbitrary shaped frames with truss and/or fiber elements. In the proposed method, there is no need for tracing the transient process between consecutive steady states, and no parametric analysis is needed for finding the steady-state limit. The proposed method is therefore much more efficient than the conventional methods for numerical response analysis.

Through the numerical examples, the following conclusions have been obtained:

1. Good agreement is observed between the results of the steady-state limit analysis and those of the conventional response analysis when the loading conditions for these analyses are close.
2. The limiting values below which elastic shakedown occurs depend on the loading history. Obviously, Melan-type or path-independent shakedown criterion cannot be extended to such cases.
3. The steady-state limits, defined under an idealized cyclic loading program with continuously increasing amplitude, provide lower bounds for the limiting values obtained by the response analysis performed under the two typical and realistic cyclic loading programs.

Appendix A. Formulation with Higher-Order Derivatives

A formulation with higher-order derivatives is presented for the steady-state limit analysis. By using the higher-order derivatives, terminal points of incremental steps can be found with the desired accuracy. We derive here only the second-order derivatives for brevity. But the higher-order derivatives can be obtained similarly.

Differentiation of the rate equations (2.21)-(2.28) with respect to the steady-state path parameter τ yields the second-order perturbation equations as follows:

$$\ddot{\varepsilon}^{\mathrm{I}} = \frac{\partial\, \varepsilon^{\mathrm{I}}}{\partial\, u_i{}^{\mathrm{I}}}\ddot{u}_i^{\mathrm{I}} + \frac{\partial^2\, \varepsilon^{\mathrm{I}}}{\partial\, u_i{}^{\mathrm{I}}\, \partial\, u_j{}^{\mathrm{I}}}\dot{u}_i^{\mathrm{I}}\dot{u}_j^{\mathrm{I}} \tag{2.43}$$

for the compatibility conditions,

$$\ddot{f}_i^{\mathrm{I}} = AL_0\left\{\ddot{\sigma}^{\mathrm{I}}\frac{\partial\, \varepsilon^{\mathrm{I}}}{\partial\, u_i^{\mathrm{I}}} + \sigma^{\mathrm{I}}\frac{\partial^2\, \varepsilon^{\mathrm{I}}}{\partial\, u_i{}^{\mathrm{I}}\, \partial\, u_j{}^{\mathrm{I}}}\ddot{u}_j^{\mathrm{I}} + 2\dot{\sigma}^{\mathrm{I}}\frac{\partial^2\, \varepsilon^{\mathrm{I}}}{\partial\, u_i{}^{\mathrm{I}}\, \partial\, u_j{}^{\mathrm{I}}}\dot{u}_j^{\mathrm{I}}\right\} \tag{2.44}$$

for the equilibrium conditions, and

$$\ddot{\sigma}^{\mathrm{I}} = C^{\mathrm{II}}\ddot{\varepsilon}^{\mathrm{I}} + C^{\mathrm{III}}\ddot{\varepsilon}^{\mathrm{II}} \tag{2.45}$$

for the stress-strain relations. Note that $\dot{C}^{\mathrm{II}} = \dot{C}^{\mathrm{III}} = 0$ because the bi-linear constitutive relation is assumed.

From Eqs. (2.43)-(2.45), we have the second-order perturbation equations for each element

$$\ddot{f}_i^{\mathrm{I}} = k_{ij}^{\mathrm{II}}\ddot{u}_j^{\mathrm{I}} + k_{ij}^{\mathrm{III}}\ddot{u}_j^{\mathrm{II}} + \hat{f}_i^{\mathrm{I}}, \tag{2.46}$$

$$\hat{f}_i^{\mathrm{I}} = AL_0\frac{\partial\, \varepsilon^{\mathrm{I}}}{\partial\, u_i^{\mathrm{I}}}\left(C^{\mathrm{II}}\frac{\partial^2\, \varepsilon^{\mathrm{I}}}{\partial\, u_j{}^{\mathrm{I}}\, \partial\, u_k{}^{\mathrm{I}}}\dot{u}_j^{\mathrm{I}}\dot{u}_k^{\mathrm{I}} + C^{\mathrm{III}}\frac{\partial^2\, \varepsilon^{\mathrm{II}}}{\partial\, u_j{}^{\mathrm{II}}\, \partial\, u_k{}^{\mathrm{II}}}\dot{u}_j^{\mathrm{II}}\dot{u}_k^{\mathrm{II}}\right) \tag{2.47}$$

$$+2AL_0\dot{\sigma}^{\mathrm{I}}\frac{\partial^2\, \varepsilon^{\mathrm{I}}}{\partial\, u_i{}^{\mathrm{I}}\, \partial\, u_j{}^{\mathrm{I}}}\dot{u}_j^{\mathrm{I}}$$

in which a hat indicates the variables expressed in terms of the first-order derivatives. Note that the coefficients k_{ij}^{II} and k_{ij}^{III} are identical to those in Eq. (2.29). We have the perturbation equations for the Γ^{II} state by replacing the superscripts I and II with II and I, respectively. Assembling the perturbation equations for the elements leads to the second-order perturbation equations for the total system

$$\ddot{\mathbf{F}}^{\mathrm{I}} = \mathbf{K}^{\mathrm{II}}\ddot{\mathbf{U}}^{\mathrm{I}} + \mathbf{K}^{\mathrm{III}}\ddot{\mathbf{U}}^{\mathrm{II}} + \hat{\mathbf{F}}^{\mathrm{I}}, \tag{2.48}$$

$$\ddot{\mathbf{F}}^{\mathrm{II}} = \mathbf{K}^{\mathrm{III}}\ddot{\mathbf{U}}^{\mathrm{I}} + \mathbf{K}^{\mathrm{III}}\ddot{\mathbf{U}}^{\mathrm{II}} + \hat{\mathbf{F}}^{\mathrm{II}}. \tag{2.49}$$

Note again that the coefficient matrices are same as those in the rate equations (2.35) and (2.36). These $2 \times 3N$ simultaneous linear equations (2.48) and (2.49) are to be solved using the boundary conditions after the value of $\ddot{\psi}$ is specified.

When the derivatives are employed up to the second order, the termination conditions Eqs. (2.37)-(2.39) of the incremental step become quadratic equations of the step length $\Delta\tau$, while the conditions are linear equations when only the first derivatives are used. Besides these termination conditions, we must consider the conditions

$$\dot{\varepsilon}^t(\tau_{h+1}) = \dot{\varepsilon}^t(\tau_h) + \ddot{\varepsilon}^t(\tau_h)\Delta\tau = 0, \tag{2.50}$$

$$\dot{\varepsilon}^c(\tau_{h+1}) = \dot{\varepsilon}^c(\tau_h) + \ddot{\varepsilon}^c(\tau_h)\Delta\tau = 0 \tag{2.51}$$

for the transitions T $\rightarrow$ E and C $\rightarrow$ E, respectively. Note that, by using the higher-order terms, we do not have to find the consistent set of stress rate-strain rate relations as far as no discontinuous change occurs in the derivatives with respect to τ. But, if the discontinuous change occurs, e.g. types of the cyclic stress-strain response changes, the consistent set should be found at the moment.

Substituting the step length and the derivatives up to the second order into Eqs. (2.16)-(2.20), we obtain the values of the state variables at $\tau = \tau_{h+1}$.

Appendix B. Formulation and Convergence Criteria for Response Analysis

As a solution method for the response analysis, the incremental perturbation method [26] is used in this chapter. In this method, the equilibrium path is traced using the higher-order derivatives up to the desired order with respect to the equilibrium path parameter t. Hence yielding and unloading can be predicted with the desired accuracy.

Differentiating the kinematic relations (2.1)-(2.3), we obtain the following equations

$$\varepsilon' = \frac{\partial\, \varepsilon}{\partial\, u_i} u_i' \tag{2.52}$$

where prime indicates partial differentiation with respect to t. The equilibrium condition is written as

$$f_i' = AL_0 \left(\sigma' \frac{\partial\, \varepsilon}{\partial\, u_i} + \sigma \frac{\partial^2\, \varepsilon}{\partial\, u_i\, \partial\, u_j} u_j' \right). \tag{2.53}$$

The constitutive relations is expressed as

$$\sigma' = C\varepsilon' \tag{2.54}$$

in which

$$C = E \qquad \text{in the elastic range,} \tag{2.55}$$

$$C = E_t,\ \varepsilon' \geq 0 \qquad \text{for the loading response in tension,} \tag{2.56}$$

$$C = E,\ \varepsilon' < 0 \qquad \text{for the unloading response in tension,} \tag{2.57}$$

$$C = E_t,\ \varepsilon' \leq 0 \qquad \text{for the loading response in compression,} \tag{2.58}$$

$$C = E,\ \varepsilon' > 0 \qquad \text{for the unloading response in compression.} \tag{2.59}$$

Differentiating Eq. (2.5) with respect to t, we have the equations for each element

$$f_i' = k_{ij} u_j', \tag{2.60}$$

$$k_{ij} = C \frac{\partial\, \varepsilon}{\partial\, u_i} \frac{\partial\, \varepsilon}{\partial\, u_j} + \sigma \frac{\partial^2\, \varepsilon}{\partial\, u_i\, \partial\, u_j}. \tag{2.61}$$

By assembling the equations for each element, we obtain the equations for the total system as

$$\mathbf{F}' = \mathbf{K}\mathbf{U}'. \tag{2.62}$$

Note that we should find the set of tangent stiffnesses that are consistent with the resulting signs of $\mathbf{F}'$. Differentiating Eqs. (2.52)-(2.62), higher-order perturbation equations are derived. Solving the perturbation equations, we obtain the higher-order derivatives. An increment is terminated when yielding, unloading or load reversal occurs. In addition, the step length Δt is kept smaller than the maximum allowable value $\Delta \bar{t}_{max}$ specified for preventing excessive accumulation of the truncation errors. Repeating these procedures, the equilibrium path is traced step by step.

In the numerical examples, the higher-order terms are employed up to the second order. The response is regarded to be divergent if buckling occurs or if one of the absolute maximum value of $\mathbf{U}$ exceeds the specified value $\bar{U}_{max}$. On the other hand, the response is judged to be convergent when the following condition is satisfied.

$$\max \left| \frac{U_{n(l+1)} - U_{n(l)}}{U_{n(l)}} \right| < \bar{e} \quad (n = 1, 2, \cdots, 3N) \tag{2.63}$$

where U_n is the nth component of $\mathbf{U}$, subscript l indicates the number of cycles and $\bar{e}$ is the specified value of the relative error. These values are set to be $\bar{U}_{max}$ =5cm, $\Delta \bar{t}_{max}$ =0.001 , and $\bar{e} = 1 \times 10^{-4}$ for the two-bar truss, and $\bar{U}_{max}$ =80cm, $\Delta \bar{t}_{max}$ =0.2 , and $\bar{e} = 1 \times 10^{-6}$ for the ten-bar truss.

Nomenclature

The following symbols are used in this chapter:

A initial cross sectional area;

C coefficient of ε';

$C^{tt}, C^{tc}, C^{ct}, C^{cc}$ coefficients of $\dot{\varepsilon}^t$ and $\dot{\varepsilon}^c$;

$C^{\mathrm{II}}, C^{\mathrm{I\,II}}, C^{\mathrm{III}}, C^{\mathrm{III}}$ coefficients of $\dot{\varepsilon}^{\mathrm{I}}$ and $\dot{\varepsilon}^{\mathrm{II}}$;

E Young's modulus;

E_t tangent modulus after yielding;

$\mathbf{E}$ strain vector for total system;

$\mathbf{E}_p$ plastic strain vector for total system;

$\bar{e}$ specified value of relative error;

$\mathbf{F}$ nodal force vector for total system;

f_i nodal force;

H Height of truss;

$\mathbf{K}$ tangent stiffness matrix;

$\mathbf{K}^{\mathrm{II}}$ $\mathbf{K}^{\mathrm{I\,II}}$, $\mathbf{K}^{\mathrm{III}}$, $\mathbf{K}^{\mathrm{III}}$ coefficient matrices of $\dot{\mathbf{U}}^{\mathrm{I}}$ and $\dot{\mathbf{U}}^{\mathrm{II}}$;

k_{ij} coefficient of u'_j;

k_{ij}^{II} $k_{ij}^{\mathrm{I\,II}}$, k_{ij}^{III}, k_{ij}^{III} coefficients of $\dot{u}_j^{\mathrm{I}}$ and $\dot{u}_j^{\mathrm{II}}$;

L current length;

L_0 initial length;

M number of elements;

N number of nodes;

$\bar{\mathbf{P}}_0$ constant vector for constant loads;

$\bar{\mathbf{P}}_c$ constant vector for cyclic load;

$\mathbf{S}$ stress vector for total system;

t equilibrium path parameter;

$\mathbf{U}$ nodal displacement vector for total system;

$\bar{U}_{max}$ maximum allowable value of U_n;

$U_{n(l)}$ nth component of $\mathbf{U}$ at lth cycle;

u_i nodal displacement;

V initial volume;

x_i current position of nodes;

x_i^0 initial position of nodes;

ε Green-Lagrangian strain;

ε_p plastic strain;

λ_0 load factor for constant load;

λ_b load factor at initial buckling load;

λ_c load factor for cyclic loads;

λ_y load factor at initial yielding load;

σ second Piola-Kirchhoff stress;

σ_y initial tensile yield stress;

$\bar{\sigma}_y$ $\bar{\sigma}_y = (1 - E_t/E)\sigma_y$;

σ_{yc} subsequent yield stress in compression;

σ_{yt} subsequent yield stress in tension;

τ steady-state path parameter;

τ_h τ at h step;

Δt increment of equilibrium path parameter;

$\Delta \bar{t}_{max}$ maximum allowable value of Δt;

$\Delta\tau$ increment of steady-state path parameter;

$\Delta \bar{\tau}_{max}$ maximum allowable value of $\Delta\tau$;

$\Delta\psi$ increment of amplitude;

$\Delta\bar{\psi}$ specified increment of amplitude for STIDAC program;

$\delta\varepsilon$ virtual strain;

δu_i virtual nodal displacement;

ψ amplitude of λ_c;

ψ_{ssl} amplitude at steady-state limit;

$\bar{\psi}$ constant amplitude for STIDAD program; and

$\bar{\psi}_{max}$ maximum amplitude for STIDAC program.

Superscripts

t variables for the equilibrium states at strain reversals in tension;

c variables for the equilibrium states at strain reversals in compression;

I variables for the equilibrium states at $\lambda_c = \psi$; and

II variables for the equilibrium states at $\lambda_c = -\psi$.

Signs

$\dot{(\ )}$ derivatives with respect to τ;

$\ddot{(\ )}$ second order derivatives with respect to τ;

$\hat{(\ )}$ quantities expressed with first-order derivatives with respect to τ; and

$(\ )'$ derivatives with respect to t.

References

[1] K. Uetani and T. Nakamura. Symmetry limit theory for cantilever beam-columns subjected to cyclic reversed bending. *Journal of the Mechanics and Physics of Solids*, 31(6):449–484, 1983.

[2] K. Uetani. *Symmetry Limit Theory and Steady-State Limit Theory for Elastic-Plastic Beam-Columns Subjected to Repeated Alternating Bending.* PhD thesis, Kyoto University, 1984. (in Japanese).

[3] K. Uetani. Uniqueness criterion for incremental variation of steady state and symmetry limit. *Journal of the Mechanics and Physics of Solids*, 37(4):495–514, 1989.

[4] F. R. Shanley. Inelastic column theory. *Journal of Aeronautical Sciences*, 14:261–268, 1947.

[5] R. Hill. A general theory of uniqueness and stability in elastic-plastic solids. *Journal of the Mechanics and Physics of Solids*, 6:236–249, 1958.

[6] W. T. Koiter. General theorems for elastic-plastic structures. In J. N. Sneddon and R. Hill, editors, *Progress in Solid Mechanics*, volume 1, pages 167–221, North Holland, Amsterdam, 1960.

[7] J. A. König. *Shakedown of Elastic-Plastic Structures.* Elsevier, Amsterdam, 1987.

[8] G. Maier. A shakedown matrix theory allowing for workhardening and second-order geometric effects. In A. Sawczuk, editor, *Foundations of plasticity*, volume 1, pages 417–433, Noordhoff, Leyden, 1972.

[9] Q. S. Nguyen, G. Gary, and G. Baylac. Interaction buckling-progressive deformation. *Nuclear Engineering and Design*, 75:235–243, 1983.

[10] A. Siemaszko and J. A. König. Analysis of stability of incremental collapse of skeletal structures. *Journal of Structural Mechanics*, 13:301–321, 1985.

[11] D. Weichert. On the influence of geometrical nonlinearities on the shakedown of elastic-plastic structures. *International Journal of Plasticity*, 2:135–148, 1986.

[12] J. Gross-Weege. A unified formulation of statical shakedown criteria for geometrically nonlinear problems. *International Journal of Plasticity*, 6:433–447, 1990.

[13] S. Pycko and J. A. König. Steady plastic cycles on reference configuration in the presence of second-order geometric effects. *European Journal of Mechanics. A, Solids*, 10(6), 1991.

[14] H. Stumpf. Theoretical and computational aspects in the shakedown analysis of finite elastoplasticity. *International Journal of Plasticity*, pages 583–602, 1993.

[15] Z. Mroz, D. Weichert, and S. Dorosz, editors. *Inelastic Behavior of Structures under Variable Loads.* Kluwer Academic Publishers, Netherlands, 1995.

[16] C. Polizzotto and G. Borio. Shakedown and steady-state responses of elastic-plastic solids in large displacements. *International Journal of Solids and Structures*, 33:3415–3437, 1996.

[17] K. Morisako, K. Uetani, and S. Ishida. Analysis of collapse behavior of 2-story 1-bay planar frames subjected to repeated lateral loading under gravity loads. *Journal of Structural Engineering*, 38B:531–536, 1992. (in Japanese).

[18] G. Maier, L. G. Pan, and U. Perego. Geometric effects on shakedown and ratchetting of axisymmetric cylindrical shells subjected to variable thermal loading. *Engineering Structures*, 15:453–465, 1993.

[19] K. Uetani. Cyclic plastic collapse of steel planar frames. In Y. Fukumoto and Lee G, editors, *Stability and Ductility of Steel Structures under Cyclic loading*, pages 261–271. CRC press, 1992.

[20] K. J. Bathe, E. Ramm, and E. L. Wilson. Finite element formulations for large deformation dynamic analysis. *International Journal for Numerical Methods in Engineering*, 9:353–386, 1975.

[21] K. Washizu. *Variational Method in Elasticity and Plasticity*, chapter 16 Two incremental theories for a solid-body problem with geometrical and material nonlinearities, pages 456–474. Pergamon press, third edition, 1982.

[22] M. A. Crisfield. *Non-linear Finite Element Analysis of Solids and Structures*, volume 1. John Wiley & Sons, New York, 1991.

[23] K. J. Bathe. *Finite Element Procedures.* Prentice Hall, New Jersey, 1996.

[24] J. C. Simo and R. L. Taylor. Consistent tangent operators for rate-independent elastoplasticity. *Computer Methods in Applied Mechanics and Engineering*, 22:649–670, 1985.

[25] M. A. Crisfield. *Non-linear Finite Element Analysis of Solids and Structures*, volume 2. John Wiley & Sons, New York, 1997.

[26] Y. Yokoo, T. Nakamura, and K. Uetani. The incremental perturbation method for large displacement analysis of elastic-plastic structures. *International Journal for Numerical Methods in Engineering*, 10:503–525, 1976.

[27] P. Z. Bazant and L. Cedolin. *Stability of Structures.* Oxford University Press, New York, 1991.

Chapter 3

Steady-State Limit for Plastic Shakedown Region

3.1 INTRODUCTION

When structures are subjected to initial constant loads and additive quasi-static cyclic loads, their responses are classified into the following three types (see for instance [1, 2, 3, 4]): (1) Convergent behavior to *elastic shakedown* or *classical shakedown*, which is a cyclic and fully elastic response after some histories of plastic deformations; (2) Convergent behavior to *plastic shakedown* or *alternating plasticity*, where structures behave cyclically but plastic deformations are included in the steady cycle; and (3) *ratchetting* or *incremental collapse*, in which no convergence is observed to the elastic or plastic shakedown state. If excessive deformations are induced by the ratchetting, total or local buckling may occur (see e.g. [5, 6, 7, 8]). Including such cases, as defined in the last chapter, the phenomena characterized by the unbounded growth of plastic deformations is referred to as *cyclic instability*. The classification of the types of responses are schematically illustrated in the plane of the loading combinations (Fig. 3.1), where ψ and λ_0 indicate the amplitude of the cyclic loads and the

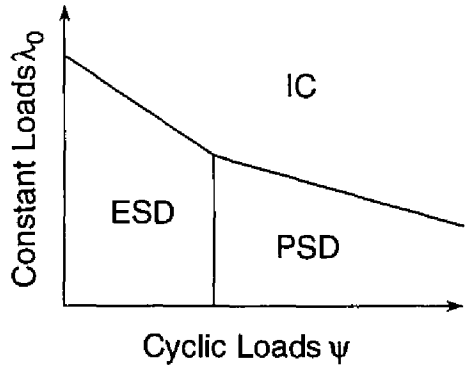

Figure 3.1: Classification of structural responses in the plane of loading combination.

magnitude of the constant loads, respectively. The regions in which the elastic shakedown and the plastic shakedown take place are called respectively the elastic shakedown region and the plastic shakedown region.

To design structures subjected to cyclic loads, one should obtain the boundary between the shakedown regions and the region where cyclic instability occurs. For this purpose, a number of studies have been conducted on the structural responses under cyclic loading. The approaches employed in the studies are roughly classified in the following two categories: one is to trace all loading histories and the other is to predict the boundary theoretically without tracing the loading histories.

To investigate the elastoplastic responses and to bound convergence and divergence of plastic deformations, a direct but elaborating approach is to trace all the loading histories of the structures. Experimental, analytical, and numerical methods are available to this end [3]. By tracing all the loading histories, we can observe the process of deformations and bound the loading conditions below which the structures behave in a stable manner. Nonetheless, generally, analytical methods can be applied only to very simple models. And experimental and numerical approaches require a number of parametric analyses to bound the structural responses. Moreover, it is very difficult to derive theoretical conditions similar to the Euler buckling load from the parametric analyses

To obtain the theoretical condition below which the elastic shakedown occurs, numerous papers have been published on the *shakedown theory* [1, 4]. The classical shakedown is extended in several papers [9, 10, 11, 12] to derive the condition below which plastic shakedown occurs. But only a little research [5, 13] has been made to derive the conditions that bounds the plastic shakedown and the cyclic instability taking the geometrical nonlinearity into account. Furthermore, the path-independent shakedown theories are not promising when strong influence of geometrical nonlinearity exists because the responses are inherently path-dependent in such cases.

To overcome these difficulties, the steady-state limit theory was proposed by Uetani [14, 15] for cantilever beam-columns. Under cyclic bending with stepwisely increasing amplitude in the presence of a certain compressive axial force, a beam-column exhibits convergence to steady states before the amplitude reaches a limit, and, after the limit, the beam-column will no longer exhibit any convergence. This limit is called the *steady-state limit* [7, 14]. With the steady-state limit theory, though under a specified loading history, the steady-state limit can be predicted as a theoretical critical point even if the strong effect of the geometrical nonlinearity exist. In the previous chapter, based on the steady-state limit

theory for cantilever beam-columns, a method has been presented for finding the steady-state limit of trusses that bounds the elastic shakedown and the cyclic instability. But several cases have been observed in which the method fail to find the steady-state limit that bounds plastic shakedown and cyclic instability.

The purpose of this chapter is to present a method for predicting the steady-state limit for the plastic shakedown region. For brevity, the method presented in the previous chapter is simply called the previous method throughout this chapter. In this chapter, first, properties of the structural responses with the plastic shakedown are studied to clarify the reason why the previous method fail to find the steady-state limit when the plastic shakedown takes place. In the study, our attention is focused on the validity of the hypothesis on strain reversals employed in the previous method. Then, on the basis of the reason made clear, the hypothesis on strain reversals is extended and fundamental concepts are outlined. Second, incremental relations for variation of a steady state are formulated with respect to the variation of the amplitude of the cyclic loads. Finally, validity of the proposed method is demonstrated through numerical examples.

3.2 GOVERNING EQUATIONS

3.2.1 Analytical Model

Consider pin-jointed space trusses with M elements and N nodes. Buckling of the element is ruled out but that of a global type is taken into account using the Total Lagrangian formulation. Under the assumption of large displacement-small strain, compatibility conditions

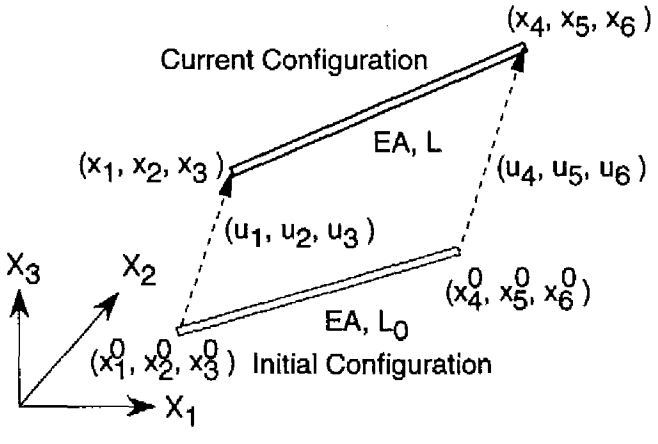

Figure 3.2: A truss element.

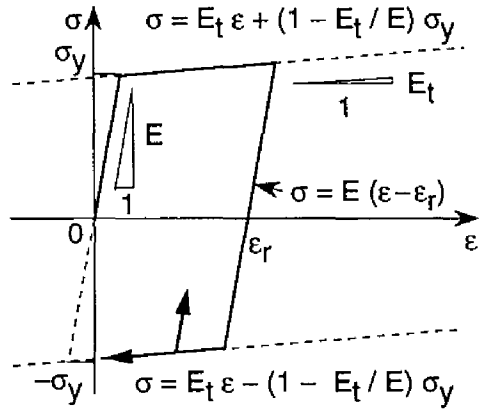

Figure 3.3: A bi-linear kinematic hardening rule.

for an element illustrated in Fig. 3.2 are given by

$$\varepsilon = \frac{L^2 - L_0^2}{2L_0^2}, \tag{3.1}$$

$$L^2 = (x_4 - x_1)^2 + (x_5 - x_2)^2 + (x_6 - x_3)^2, \tag{3.2}$$

$$x_i = x_i^0 + u_i; \qquad i = 1, \cdots, 6 \tag{3.3}$$

where ε is the Green-Lagrangian strain, L and L_0 are the current length and the initial length of the element, respectively, u_i is the nodal displacement, and x_i and x_i^0 indicate the current position and the initial position of the nodes at the two ends, respectively. For equilibrium, we require

$$f_i = AL_0\sigma\frac{\partial\,\varepsilon}{\partial\,u_i} \tag{3.4}$$

in which f_i is the nodal force, A is the cross sectional area, and σ is the second Piola-Kirchhoff stress. By assembling the equilibrium equation (3.4) for the element, we have the equilibrium equations for the total system.

As a constitutive model, we employ a bi-linear kinematic hardening rule shown in Fig. 3.3. Let E, E_t, σ_y and ε_p indicate the Young's modulus, the tangent modulus after yielding, the initial yield stress and plastic strain, respectively Then the constitutive law is expressed as follows:

$$\sigma = E(\varepsilon - \varepsilon_p) \qquad \text{in the elastic and unloading ranges,} \tag{3.5}$$

$$\sigma = E_t\varepsilon + \bar{\sigma}_y \qquad \text{for the plastic loading in tension,} \tag{3.6}$$

$$\sigma = E_t\varepsilon - \bar{\sigma}_y \qquad \text{for the plastic loading in compression} \tag{3.7}$$

where $\bar{\sigma}_y = (1 - E_t/E)\sigma_y$. Let σ_{yt} and σ_{yc} denote the subsequent yield stresses in tension and compression, respectively. Then the subsequent yield stresses are expressed in terms of the plastic strains as

$$\sigma_{yt} = \frac{EE_t}{E - E_t}\varepsilon_p + \sigma_y, \tag{3.8}$$

$$\sigma_{yc} = \frac{EE_t}{E - E_t}\varepsilon_p - \sigma_y. \tag{3.9}$$

3.2.2 Loading Conditions

The trusses are subjected to initial constant loads $\lambda_0\bar{\mathbf{P}}_0$ and subsequent cyclic loads $\lambda_c\bar{\mathbf{P}}_c$. Here, λ and $\bar{\mathbf{P}}$ denote the load factor and the constant vector, respectively. The subscripts 0 and c indicate the variables refer to the constant loads and the cyclic loads, respectively. External forces and/or forced displacements are applied as the external loads. In other words, according to the boundary conditions, one of the nodal force and the nodal displacement components is given as external loads for every degree of freedom.

The load factor λ_c is varied between the maximum value $\lambda_c^{\mathrm{I}} = \psi$ and the minimum value $\lambda_c^{\mathrm{II}} = -\psi$ in a cycle, where ψ denotes the amplitude of λ_c. Variation of λ_c is defined by a monotonically increasing parameter t, called equilibrium path parameter. The equilibrium states at which $\lambda_c = \lambda_c^{\mathrm{I}}$ and $\lambda_c = \lambda_c^{\mathrm{II}}$ are called Γ^{I} state and Γ^{II} state, respectively. The superscripts I and II indicate that the state variables, such as stresses, strains and displacements, refer to those for Γ^{I} and Γ^{II}, respectively.

3.2.3 Steady-State Responses in Stress-Strain Plane

For later formulation, we classify all the possible types of the steady-state responses. The calcification is schematically shown in Fig. 3.4. The superscripts t and c indicate the

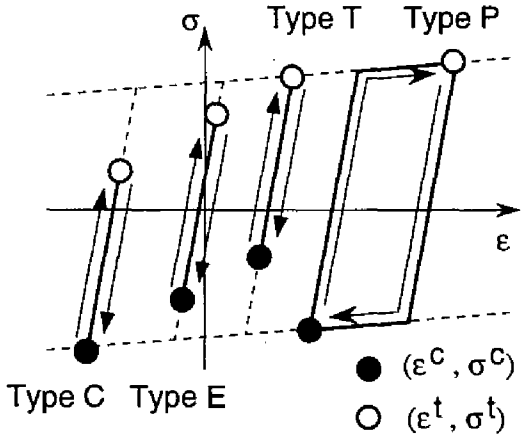

Figure 3.4: Possible classification of cyclic responses.

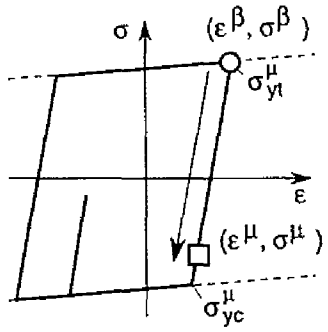

Figure 3.5: Relation between Γ^μ and Γ^β.

state variables belonging to the equilibrium states at which strain take its maximum and minimum values in a cycle, respectively. The type E is the elastic shakedown state in elastic region. The type T is the elastic shakedown state whose maximum stress reaches the strain hardening line in tension. The type C is the elastic shakedown state whose minimum stress reaches the strain hardening line in compression. The type P is the plastic shakedown state. Throughout this chapter, the elements exhibiting the types E, C, T and P are called E element, C element, T element and P element, respectively.

Let the superscript μ indicate the state variables for an arbitrary equilibrium state Γ^μ in a steady state. And let the superscript β indicate the variables for the equilibrium states at which the last unloading occurs before $t = t^\mu$. According to the types of the cyclic responses, we can express the stress σ^μ in terms of the strains ε^μ, ε^t, ε^c and ε^β as follows:

$$\text{type E: } \sigma^\mu = E(\varepsilon^\mu - \varepsilon_p^\mu), \tag{3.10}$$

$$\text{type T: } \sigma^\mu = E_t\varepsilon^\mu + \bar{\sigma}_y, \qquad \text{if } \sigma^\mu = \sigma^t, \tag{3.11}$$

$$\sigma^\mu = E\varepsilon^\mu - (E - E_t)\varepsilon^t + \bar{\sigma}_y, \quad \text{if } \sigma^\mu \neq \sigma^t, \tag{3.12}$$

$$\text{type C: } \sigma^\mu = E\varepsilon^\mu - (E - E_t)\varepsilon^c + \bar{\sigma}_y, \quad \text{if } \sigma^\mu \neq \sigma^c, \tag{3.13}$$

$$\sigma^\mu = E_t\varepsilon^\mu - \bar{\sigma}_y, \qquad \text{if } \sigma^\mu = \sigma^c, \tag{3.14}$$

$$\text{type P: } \sigma^\mu = E_t\varepsilon^\mu + \bar{\sigma}_y, \qquad \text{if } \sigma^\mu = \sigma_{yt}^\mu, \tag{3.15}$$

$$\sigma^\mu = E_t\varepsilon^\mu - \bar{\sigma}_y, \qquad \text{if } \sigma^\mu = \sigma_{yc}^\mu, \tag{3.16}$$

$$\sigma^\mu = E\varepsilon^\mu - (E - E_t)\varepsilon^\beta + \bar{\sigma}_y, \quad \text{for } \sigma_{yc}^\mu < \sigma^\mu < \sigma_{yt}^\mu. \tag{3.17}$$

The relation between Γ^μ and Γ^β is shown in Fig. 3.5. Note that the plastic strain in Eq. (3.12) is eliminated using the relation $\varepsilon_p^\mu = \varepsilon_p^t$ The plastic strains are eliminated similarly in Eqs. (3.13) and (3.17).

3.3 PRELIMINARY CONSIDERATIONS

As mentioned in the introduction, the previous method for the elastic shakedown region may fail to find the steady-state limit when plastic shakedown occurs. In this section, first, the fundamental concepts and hypotheses of the previous method is summarized. Then numerical response analysis is performed for simple truss model to clarify the reason of the failure. In the study, our attention is focused on the validity of the hypothesis on strain reversals employed in the previous method. Second, more general consideration is made on strain reversals. Finally, key concepts are shown for finding the steady-state limit that bounds the plastic shakedown region and the region where cyclic instability occur.

3.3.1 Fundamental Concepts for Steady-State Limit Theory in Elastic Shakedown Region

The key concepts of the steady-state limit theory are summarized as follows:

1. A steady state is recognized as a point in a special space schematically illustrated in Fig. 3.6.
2. Under an idealized cyclic loading program with continuously increasing amplitude, variation of the point is recognized as a continuous path, called *steady-state path.*
3. The steady-state limit is found as the first limit point of the steady-sate path.

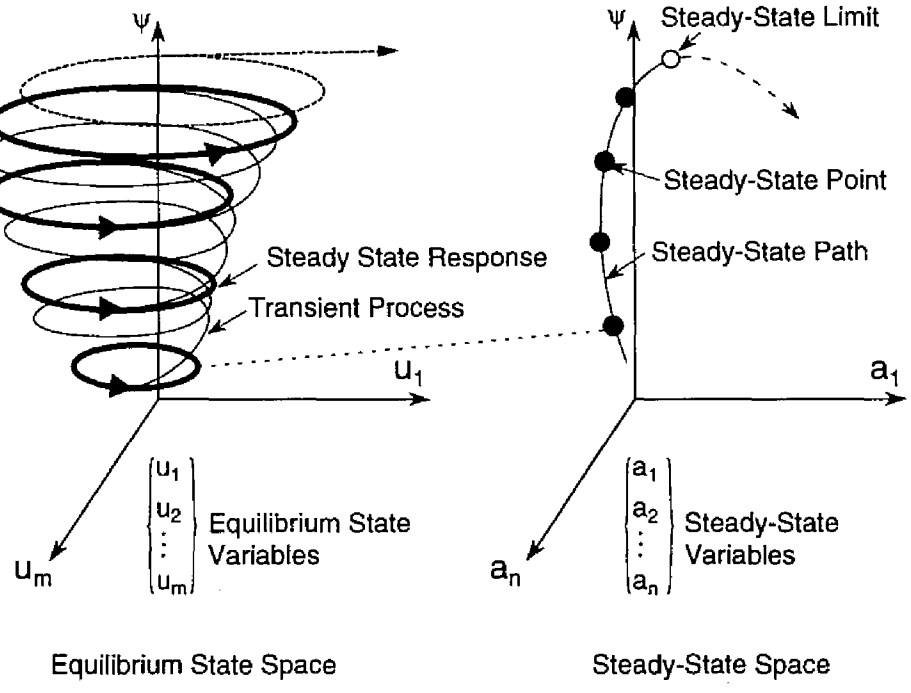

Figure 3.6: Fundamental concepts of steady-state limit theory.

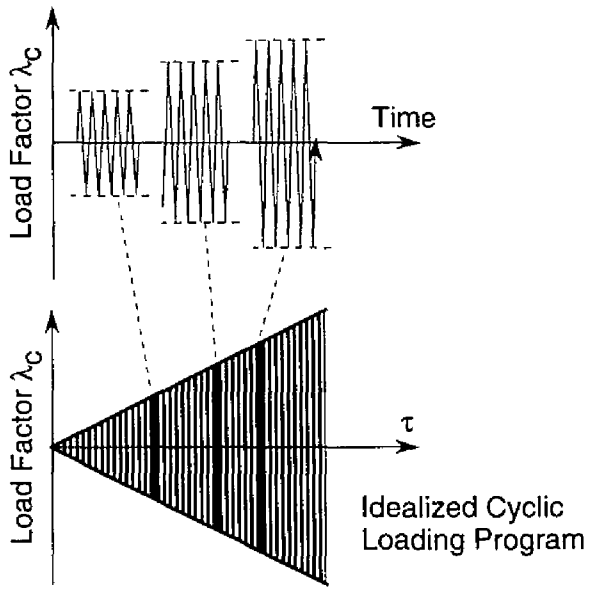

Figure 3.7: The idealized cyclic loading program.

Note that, in the idealized cyclic loading program, the loading cycle is repeated as many times as necessary for the trusses to converge to a steady state at each level of the amplitude as shown in Fig. 3.7. And variation of its amplitude is defined by a parameter τ. More rigorous definition of the idealized program is given in the previous chapter.

In the previous method, a steady state and its variation are formulated in terms of the state variables at load reversals based on the following hypotheses:

Hypothesis 2.1 All the state variables for Γ^{I} and Γ^{II} are continuous and piecewise differentiable functions of τ.

Hypothesis 2.2 For all elements, strain reversals occur only at Γ^{I} or Γ^{II}.

These hypotheses are the alternative ones for hypotheses 2 and 3 in the paper by Uetani [7, 14], respectively. Note that hypothesis 2.2 is applied not for the transient response but for the steady-state response after convergence.

3.3.2 Numerical Study on Strain Reversals

To clarify the reason why the previous method fails to find the steady-state limit for the plastic shakedown region, all loading history of a simple truss is traced by performing a conventional response analysis. The truss is shown in Fig. 3.8. Its elastic shakedown boundaries have been obtained in the previous chapter. The cross-sectional areas are $A_{(1)}$ = 1 cm^2 and $A_{(2)}$ = 2 cm^2. Material properties are $E = 1.961 \times 10^2$GPa, $E_t = 0.01E$,

$\sigma_y = 2.942 \times 10^2$MPa. The truss is subjected to the initial constant force $\lambda_0 \bar{F}_0$ and the additive forced displacement $\lambda_c \bar{U}_c$. Throughout all cycles, the amplitude ψ of the load factor λ_c is kept a constant value $\bar{\psi}$. The constants for the external loads are determined so that the loading condition lies in the plastic shakedown region: $\bar{\psi} = 0.13$, $\bar{F}_0 = 9.807 \times 10^3$N, $\bar{U}_c = 1$cm and $\lambda_0/\lambda_b = 0.375$, where $\lambda_b = 0.7477$ is the load factor at buckling in the sense of Hill [16] when only the initial loads are applied.

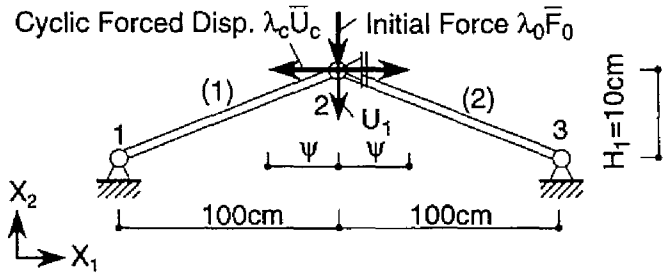

Figure 3.8: The two-bar truss.

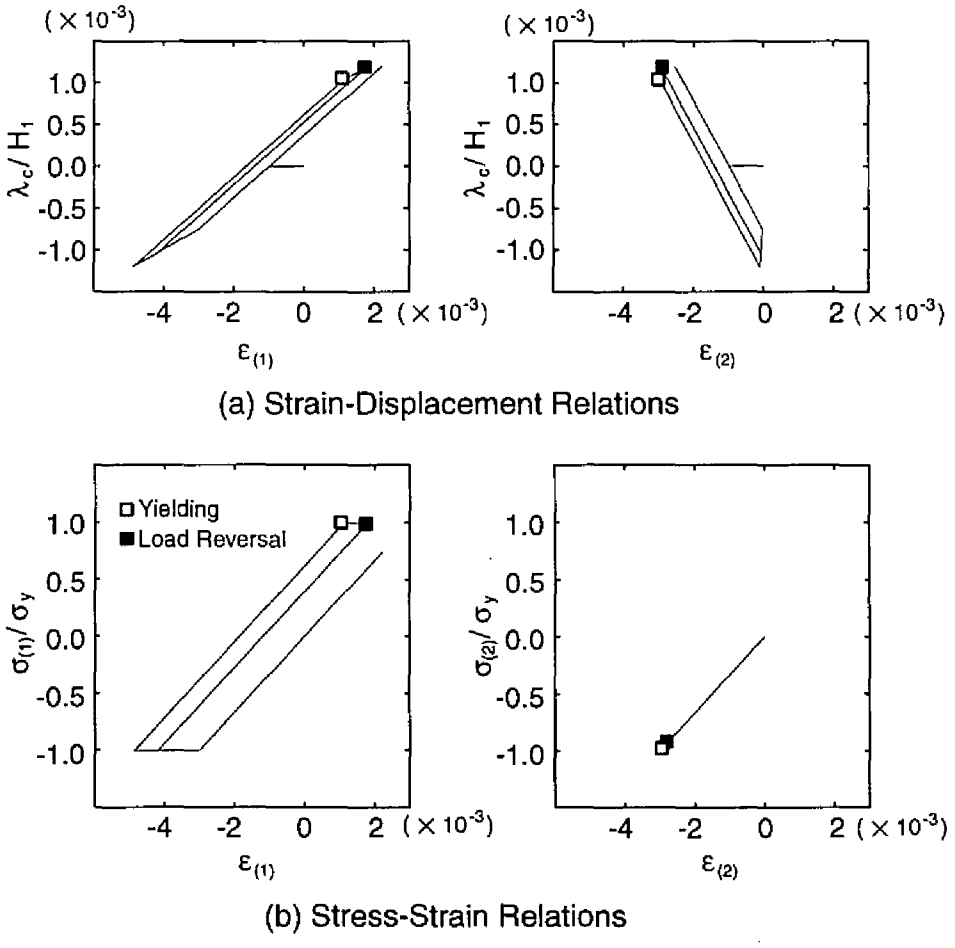

Figure 3.9: Strain-displacement relations and stress-strain relations.

Figure 3.9 (a) illustrate the strain-displacement relations. And Fig. 3.9 (b) depicts the stress-strain relations. From these figures, it is observed that strain reversals in the element 2 occur at the yielding points of the element 1 even after convergence. Namely, hypothesis 2.2 is disproved. This is considered to be the reason of the failure of the previous method to find the steady-state limit for the plastic shakedown region.

3.3.3 General Consideration on Strain Reversals

More general consideration is made on strain reversals. Let prime indicate differentiation with respect to the equilibrium path parameter t, and let C denote the tangent stiffness defined by $C = \sigma'/\varepsilon'$. Then all the possible reasons of strain reversals for the trusses considered in this paper are: (1) discontinuous change of λ_c', e.g. load reversals, (2) discontinuous change of C in other elements, for instance yielding and unloading, and (3) geometrical nonlinearity.

The cases (1) and (2) have been demonstrated in the last subsection. It is true the case (3) can occur, but the case (3) does not seem to occur frequently. Hence, in this chapter, our discussion is limited to the cases (1) and (2), and the case (3) is excluded.

3.3.4 Fundamental Concepts for Steady-State Limit Theory in Plastic Shakedown Region

The key concept of the steady-state limit theory for plastic shakedown region is to relax hypothesis 2.2 so that the strain reversals due to yielding is taken into account. For this purpose, hypotheses 2.1 and 2.2 are relaxed as follows:

Hypothesis 3.1 All the state variables for the equilibrium states at which load reversal or yielding occurs are continuous and piecewise differentiable functions of τ

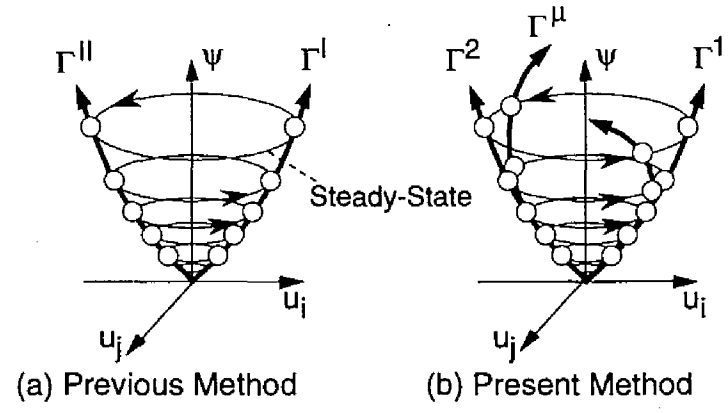

Figure 3.10: Key difference between the previous and the present methods.

Hypothesis 3.2 For all elements, strain reversals occur only at load reversals or at yielding of the elements exhibiting the plastic shakedown.

Similar to hypothesis 2.2, hypothesis 3.2 is applied not for the transient response but for the steady-states response after convergence.

Based on these relaxed hypothesis, a steady state is represented by the yielding points of the elements exhibiting the plastic shakedown in addition to the load-reversal points as shown in Fig. 3.10. That is, a steady state is described by the equilibrium states at which strain reversals occur. For brevity, these equilibrium states for expressing a steady state are called *representative equilibrium states* or RES in this chapter.

To sum up, the way of description of a steady state is the key difference between the previous and the present methods. Once a steady state is represented by the RES, similar to the previous method, the steady-state path is traced incrementally, and the steady-state limit is found as the first limit point of the steady-state path.

3.4 FORMULATION

3.4.1 Incremental Relations for Variation of Steady State

Consider a steady state at $\tau = \tau_h$ represented by J RES Γ^μ $(\mu = 1, 2, \cdots, J)$. Here, Γ^1 and Γ^2 are defined so that they correspond to Γ^{I} and Γ^{II}, respectively. When all the state variables for the RES are known in the current steady state at $\tau = \tau_h$, our problem is to find those in the neighboring steady state at $\tau = \tau_{h+1} = \tau_h + \Delta\tau$.

Let dot indicate the differentiation with respect to τ. Then, owing to hypothesis 3.1, the state variables at the neighboring steady state is expressed using Taylor-series expansion with respect to τ.

$$\mathbf{U}^\mu(\tau_{h+1}) = \mathbf{U}^\mu(\tau_h) + \dot{\mathbf{U}}^\mu(\tau_h)\Delta\tau + \frac{1}{2}\ddot{\mathbf{U}}^\mu(\tau_h)\Delta\tau^2 + \cdots, \tag{3.18}$$

$$\mathbf{F}^\mu(\tau_{h+1}) = \mathbf{F}^\mu(\tau_h) + \dot{\mathbf{F}}^\mu(\tau_h)\Delta\tau + \frac{1}{2}\ddot{\mathbf{F}}^\mu(\tau_h)\Delta\tau^2 + \cdots, \tag{3.19}$$

$$\mathbf{E}^\mu(\tau_{h+1}) = \mathbf{E}^\mu(\tau_h) + \dot{\mathbf{E}}^\mu(\tau_h)\Delta\tau + \frac{1}{2}\ddot{\mathbf{E}}^\mu(\tau_h)\Delta\tau^2 + \cdots, \tag{3.20}$$

$$\mathbf{E}_p^\mu(\tau_{h+1}) = \mathbf{E}_p^\mu(\tau_h) + \dot{\mathbf{E}}_p^\mu(\tau_h)\Delta\tau + \frac{1}{2}\ddot{\mathbf{E}}_p^\mu(\tau_h)\Delta\tau^2 + \cdots, \tag{3.21}$$

$$\mathbf{S}^\mu(\tau_{h+1}) = \mathbf{S}^\mu(\tau_h) + \dot{\mathbf{S}}^\mu(\tau_h)\Delta\tau + \frac{1}{2}\ddot{\mathbf{S}}^\mu(\tau_h)\Delta\tau^2 + \cdots \tag{3.22}$$

where $\mathbf{F}$ and $\mathbf{U}$ are the nodal force vector and the nodal displacements vector, respectively, with $3N$ components, and $\mathbf{E}$, $\mathbf{E}_p$ and $\mathbf{S}$ denote the strain vector, the plastic strain vector, and the stress vector, respectively, with M components.

To determine the state variables at the neighboring steady state, we should calculate the step length $\Delta\tau$ and the derivatives of the state variables with respect to τ. In the following subsections, the formulation for obtaining these variables are shown. For clarity and simplicity of presentation, we show the formulation in which only the first-order derivatives with respect to τ are used. But, for more accurate approximation, the formulation taking higher-order terms into account is presented in Appendix A.

3.4.2 Rate Forms of Governing Equations

To derive the rate forms of the governing equations, all the governing equations for Γ^μ are differentiated with respect to τ. Similar to the last chapter, the rate forms of the governing equations are simply called *rate equations*. Differentiating Eqs. (3.1)-(3.4), we have

$$\dot{\varepsilon}^\mu = \frac{\partial\, \varepsilon^\mu}{\partial\, u_i^\mu} \dot{u_i}^\mu, \tag{3.23}$$

$$\dot{f}_i^\mu = AL_0 \left(\dot{\sigma}^\mu \frac{\partial\, \varepsilon^\mu}{\partial\, u_i^\mu} + \sigma^\mu \frac{\partial^2\, \varepsilon^\mu}{\partial\, u_i^\mu\, \partial\, u_j^\mu} \dot{u}_j^\mu \right). \tag{3.24}$$

Suppose that for all the elements the superscripts corresponding to t and c are known. And assume that for all the elements all of the relations between μ and corresponding β are

Table 3.1: Stress rate-strain rate relations for the elements exhibiting elastic shakedown.

	E	T			C		
		$\dot{\varepsilon}^t \geq 0$		$\dot{\varepsilon}^t < 0$	$\dot{\varepsilon}^c \leq 0$		$\dot{\varepsilon}^c > 0$
		$\sigma^\mu = \sigma^t$	$\sigma^\mu \neq \sigma^t$		$\sigma^\mu = \sigma^c$	$\sigma^\mu \neq \sigma^c$	
$C^{\mu\mu}$	E	E_t	E	E	E_t	E	E
$C^{\mu t}$	0	0	$E_t - E$	0	0	0	0
$C^{\mu c}$	0	0	0	0	0	$E_t - E$	0

Table 3.2: Stress rate-strain rate relations for the elements exhibiting plastic shakedown.

	$\sigma^\mu = \sigma^\mu_{yt}$	$\sigma^\mu = \sigma^\mu_{yc}$	$\sigma^\mu_{yc} < \sigma^\mu < \sigma^\mu_{yt}$
$C^{\mu\mu}$	E_t	E_t	E
$C^{\mu\beta}$	0	0	$E_t - E$

known. Differentiating Eqs. (3.10)-(3.13), we have the stress rate-strain rate relations for the E, T and C elements. The rate relations are expressed as

$$\dot{\sigma}^\mu = C^{\mu\mu}\dot{\varepsilon}^\mu + C^{\mu t}\dot{\varepsilon}^t + C^{\mu c}\dot{\varepsilon}^c \tag{3.25}$$

where $C^{\mu\mu}$, $C^{\mu t}$ and $C^{\mu c}$ are the coefficients that are chosen according to Table 3.1. For the P elements, differentiation of Eqs. (3.15)-(3.17) leads to

$$\dot{\sigma}^\mu = C^{\mu\mu}\dot{\varepsilon}^\mu + C^{\mu\beta}\dot{\varepsilon}^\beta \tag{3.26}$$

in which $C^{\mu\mu}$ and $C^{\mu\beta}$ are the coefficients that are selected according to Table 3.2. After replacing the superscripts t, c and β with those indicating the corresponding RES, we can express the rate forms of stress-strain relations

$$\dot{\sigma}^\mu = \sum_{\nu=1}^{J} C^{\mu\nu}\dot{\varepsilon}^\nu \tag{3.27}$$

where $C^{\mu\nu}$ is the coefficient of the strain rates. Substituting Eqs. (3.23) and (3.27) into Eq. (3.24), we have the rate equations for element

$$\dot{f}_i^\mu = \sum_{\nu=1}^{J} k_{ij}^{\mu\nu}\dot{u}_j^\nu, \tag{3.28}$$

$$k_{ij}^{\mu\nu} = AL_0 \sum_{\nu=1}^{J} C^{\mu\nu}\frac{\partial\,\varepsilon^\mu}{\partial\,u_i^\mu}\frac{\partial\,\varepsilon^\nu}{\partial\,u_j^\nu} + AL_0\delta_{\mu\nu}\sigma^\mu\frac{\partial^2\,\varepsilon^\mu}{\partial\,u_i^\mu\,\partial\,u_j^\mu}$$

where $\delta_{\mu\nu}$ is the Kronecker's delta and $k_{ij}^{\mu\nu}$ is the coefficient relating $\dot{f}_i^\mu$ and $\dot{u}_j^\nu$. By assembling Eq. (3.28), the following rate equations are derived for the total system

$$\dot{\mathbf{F}}^\mu = \sum_{\nu=1}^{J} \mathbf{K}^{\mu\nu}\dot{\mathbf{U}}^\nu \tag{3.29}$$

where $\mathbf{K}^{\mu\nu}$ is coefficient matrix of $\dot{\mathbf{U}}^\nu$.

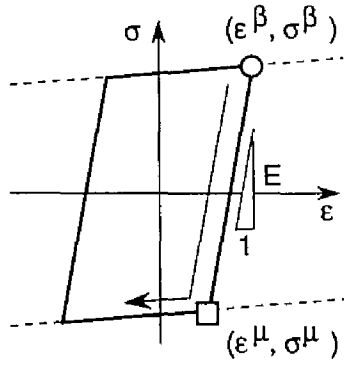

Figure 3.11: Γ^{μ} as an yielding point.

Now we have $J \times 3N$ equations that relates the rate vectors of the nodal forces and the nodal displacements. On the other hand, there are J unknowns of $\dot{\lambda}^{\mu}$ in addition to $J \times 3N$ unknown components of the rate vectors of the nodal forces and/or nodal displacements. Namely, we have $J \times (3N+1)$ unknowns. Consequently, additional J equations are apparently needed to solve the rate equations.

Assume that for all the RES Γ^{μ} ($\mu \geq 3$) the element whose yielding characterize Γ^{μ} are known. For the equilibrium states at load reversals, we have

$$\dot{\lambda}_c^1 = \dot{\lambda}_c^{\mathrm{I}} = \dot{\psi}, \tag{3.30}$$

$$\dot{\lambda}_c^2 = \dot{\lambda}_c^{\mathrm{II}} = -\dot{\psi} \tag{3.31}$$

which characterize the load reversals Γ^{I} and Γ^{II}. In contrast, the equilibrium states Γ^{μ} ($\mu \geq 3$) are characterized as the yielding point of the element exhibiting the plastic shakedown. Consider the case Γ^{μ} is characterized as the equilibrium state at which compressive yielding occurs as shown in Fig. 3.11. At the yielding point of the element whose yielding defines Γ^{μ}, both Eqs. (3.15) and (3.17) are satisfied. Hence we have

$$E(\varepsilon^{\mu} - \varepsilon^{\beta}) + 2\sigma_y = 0. \tag{3.32}$$

Differentiation of Eq. (3.32) yields the rate relation

$$\dot{\varepsilon}^{\mu} - \dot{\varepsilon}^{\beta} = 0. \tag{3.33}$$

The condition (3.33) is expressed in terms of the nodal displacements for the element as

$$\frac{\partial\, \varepsilon^{\mu}}{\partial\, u_i^{\mu}} \dot{u}_i^{\mu} - \frac{\partial\, \varepsilon^{\beta}}{\partial\, u_i^{\beta}} \dot{u}_i^{\beta} = 0. \tag{3.34}$$

The condition Eq. (3.34) can be rewritten in terms of the nodal displacement for the total system as

$$\mathbf{L}^{\mu}\dot{\mathbf{U}}^{\mu} + \mathbf{L}^{\beta}\dot{\mathbf{U}}^{\beta} = \mathbf{0} \tag{3.35}$$

where $\mathbf{L}$ is the coefficient matrix of $\dot{\mathbf{U}}$, and $\mathbf{0}$ is zero vector. The conditions that characterize the yielding in tension is derived similarly and is expressed in the same form of Eq. (3.35). After replacing the superscript β to that for the corresponding RES, we have $J-2$ equations in addition to Eqs. (3.30) and (3.31). Thus we have the same number of the equations as that of the unknowns. These equations are to be solved by specifying the value of $\dot{\psi}$ and by using the boundary conditions.

3.4.3 Consistent Set of Stress Rate-Strain Rate Relations

If an element exhibits type T or type C behavior, the coefficients of the strain rates should be chosen according to the signs of the strain rates as shown in Table 3.1. Therefore, for all the elements exhibiting the type T or the type C behavior, we should choose a set of the coefficients that are consistent with the signs of the resulting strain rates.

To find the consistent set of the coefficients, we employ a trial and error approach, which is also used in the conventional response analysis [17]. In the trial and error approach, first, the signs of the strain rates $\dot{\mathbf{E}}^{\mu}$ are assumed to be equal to those in the last step. Then, the coefficients $C^{\mu\mu}$, $C^{\mu t}$ and $C^{\mu c}$ are determined according to the assumptions, and the rate equations are constructed. After the rate equations are solved and $\dot{\mathbf{E}}^{\mu}$ are calculated, the consistency is checked between the assumed signs of the strain rates and the resulting ones for all the elements exhibiting the type T or the type C behavior. If the signs are not consistent, the assumed signs are reversed. This procedure is continued until all the resulting signs of the strain rates are consistent with the assumed ones.

3.4.4 Termination Conditions for Incremental Steps

Different stress rate-strain rate relations should be employed in Eq. (3.27) for the steady states at $\tau \geq \tau_{h+1}$ when the types of stress-strain cyclic responses, the order of the RES or the number of the RES may change at $\tau = \tau_{h+1}$. In such cases, an incremental step is terminated at $\tau = \tau_{h+1}$. The conditions for terminating the incremental steps are given by the following equations. The step length $\Delta\tau$ is determined as the smallest value among $\Delta\bar{\tau}_{max}$, specified for preventing excessive accumulation of truncation errors, and the values obtained from these conditions.

First, consider the transition of the types of the cyclic responses. For E elements, $\Delta\tau$ is calculated using the following conditions:

$$\sigma^t(\tau_{h+1}) - \sigma^t_{yt}(\tau_h) = 0, \tag{3.36}$$

$$\sigma^c(\tau_{h+1}) - \sigma^c_{yc}(\tau_h) = 0, \tag{3.37}$$

where the subsequent yield stresses are expressed in terms of $\varepsilon_p(\tau_h)$ using Eqs. (3.8) and (3.9), and $\sigma(\tau_{h+1})$ is expressed as $\sigma(\tau_h) + \dot{\sigma}(\tau_h)\Delta\tau$ in the linear approximation. Equations (3.36) and (3.37) are the conditions for E $\rightarrow$ T and E $\rightarrow$ C, respectively. For every E, T and C element, the condition for the transition to the type P is written as

$$\sigma^t(\tau_{h+1}) - \sigma^c(\tau_{h+1}) - 2\sigma_y = 0. \tag{3.38}$$

An example of the transition is shown in Fig. 3.12 (a).

Next, let us discuss the change of the order or the number of the RES. Let the superscripts α and $\alpha+1$ indicate the stresses at two consecutive instants in a cycle. Then the condition for the change of the order of the RES is written by

$$\sigma^\alpha(\tau_{h+1}) - \sigma^{\alpha+1}(\tau_{h+1}) = 0. \tag{3.39}$$

The condition for increasing the number of the RES are given by

$$\sigma^\mu(\tau_{h+1}) - \sigma^\beta_{yt}(\tau_{h+1}) = 0, \quad \text{if } \sigma^\beta = \sigma^\beta_{yc} \text{ at } \tau = \tau_h, \tag{3.40}$$

$$\sigma^\mu(\tau_{h+1}) - \sigma^\beta_{yc}(\tau_{h+1}) = 0, \quad \text{if } \sigma^\beta = \sigma^\beta_{yt} \text{ at } \tau = \tau_h. \tag{3.41}$$

Note that, obviously, the number of the RES should be increased when the transition E, T or C $\rightarrow$ P occurs.

3.4.5 Examination of Strain Reversals

In constructing the rate equations and in determining the incremental steps, the following things are assumed to be known: (1) the element whose yielding characterize Γ^μ ($\mu \geq 3$); (2) the equilibrium states corresponding to Γ^t and Γ^c for all the elements; and (3) the relations between μ and corresponding β for all the P elements. These relations may change if the order or the number of the RES changes. In the previous section, the conditions (3.38)-(3.41) have been given for terminating incremental steps at these instants. If the incremental steps are terminated using at least one of these conditions, it must be examined whether the relations (1)-(3) change or not. For this purpose, we examine strain reversals.

When at least one of the conditions (3.38)-(3.41) are satisfied, an equilibrium state in the steady state may be characterized by more than one condition. For instance, the case where the number of the RES may increase is illustrated in Fig. 3.12. The equilibrium state indicated by the black square at $\tau = \tau_h$ in Fig. 3.12 (a) is characterized as both load reversal point and yielding point. For simplicity, we consider here only the case in which an equilibrium state is characterized by only two conditions. When an equilibrium state is characterized by more than two conditions, the combination of the order should be assumed and the consistency between the assumed and resulting order should be examined in the process of obtaining the incremental relations with respect to τ.

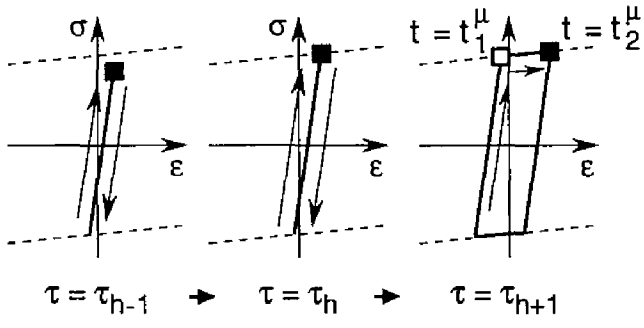

(a) The Element Exhibitting Transition C → P

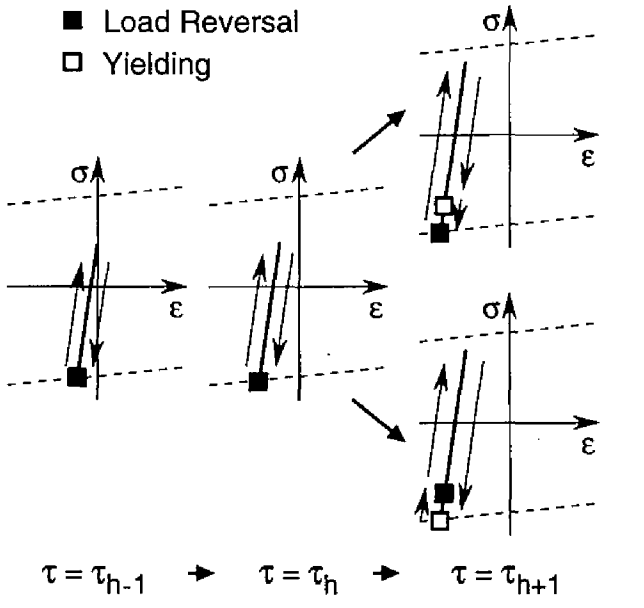

(b) Another Element

Figure 3.12: Examination of strain reversals.

Let Γ^μ be characterized by two conditions at $\tau = \tau_h$. First, to examine the strain reversals, the order of the equilibrium states are determined in the steady state for $\tau > \tau_h$. If the number of the RES may increase, the new yielding is considered to occur preceding Γ^μ. An example is shown in Fig. 3.12, where the black square indicate the load reversal point Γ^μ and the white square indicate the new yielding point. On the other hand, if the order of the RES in a steady state is changed, the order in the steady state for $\tau < \tau_h$ is reversed.

Second, it is checked whether or not strain reversals occur at the two equilibrium states in the steady state for $\tau > \tau_h$. For this purpose, the partial derivatives with respect to t is used. Let t_1^μ and t_2^μ $(t_1^\mu \leq t_2^\mu)$ denote respectively the instants for the equilibrium states in a steady sate at $\tau > \tau_h$ as shown in Fig. 3.12. A strain reversal is judged to occur at $t = t_1^\mu$ if the following condition

$$\left.\frac{\partial \varepsilon}{\partial t}\right|_{t=t_1^\mu}^{-} \times \left.\frac{\partial \varepsilon}{\partial t}\right|_{t=t_1^\mu}^{+} < 0 \tag{3.42}$$

is satisfied. Otherwise, no stain reversal is judged to take place. The condition for $t = t_2^\mu$ is written in the same form as Eq. (3.42). These conditions are checked for every the element. The procedures for calculating the partial derivatives are shown in Appendix B.

Finally, if the strain reversals are judged to occur in at least one element at the time where no strain reversal occurs in the steady state for $\tau < \tau_h$, the yielding point is added to the RES. And according to the result of the examination of the strain reversals, the relations (1)-(3) are changed if changes are needed.

3.4.6 Steady-State Limit Condition

Now, all the first-order derivatives and the step length $\Delta\tau$ have been obtained. Substituting $\Delta\tau$ and the first-order derivatives into Eq. (3.18) we have all the state variables at $\tau = \tau_{h+1}$. Repeating these procedures, the steady-state path is traced incrementally.

As mentioned before, the steady-state limit is characterized as the first limit point of the steady-state path. The steady-state limit condition is therefore given as

$$\dot{\psi} \leq 0 \tag{3.43}$$

Note that, to find the limit point and to trace the steady-state path after the limit point, a procedure should be employed similar to displacement control schemes [17, 18].

3.5 NUMERICAL EXAMPLES

The proposed method has been developed on the basis of hypotheses 3.1 and 3.2. And the steady-state limit is predicted regardless of the transient process between the two consecutive steady states. Hence validity of the two hypotheses and the steady-state limit should be examined. In addition, the steady-state limit is defined for the structures under an idealized cyclic loading program. Therefore the effect of the differences of the loading histories should be examined.

For these reasons and to demonstrate the present method, the steady-state limit analysis and the conventional response analysis, in which the entire history is traced, are performed. The analyses are applied for the two-bar arch truss and the ten-bar cantilever truss, whose elastic shakedown boundaries have been obtained in the previous chapter.

3.5.1 Steady-state limit Analysis

Numerical data for the two-bar truss has been shown in subsection 3.3.2. Initial shape, boundary conditions and loading conditions of the ten-bar truss are shown in Fig. 3.8. The cross-sectional areas of the ten-bar truss are as follows: $A_{(1)} = A_{(4)} = A_{(5)} = 11$ cm^2, $A_{(2)} = A_{(3)} = 1.1$ cm^2, $A_{(6)} = A_{(9)} = A_{(10)} = 10$ cm^2, and $A_{(7)} = A_{(8)} = 1$ cm^2. Material properties of the ten-bar truss is same as those for the two-bar truss. Throughout the steady-state limit analysis, the higher-order terms are employed up to the second order (see Appendix A). And the maximum allowable step lengths $\Delta\bar{\tau}_{max}$ are set to be $\Delta\bar{\tau}_{max} = 0.05$ and $\Delta\bar{\tau}_{max} = 0.2$ for the two-bar and the ten-bar trusses, respectively. For the ten-bar truss, the load factor at the buckling is $\lambda_b = 40.38$ when only the initial loads are applied.

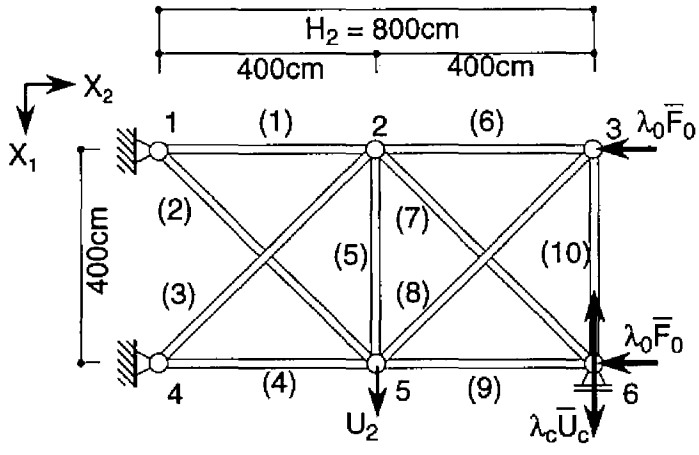

Figure 3.13: The ten-bar truss.

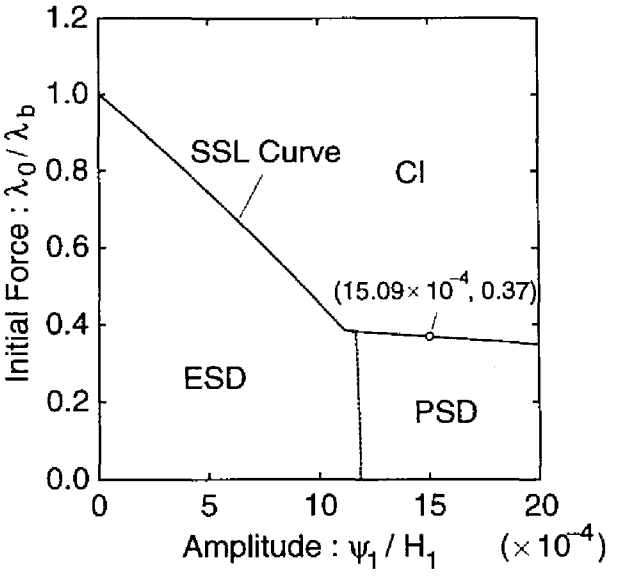

Figure 3.14: The steady-state limit curve for the two-bar truss.

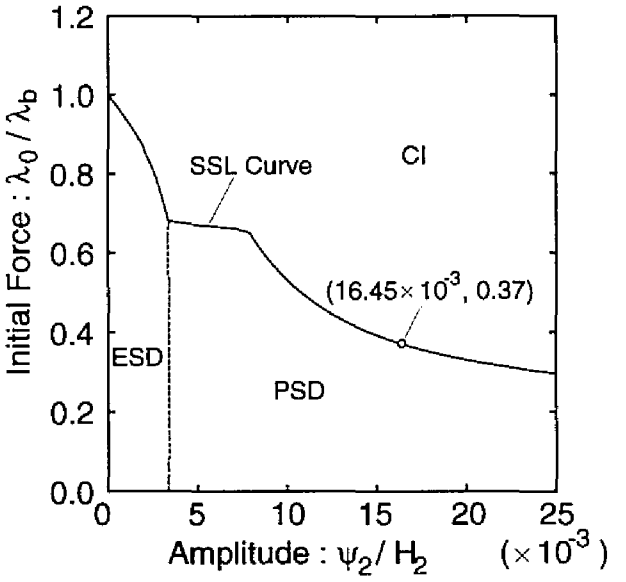

Figure 3.15: The steady-state limit curve for the ten-bar truss.

Figures 3.14 and 3.15 illustrate the load combinations at the steady-state limit predicted for each value of normalized load factor λ_0/λ_b. The value of λ_0/λ_b is parametrically changed between 0 and 1 with increments of 0.005 and 0.01 for two-bar and ten-bar trusses, respectively. From these figures, several points can be observed at which the slope is discontinuously changed. The reason is considered to be that distribution of the types of the stress-strain cyclic responses changes at the points.

3.5.2 Response Analysis

All the loading histories are traced under the two typical and realistic cyclic loading programs STIDAC and STIDAD shown in Fig. 3.16. The STIDAC is the loading program that in which the amplitude ψ of the forced displacement is increased every half cycle with an increment $\Delta\bar{\psi}$ from zero to a specified value $\bar{\psi}_{max}$, and then ψ is kept constant in the following cycles. In the STIDAD program, the amplitude ψ of the load factor λ_c is kept a constant value throughout all cycles. The solution method for the conventional response analysis and the criteria for convergence are exactly identical to those shown in Appendix B in the previous chapter. The constants for the loading conditions are $\bar{\psi}_{max} = (1 \pm 0.001)\psi_{ssl}$, $\Delta\bar{\psi} = 0.001\psi_{ssl}$ and $\bar{\psi} = (1 \pm 0.001)\psi_{ssl}$.

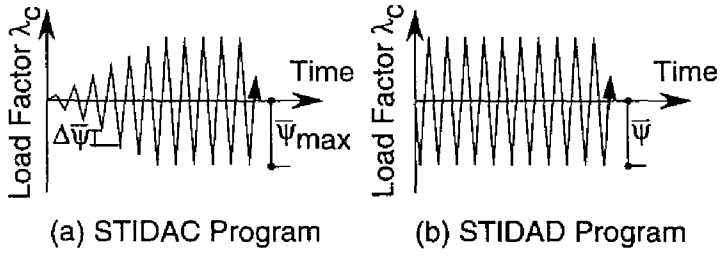

Figure 3.16: STIDAC program and STIDAD program.

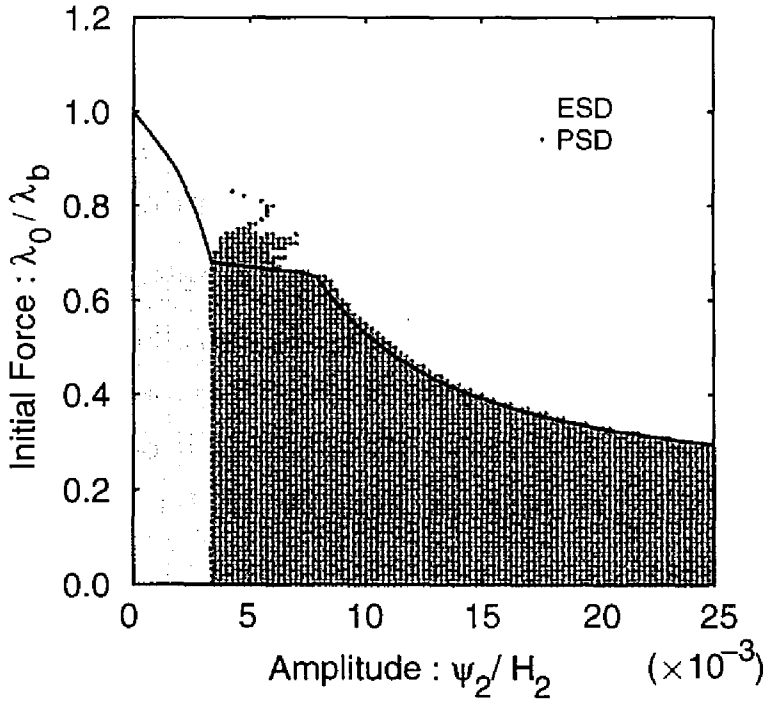

Figure 3.17: Steady-state curve and the results of the parametric analysis.

Under the STIDAC program, good agreement is observed between the the steady-state limit predicted by the proposed method and the results of the response analysis. Convergence is observed if $\bar{\psi}_{max} < \psi_{ssl}$, and divergence is obtained if $\bar{\psi}_{max} > \psi_{ssl}$. From this result, it may be stated that the proposed method is directly verified. On the other hand, inconsistent results are seen for the ten-bar truss under STIDAD program. Convergence is observed regardless of $\bar{\psi} > \psi_{ssl}$.

To clarify when this inconsistency occurs, a complete parametric analysis is carried out. In the parametric analysis, not only λ_0 but also $\bar{\psi}$ are changed. The load factor λ_0 of the constant load is changed in the same manner as the steady-state limit analysis. The constant amplitude of the cyclic forced displacement is changed from $\bar{\psi}/H_2(\times^{-3}) = 0$ to 25 with an increment of 0.25. Namely, the response analysis is performed for 10,000 different load combinations of $(\lambda_0, \bar{\psi})$.

The results of the complete parametric analyses is illustrated in Fig. 3.17. When convergence is observed, the load combinations are plotted by the circular symbols. The darker and lighter grey circles indicate the convergence to the plastic shakedown and the elastic shakedown, respectively. From Fig. 3.17, we may state that the values of the steady-state limit predicted under the idealized cyclic loading program may be smaller than the limiting values that bound convergence and divergence predicted under the STIDAD program.

3.6 CONCLUSIONS

For elastoplastic trusses subjected to the cyclic loads in the presence of the constant loads, a new method has been presented for finding the critical load combinations that bounds convergence to plastic shakedown and divergence of plastic deformations.

The conclusions of this research are:

1. The reason has been clarified why the method presented in the previous chapter fails to find the steady-state limit when plastic shakedown occurs. When an element exhibits the plastic shakedown, strain reversals of the other elements may take place not only at load reversals but also at yielding of the elements exhibiting the plastic shakedown. Nevertheless it was assumed that the strain reversals occur only at the load reversals in the previous method.
2. The hypothesis on the strain reversals has been relaxed so that the strain reversals due to yielding is taken into account. Based on the relaxed assumption, incremental relations have been formulated for tracing the variation of the steady state with respect to the parameter that defined the amplitude of the cyclic loads.

3. From the results in the numerical examples, the following results have been obtained: (1) Good agreements are obtained between the results of the steady-state limit analysis and the response analysis if the loading programs employed in the both analyses are close enough; (2) The limiting values below which elastic shakedown or plastic shakedown occurs depend on the loading history; and (3) The values of the steady-state limit, defined for an idealized cyclic loading program, are smaller than the limiting values that bounds convergence and divergence under the two typical and realistic cyclic loading programs.

The last statement 3. (3) is not a quantitative conclusion. Further investigations is therefore required on this subject.

Appendix A. Formulation with Higher-Order Derivatives

A formulation with higher-order derivatives is presented for the steady-state limit analysis. We derive here the derivatives up to only the second order. But more higher-order derivatives can be obtained similarly.

Differentiation of the rate equations (3.23)-(3.34) with respect to the steady-state path parameter τ yields the second-order perturbation equations as follows:

$$\ddot{\varepsilon}^{\mu} = \frac{\partial\, \varepsilon^{\mu}}{\partial\, u_i{}^{\mu}} \ddot{u}_i^{\mu} + \frac{\partial^2\, \varepsilon^{\mu}}{\partial\, u_i{}^{\mu}\, \partial\, u_j{}^{\mu}} \dot{u}_i^{\mu} \dot{u}_j^{\mu} \tag{3.44}$$

for the compatibility conditions,

$$\ddot{f}_i^{\mu} = AL_0 \left\{ \ddot{\sigma}^{\mu} \frac{\partial\, \varepsilon^{\mu}}{\partial\, u_i^{\mu}} + \sigma^{\mu} \frac{\partial^2\, \varepsilon^{\mu}}{\partial\, u_i{}^{\mu}\, \partial\, u_j{}^{\mu}} \ddot{u}_j^{\mu} + 2\dot{\sigma}^{\mu} \frac{\partial^2\, \varepsilon^{\mu}}{\partial\, u_i{}^{\mu}\, \partial\, u_j{}^{\mu}} \dot{u}_j^{\mu} \right\} \tag{3.45}$$

for the equilibrium conditions, and

$$\ddot{\sigma}^{\mu} = \sum_{\nu=1}^{J} C^{\mu\nu} \ddot{\varepsilon}^{\nu} \tag{3.46}$$

for the stress-strain relations. Note that $\dot{C}^{\mu\mu} = 0$ because the piecewise-linear constitutive relation is assumed. Differentiating Eq. (3.28), we have the second-order perturbation equations for each element

$$\ddot{f}_i^{\mu} = \sum_{\nu=1}^{J} k_{ij}^{\mu\nu} \ddot{u}_j^{\nu} + \hat{f}_i^{\mu}, \tag{3.47}$$

where the coefficients $k_{ij}^{\mu\nu}$ is identical to that in Eq. (3.29) and hat indicates the variables expressed in terms of the first-order derivatives as follows

$$\hat{f}_i^{\mu} = 2AL_0 \dot{\sigma}^{\mu} \frac{\partial^2\, \varepsilon^{\mu}}{\partial\, u_i{}^{\mu}\, \partial\, u_j{}^{\mu}} \dot{u}_j^{\mu} + AL_0 \frac{\partial\, \varepsilon^{\mu}}{\partial\, u_i^{\mu}} \sum_{\nu=1}^{J} C^{\nu\nu} \frac{\partial^2\, \varepsilon^{\nu}}{\partial\, u_j{}^{\nu}\, \partial\, u_k{}^{\nu}} \dot{u}_j^{\nu} \dot{u}_k^{\nu}. \tag{3.48}$$

Assembling the perturbation equations for the elements leads to the second-order perturbation equations for the total system

$$\ddot{\mathbf{F}}^{\mu} = \mathbf{K}^{\mu\nu} \ddot{\mathbf{U}}^{\nu} + \hat{\mathbf{F}}^{\mu}, \tag{3.49}$$

where the coefficient matrices are same as those in the rate equation (3.29). Differentiation of Eqs. (3.30), (3.31) and (3.34) leads to

$$\ddot{\lambda}_c^1 - \ddot{\psi} = 0, \tag{3.50}$$

$$\ddot{\lambda}_c^2 + \ddot{\psi} = 0, \tag{3.51}$$

$$\frac{\partial\, \varepsilon^{\mu}}{\partial\, u_i^{\mu}} \ddot{u}_i^{\mu} - \frac{\partial\, \varepsilon^{\beta}}{\partial\, u_i^{\beta}} \ddot{u}_i^{\beta} + \hat{u}^{\mu\beta} = 0 \tag{3.52}$$

where

$$\hat{u}^{\mu\beta} = \frac{\partial^2 \varepsilon^\mu}{\partial u_i^\mu \partial u_j^\mu} \dot{u}_i^\mu \dot{u}_j^\mu - \frac{\partial^2 \varepsilon^\beta}{\partial u_i^\beta \partial u_j^\beta} \dot{u}_i^\beta \dot{u}_j^\beta \tag{3.53}$$

Equation (3.53) can be expressed in terms of nodal displacements for the total system as

$$\mathbf{L}^\mu \ddot{\mathbf{U}}^\mu + \mathbf{L}^\beta \ddot{\mathbf{U}}^\beta + \hat{\mathbf{U}}^{\mu\beta} = 0. \tag{3.54}$$

By specifying the value of $\ddot{\psi}$, we have $J \times (3N+1)$ simultaneous linear equations (3.49) and (3.54).

When the derivatives are employed up to the second order, the termination conditions Eqs. (3.36)-(3.38) of the incremental step become quadratic equations of the step length $\Delta\tau$, while the conditions are linear equations when only the first derivatives are used. Besides these termination conditions, we must consider the conditions

$$\dot{\varepsilon}^t(\tau_{h+1}) = \dot{\varepsilon}^t(\tau_h) + \ddot{\varepsilon}^t(\tau_h)\Delta\tau = 0, \tag{3.55}$$

$$\dot{\varepsilon}^c(\tau_{h+1}) = \dot{\varepsilon}^c(\tau_h) + \ddot{\varepsilon}^c(\tau_h)\Delta\tau = 0 \tag{3.56}$$

for the transitions T $\rightarrow$ E and C $\rightarrow$ E, respectively.

Appendix B. Formulation for Examination of Strain Reversals

A formulation is shown here for examining the strain reversals. Differentiating the kinematic relations (3.1)-(3.3) with respect to t, we obtain the following equations

$$\varepsilon^{\mu\prime} = \frac{\partial \varepsilon^\mu}{\partial u_i^\mu} u_i^{\mu\prime}. \tag{3.57}$$

where the prime indicates partial differentiation with respect to t. Differentiation of equilibrium condition (3.4) yields

$$f_i^{\mu\prime} = AL_0 \left(\sigma^{\mu\prime} \frac{\partial \varepsilon^\mu}{\partial u_i^\mu} + \sigma^\mu \frac{\partial^2 \varepsilon^\mu}{\partial u_i^\mu \partial u_j^\mu} u_j^{\mu\prime} \right). \tag{3.58}$$

These equations (3.57) and (3.58) are used for both $t = t_1^\mu$ and $t = t_2^\mu$.

On the other hand, the constitutive relations may be different for the two instants. Consider first the case where $t = t_1^\mu$. Define C_1^+ and C_1^- by

$$C_1^{\mu+} = \left. \frac{\partial \varepsilon}{\partial \sigma} \right|_{t=t_1^\mu}^{+}, \quad C_1^{\mu-} = \left. \frac{\partial \varepsilon}{\partial \sigma} \right|_{t=t_1^\mu}^{-}. \tag{3.59}$$

Then these coefficients $C_1^{\mu+}$ and $C_1^{\mu-}$ are determined according to the type of the stress-strain cyclic response. For the E, T and C elements, these coefficients are given by

$$C_1^{\mu-} = C_1^{\mu+} = E \tag{3.60}$$

because these elements exhibit elastic shakedown responses in the neighboring steady state for $\tau \geq \tau_h$. Recall that only the steady-state responses after convergence is considered in the steady-state limit theory. For P elements, the coefficients are selected according to the location of state point in the stress-strain plane. For the element whose yielding occurs at $t = t_1^\mu$, the coefficients are given by

$$C_1^{\mu-} = E, \quad C_1^{\mu+} = E_t. \tag{3.61}$$

For the element whose yielding occurs at $t = t_2^\mu$, the coefficients are determined by

$$C_1^{\mu-} = C_1^{\mu+} = E. \tag{3.62}$$

For the other elements, the coefficients are given by

$$C_1^{\mu-} = C_1^{\mu+} = E_t, \quad \text{if } \sigma^\mu = \sigma_{yt}^\mu \text{ or } \sigma^\mu = \sigma_{yc}^\mu \tag{3.63}$$

$$C_1^{\mu-} = C_1^{\mu+} = E, \quad \text{if } \sigma_{yc}^\mu < \sigma^\mu < \sigma_{yt}^\mu. \tag{3.64}$$

Note that consistency between the assumed and resulting sign of ε' must be checked when the tangent stiffness E_t is used.

Substitution of the coefficients $C_1^{\mu-}$ and $C_1^{\mu+}$ into Eq. (3.58) and assemblage of the tangent stiffness equations for elements lead to that for total system

$$\mathbf{F}_1^{\mu-\prime} = \mathbf{K}_1^{\mu-}\mathbf{U}_1^{\mu-\prime}, \quad \mathbf{F}_1^{\mu+\prime} = \mathbf{K}_1^{\mu+}\mathbf{U}_1^{\mu+\prime} \tag{3.65}$$

By using the boundary conditions and by specifying $\lambda_c^{\mu-\prime}$ and $\lambda_c^{\mu+\prime}$, we can solve Eq. (3.65). With strain-displacement relations, we have $\mathbf{E}_1^{\mu-\prime}$ and $\mathbf{E}_1^{\mu+\prime}$.

Let us turn to the case where $t = t_2^\mu$. Here, we have

$$\mathbf{E}_2^{\mu-\prime} = \mathbf{E}_1^{\mu+\prime}. \tag{3.66}$$

Our problem is then to calculate $\mathbf{E}_2^{\mu+\prime}$. The only difference between the case for obtaining $\mathbf{E}_1^{\mu+\prime}$ and $\mathbf{E}_2^{\mu+\prime}$ is the way to choose tangent stiffnesses. For the element whose yielding occurs at $t = t_2^\mu$, the coefficients are determined by

$$C_2^{\mu+} = E_t. \tag{3.67}$$

For the other elements, the coefficients $C_2^{\mu+}$ are determined so that those are identical to $C_1^{\mu+}$ after the consistent set of tangent stiffness is obtained. Note that, if unloading at $t = t_1^\mu$ and strain reversal $t = t_2^\mu$ occur in an element, the element will yield at the time $t > t_2^\mu$. The strain reversals at the yielding time should be checked in a similar manner as that at $t = t_2^\mu$.

Nomenclature

The following symbols are used in this chapter:

A initial cross sectional area;

C coefficient of ε';

$C^{\mu\mu}, C^{\mu t}, C^{\mu c}, C^{\mu\beta}$ coefficients of $\dot{\varepsilon}^{\mu}$, $\dot{\varepsilon}^{t}$, $\dot{\varepsilon}^{c}$ and $\dot{\varepsilon}^{\beta}$;

$C^{\mu\nu}$ coefficients of $\dot{\varepsilon}^{\nu}$;

E Young's modulus;

E_t tangent modulus after yielding;

$\mathbf{E}$ strain vector for total system;

$\mathbf{E}_p$ plastic strain vector for total system;

$\mathbf{F}$ nodal force vector for total system;

f_i nodal force;

J Number of RES;

H Height of truss;

$\mathbf{K}$ tangent stiffness matrix;

$\mathbf{K}^{\mu\nu}$ coefficient matrices of $\dot{\mathbf{U}}^{\nu}$;

k_{ij} coefficient of u'_j;

$k_{ij}^{\mu\nu}$ coefficients of $\dot{u}_j^{\nu}$;

L current length;

L_0 initial length;

M number of elements;

N number of nodes;

$\bar{\mathbf{P}}_0$ constant vector for constant loads;

$\bar{\mathbf{P}}_c$ constant vector for cyclic load;

$\mathbf{S}$ stress vector for total system;

t equilibrium path parameter;

$\mathbf{U}$ nodal displacement vector for total system;

u_i nodal displacement;

V initial volume;

x_i current position of nodes;

x_i^0 initial position of nodes;

ε Green-Lagrangian strain;

ε_p plastic strain;

λ_0 load factor for constant load;

λ_b load factor at initial buckling load;

λ_c load factor for cyclic loads;

σ second Piola-Kirchhoff stress;

σ_y initial tensile yield stress;

$\bar{\sigma}_y$ $\bar{\sigma}_y = (1 - E_t/E)\sigma_y$;

σ_{yc} subsequent yield stress in compression;

σ_{yt} subsequent yield stress in tension;

τ steady-state path parameter;

τ_h τ at h step;

$\Delta\tau$ increment of steady-state path parameter;

$\Delta\bar{\tau}_{max}$ maximum allowable value of $\Delta\tau$;

$\Delta\bar{\psi}$ specified increment of amplitude for STIDAC program;

ψ amplitude of λ_c;

ψ_{ssl} amplitude at steady-state limit;

$\bar{\psi}$ constant amplitude for STIDAD program; and

$\bar{\psi}_{max}$ maximum amplitude for STIDAC program.

Superscripts

t variables for the equilibrium states at strain reversals in tension;

c variables for the equilibrium states at strain reversals in compression;

I variables for the equilibrium states at $\lambda_c = \psi$;

II variables for the equilibrium states at $\lambda_c = -\psi$;

β variables at which the last strain reversal occurs before $t = t^{\mu}$;

μ variables at Γ^{μ}; and

ν variables at Γ^{ν}..

Signs

$\dot{(\ )}$ derivatives with respect to τ;

$\ddot{(\ )}$ second order derivatives with respect to τ;

$\hat{(\ )}$ quantities expressed with first-order derivatives with respect to τ; and

$(\ )'$ derivatives with respect to t.

References

[1] W. T. Koiter. General theorems for elastic-plastic structures. In J. N. Sneddon and R. Hill, editors, *Progress in Solid Mechanics*, volume 1, pages 167–221, North Holland, Amsterdam, 1960.

[2] J. Bree. Elastic-plastic behavior of thin tubes subjected to internal pressure and intermittent high-heat fluxes with application to fast-nuclear-reactor fuel elements. *Journal of Strain Analysis*, 6:236–249, 1967.

[3] J. Zarka and J. Casier. Elastic-plastic response of a structure to cyclic loading: Practical rules. In S. Nemat-Nasser, editor, *Mechanics Today*, pages 93–198. Pergamon Press, New York, 1979.

[4] J. A. König. *Shakedown of Elastic-Plastic Structures.* Elsevier, Amsterdam, 1987.

[5] Q. S. Nguyen, G. Gary, and G. Baylac. Interaction buckling-progressive deformation. *Nuclear Engineering and Design*, 75:235–243, 1983.

[6] A. Siemaszko and J. A. König. Analysis of stability of incremental collapse of skeletal structures. *Journal of Structural Mechanics*, 13:301–321, 1985.

[7] K. Uetani and T. Nakamura. Symmetry limit theory for cantilever beam-columns subjected to cyclic reversed bending. *Journal of the Mechanics and Physics of Solids*, 31(6):449–484, 1983.

[8] G. Maier, L. G. Pan, and U. Perego. Geometric effects on shakedown and ratchetting of axisymmetric cylindrical shells subjected to variable thermal loading. *Engineering Structures*, 15:453–465, 1993.

[9] A. R. S. Ponter and S. Karadeniz. An extended shakedown theory for structures that suffer cyclic thermal loadings, part 1: Theory. *Journal of Applied Mechanics*, 52:877–882, 1985.

[10] A. R. S. Ponter and S. Karadeniz. An extended shakedown theory for structures that suffer cyclic thermal loadings, part 2: Applications. *Journal of Applied Mechanics*, 52:883–889, 1985.

[11] C. Polizzotto. A study on plastic shakedown of structures, part i: Basic properties. *Journal of Applied Mechanics*, 60:318–323, 1993.

[12] C. Polizzotto. A study on plastic shakedown of structures, part ii: Theorems. *Journal of Applied Mechanics*, 60:324–330, 1993.

[13] C. Polizzotto and G. Borio. Shakedown and steady-state responses of elastic-plastic solids in large displacements. *International Journal of Solids and Structures*, 33:3415–3437, 1996.

[14] K. Uetani. *Symmetry Limit Theory and Steady-State Limit Theory for Elastic-Plastic Beam-Columns Subjected to Repeated Alternating Bending.* PhD thesis, Kyoto University, 1984. (in Japanese).

[15] K. Uetani and T. Nakamura. Steady-state limit theory for cantilever beam-columns subjected to cyclic reversed bending. *Journal of Structural and Construction Engineering, AIJ*, (438):105–115, 1992.

[16] R. Hill. A general theory of uniqueness and stability in elastic-plastic solids. *Journal of the Mechanics and Physics of Solids*, 6:236–249, 1958.

[17] Y. Yokoo, T. Nakamura, and K. Uetani. The incremental perturbation method for large displacement analysis of elastic-plastic structures. *International Journal for Numerical Methods in Engineering*, 10:503–525, 1976.

[18] M. A. Crisfield. *Non-linear Finite Element Analysis of Solids and Structures*, volume 1. John Wiley & Sons, New York, 1991.

Chapter 4

Stability of Steady States and Steady-State Limit

4.1 INTRODUCTION

The concept of stability is generally defined for dynamical systems (see for instance [1, 2]). When a dynamical system depends on parameters, the object of stability analysis is to study the change of its solution or response due to the change of the parameters.

According to the type of the perturbation, the stability has been defined in various ways. Among them, the definition due to Liapunov [1] has been used in many fields. According to this definition, roughly speaking, a solution is said to be stable if a small change in the initial conditions leads to a small change in the solution. Though the perturbation is given to initial conditions in the Liapunov stability, it may be given to other parameters.

Based on the definition of stability given by Liapunov, various criteria have been proposed for the stability of an equilibrium state in the field of structural engineering [2, 3]. The criteria is generally given in terms of the eigenvalues for ordinary differential equations. If structural systems are conservative, which constitute the majority of applications in structural engineering, the stability of equilibrium states can be determined based on energy approach. In this case, the loss of the stability occurs at the branching or limit point of an equilibrium path, which represents the variation of the equilibrium state with respect to the variation of external loads. For elastic structures, the stability criteria were derived using a potential energy [4, 5, 6]. For elastoplastic structures, where potential energy can not be defined, Hill [7] derived a stability criterion by introducing the concept of comparison solid, where any yielding element is assumed to behave with their tangent stiffness for plastic loading even if its strain changes in an unloading direction.

On the stability of cycles or closed orbits of nonlinear dynamical systems, on the other hand, a lot of research have also been made (see for instance [8, 9, 10]). In the research, it was

pointed out that there exist the relation between the stability of a cycle and the branching of a path that represent the variation of a cycle with respect to the variation of the parameter in the dynamical systems. And stability criteria were given for these nonlinear systems based on the idea of Poincare Maps, which relate the quantities at the discrete instants. These criteria is directly applicable to elastic structures. But, to the best of author's knowledge, no such criterion has been derived or formulated for elastoplastic structures.

So far, the stability of the solutions for dynamical systems has been reviewed. Let us turn on the stability of a cycle in quasi-static problem, where inertia force and damping force are neglected. For elastic structures, no instability occurs if the all the equilibrium states in a cycle are stable. In elastoplastic structures however the deviation from the cycle due to the small change of parameters may become large because of the accumulation of plastic strains even if no unstable equilibrium state exits in the cycle. This phenomena, known as incremental collapse or ratchetting [11, 12], is apparently considered to be one type of the instability, and it is called cyclic instability in this paper. But, in addition to the elastoplastic structures under dynamic loads, no stability analysis has been done for those under quasi-static loads.

For elastoplastic beam-columns under cyclic bending with continuously increasing amplitude, Uetani [13, 14, 15] proposed symmetry limit theory and steady-state limit theory for finding the critical loading condition above which cyclic instability occur. In these two theories, a steady-state path, which represents variation of a steady cycle with respect to the variation of the amplitude, is traced, and the critical loading condition is found as the branching and limit points of the steady-state path. In the preceding chapters, a method and its extension have been presented for finding the critical loading condition of elastoplastic trusses based on this concept. But these methods yield only steady states, which may be stable or unstable. It is therefore desirable to introduce the concept of stability of steady state and to find the steady-state limit as the critical steady-state at which the stability is lost.

The purpose of this chapter is to present a theory for finding the steady-state limit as the critical steady state at which loss of the stability of a steady state occurs. In this theory, for tracing the steady-state path, an alternative method is also presented in which the hypothesis on strain reversals employed in the method presented in previous chapters are completely excluded. This method is constructed based on the method for tracing the steady-state path of three dimensional continua [16]. In this method, first, a steady state is expressed by discretizing its equilibrium path with respect to an equilibrium path parameter.

Second, deviation from the steady state due to the change of the amplitude of cyclic loading is expressed using the recurrence equation that relates the two consecutive periodic instants. The recurrence equation is formulated in terms of the plastic strain increments with respect to the change of the amplitude of cyclic loads. Then the stability of the steady state is defined and the stability criterion is given in terms of the eigenvalue the coefficient matrix in the recurrence equation. The steady-state path is traced using the recurrence equation, and the steady-state limit is found as the critical steady state at which loss of the stability of a steady state occurs. Finally, validity of the proposed method is demonstrated through numerical examples.

4.2 GOVERNING EQUATIONS

4.2.1 Analytical Models

Consider pin-jointed space trusses with M elements and N nodes. Buckling of elements is ruled out but that of a global type is taken into account using the Total Lagrangian formulation. Under the assumption of large displacement-small strain, compatibility conditions for an element illustrated in Fig. 4.1 are given by

$$\varepsilon = \frac{L^2 - L_0^2}{2L_0^2}, \tag{4.1}$$

$$L^2 = (x_4 - x_1)^2 + (x_5 - x_2)^2 + (x_6 - x_3)^2, \tag{4.2}$$

$$x_i = x_i^0 + u_i; \qquad i = 1, \cdots, 6 \tag{4.3}$$

where ε is the Green-Lagrangian strain, L and L_0 are the current length and the initial length of the element, respectively, u_i is the nodal displacement, and x_i and x_i^0 indicate the current

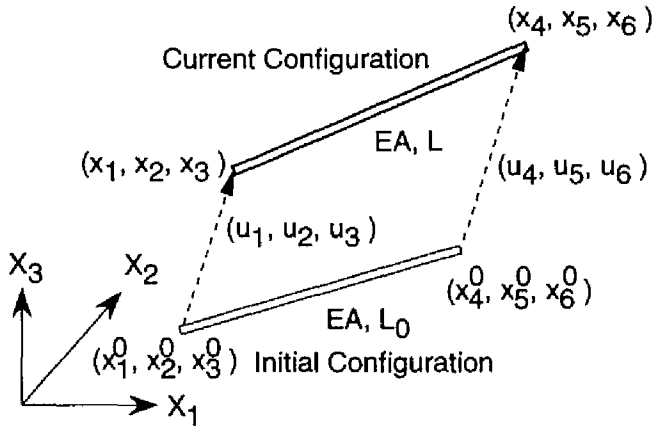

Figure 4.1: A truss element

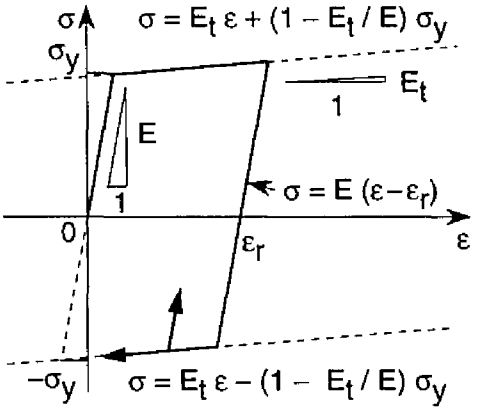

Figure 4.2: A bi-linear kinematic hardening rule.

position and the initial position of the nodes at the two ends, respectively. For equilibrium, we require

$$f_i = AL_0\sigma\frac{\partial\,\varepsilon}{\partial\,u_i} \tag{4.4}$$

in which f_i is the nodal force, A is the cross sectional area, and σ is the second Piola-Kirchhoff stress. By assembling the equilibrium equations for elements, we have the equilibrium equations for the total system.

As a constitutive model, we employ a bi-linear kinematic hardening rule shown in Fig. 4.2. Let E, E_t, σ_y and ε_p indicate the Young's modulus, the tangent modulus after yielding, the initial yield stress in tension and plastic strain, respectively Then the constitutive law is expressed as follows:

$$\sigma = E(\varepsilon - \varepsilon_p), \tag{4.5}$$

$$\sigma = E_t\varepsilon + \bar{\sigma}_y \qquad \text{for the plastic loading in tension,} \tag{4.6}$$

$$\sigma = E_t\varepsilon - \bar{\sigma}_y \qquad \text{for the plastic loading in compression} \tag{4.7}$$

where $\bar{\sigma}_y = (1 - E_t/E)\sigma_y$. Let σ_{yt} and σ_{yc} denote the subsequent yield stresses in tension and compression, respectively. Then the subsequent yield stresses are expressed in terms of the plastic strains as

$$\sigma_{yt} = \frac{EE_t}{E - E_t}\varepsilon_p + \sigma_y, \tag{4.8}$$

$$\sigma_{yc} = \frac{EE_t}{E - E_t}\varepsilon_p - \sigma_y. \tag{4.9}$$

4.2.2 Loading Conditions

The trusses are subjected to initial constant loads $\lambda_0\bar{\mathbf{P}}_0$ and subsequent cyclic loads $\lambda_c\bar{\mathbf{P}}_c$. Here, λ and $\bar{\mathbf{P}}$ denote the load factor and the constant vector, respectively. The subscripts 0 and c indicate the variables corresponding to the constant loads and the cyclic loads, respectively. External forces and/or forced displacements are applied as the external loads. In other words, according to the boundary conditions, either the nodal force or the nodal displacement components is specified for each degree of freedom.

The load factor λ_c is varied between the maximum value $\lambda_c = \psi$ and the minimum value $\lambda_c = -\psi$ in a cycle, where ψ denotes the amplitude of λ_c. The load factor λ_c is the function of an equilibrium path parameter t. The amplitude ψ is the function of a steady-state path parameter τ. Though the loading condition used here is very simple, the present theory can be extended easily to more complicate loading conditions.

4.3 STEADY STATES

4.3.1 Outline of Formulation

Consider a steady state under the loading condition defined by $\tau = \tau_h$, where τ_h is an arbitrary value of τ. To formulate this steady state, the equilibrium path in a period $IT \leq t \leq (I+1)T$ is discretized with respect to t. Here, $T(\tau_h)$ is the period of the external loads, and I is the number of cycles. Define t^0 and t^γ by $t^0 = IT$ and $t^\gamma = (I+1)T$, respectively. Let t^μ $(\mu = 0, 1, \cdots, \gamma-1, \gamma)$ indicate an arbitrary instant between t^0 and t^γ, and let the superscript μ indicate the variables at $t = t^\mu$.

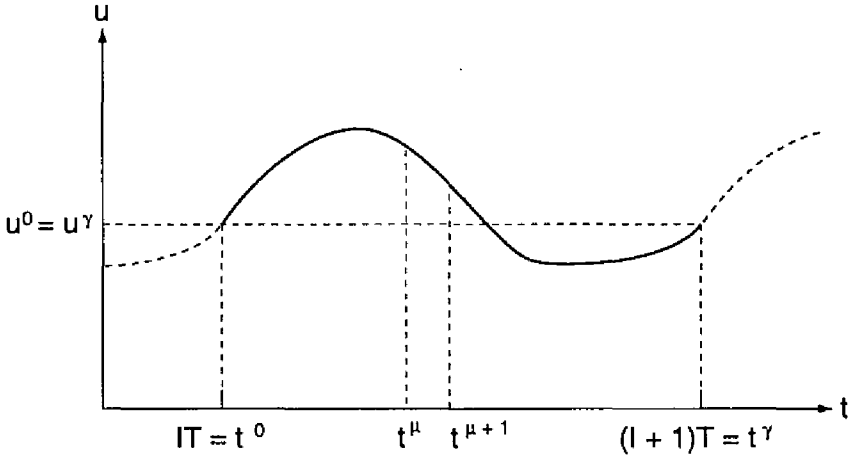

Figure 4.3: A steady state.

Suppose that, in the current steady state at $\tau = \tau_h$, all the equilibrium states are stable in the sense of Hill [7]. Then, when all the state variables are known at $t = t^\mu$, the state variables at the neighboring instant $t = t^{\mu+1}$ are expressed using Taylor-series expansions as

$$\mathbf{U}(t^{\mu+1}) = \mathbf{U}(t^\mu) + \mathbf{U}'(t^\mu)(t^{\mu+1} - t^\mu) + \frac{1}{2}\mathbf{U}''(t^\mu)\ (t^{\mu+1} - t^\mu)^2 + \cdots, \tag{4.10}$$

$$\mathbf{F}(t^{\mu+1}) = \mathbf{F}(t^\mu) + \mathbf{F}'(t^\mu)(t^{\mu+1} - t^\mu) + \frac{1}{2}\mathbf{F}''(t^\mu)\ (t^{\mu+1} - t^\mu)^2 + \cdots, \tag{4.11}$$

$$\mathbf{E}(t^{\mu+1}) = \mathbf{E}(t^\mu) + \mathbf{E}'(t^\mu)(t^{\mu+1} - t^\mu) + \frac{1}{2}\mathbf{E}''(t^\mu)\ (t^{\mu+1} - t^\mu)^2 + \cdots, \tag{4.12}$$

$$\mathbf{S}(t^{\mu+1}) = \mathbf{S}(t^\mu) + \mathbf{S}'(t^\mu)(t^{\mu+1} - t^\mu) + \frac{1}{2}\mathbf{S}''(t^\mu)\ (t^{\mu+1} - t^\mu)^2 + \cdots, \tag{4.13}$$

$$\mathbf{E}_p(t^{\mu+1}) = \mathbf{E}_p(t^\mu) + \mathbf{E}_p'(t^\mu)(t^{\mu+1} - t^\mu) + \frac{1}{2}\mathbf{E}_p''(t^\mu)\ (t^{\mu+1} - t^\mu)^2 + \cdots, \tag{4.14}$$

where the prime indicates the partial differentiation with respect to t, $\mathbf{U}$ and $\mathbf{F}$ denote respectively the nodal displacement vector and the nodal force vector, $\mathbf{E}$, $\mathbf{S}$ and $\mathbf{E}_p$ are the strain vector, the stress vector and the plastic strain vector, respectively. Both $\mathbf{U}$ and $\mathbf{F}$ have $3N$ components, and all $\mathbf{E}$, $\mathbf{S}$, $\mathbf{E}_p$ have M components.

Repeating the Taylor-series expansion, we can write the state variables at $t = t^\gamma$ $(\gamma \geq 1)$ as

$$\mathbf{U}^\gamma = \mathbf{U}^0 + \sum_{\mu=0}^{\gamma-1} \mathbf{U}^{\mu\prime}(t^{\mu+1} - t^\mu), \tag{4.15}$$

$$\mathbf{F}^\gamma = \mathbf{F}^0 + \sum_{\mu=0}^{\gamma-1} \mathbf{F}^{\mu\prime}(t^{\mu+1} - t^\mu), \tag{4.16}$$

$$\mathbf{E}^\gamma = \mathbf{E}^0 + \sum_{\mu=0}^{\gamma-1} \mathbf{E}^{\mu\prime}(t^{\mu+1} - t^\mu), \tag{4.17}$$

$$\mathbf{S}^\gamma = \mathbf{S}^0 + \sum_{\mu=0}^{\gamma-1} \mathbf{S}^{\mu\prime}(t^{\mu+1} - t^\mu), \tag{4.18}$$

$$\mathbf{E}_p^\gamma = \mathbf{E}_p^0 + \sum_{\mu=0}^{\gamma-1} \mathbf{E}_p^{\mu\prime}(t^{\mu+1} - t^\mu), \tag{4.19}$$

where the terms higher than the first order are truncated. As seen in Eqs. (4.15)-(4.19), the state variables at $t = t^\gamma$ are expressed in terms of the state variables at $t = t^0$, the instants t^μ $(0 \leq \mu \leq \gamma)$, and the derivatives with respect to t at $t = t^\mu$ $(0 \leq \mu \leq \gamma - 1)$. It should be noted that, by discretizing the equilibrium path, we can regard these quantities as the functions of only one parameter τ.

4.3.2 Tangent Stiffness Equations

In this subsection, the equations are shown for obtaining the partial derivatives with respect to t. For simplicity, we derive only the first-order derivatives. But more higher-order derivatives can be obtained with the equations derived by differentiating the tangent stiffness equations [17]. Suppose that all the state variables are known at $t = t^{\mu}$. Differentiating the strain-displacement relations (4.1)-(4.3) with respect to t, we have the following equations for $t = t^{\mu}$

$$\varepsilon^{\mu\prime} = \frac{\partial\, \varepsilon^{\mu}}{\partial\, u_i^{\mu}} u_i^{\mu\prime}. \tag{4.20}$$

Summation convention is used for the subscripts i, j and k which are varied from 1 to 6 throughout this chapter. Differentiation of the equilibrium condition (4.4) yields

$$f_i^{\mu\prime} = AL_0 \left(\sigma^{\mu\prime} \frac{\partial\, \varepsilon^{\mu}}{\partial\, u_i^{\mu}} + \sigma^{\mu} \frac{\partial^2\, \varepsilon^{\mu}}{\partial\, u_i^{\mu}\, \partial\, u_j^{\mu}} u_j^{\mu\prime} \right). \tag{4.21}$$

Differentiating Eqs. (4.5)-(4.7), we have

$$\sigma^{\mu\prime} = {}_T C^{\mu} \varepsilon^{\mu\prime} \tag{4.22}$$

in which ${}_T C^{\mu}$ is determined by

$${}_T C^{\mu} = E \qquad \text{in the elastic range,} \tag{4.23}$$

$${}_T C^{\mu} = E_t,\ \varepsilon' \geq 0 \qquad \text{for the loading response in tension,} \tag{4.24}$$

$${}_T C^{\mu} = E,\ \varepsilon' < 0 \qquad \text{for the unloading response in tension,} \tag{4.25}$$

$${}_T C^{\mu} = E_t,\ \varepsilon' \leq 0 \qquad \text{for the loading response in compression,} \tag{4.26}$$

$${}_T C^{\mu} = E,\ \varepsilon' > 0 \qquad \text{for the unloading response in compression.} \tag{4.27}$$

Substituting Eqs. (4.20) and (4.22) into Eq. (4.21), we have

$$f_i^{\mu\prime} = {}_T k_{ij}^{\mu} u_j^{\mu\prime} \tag{4.28}$$

where

$${}_T k_{ij}^{\mu} = AL_0 \left({}_T C^{\mu} \frac{\partial\, \varepsilon^{\mu}}{\partial\, u_i^{\mu}} \frac{\partial\, \varepsilon^{\mu}}{\partial\, u_j^{\mu}} + \sigma^{\mu} \frac{\partial^2\, \varepsilon^{\mu}}{\partial\, u_i^{\mu}\, \partial\, u_j^{\mu}} \right). \tag{4.29}$$

Assembling Eq. (4.28), we have the tangent stiffness equation for the total system

$$\mathbf{F}^{\mu\prime} = {}_T\mathbf{K}^{\mu} \mathbf{U}^{\mu\prime} \tag{4.30}$$

where ${}_T\mathbf{K}^{\mu}$ indicates the tangent stiffness matrix for the total system. Using the boundary conditions and specifying the value of $\lambda_c^{\mu'}$, we can solve Eq. (4.30). Substituting the solution $\mathbf{U}^{\mu'}$ into Eq. (4.20), we have $\mathbf{E}^{\mu'}$. Note that we should find the set of tangential stiffness coefficients ${}_TC^{\mu}$ that are consistent with the resulting signs of the components of $\mathbf{E}^{\mu'}$ [17]. Substitution of $\mathbf{E}^{\mu'}$ into Eq. (4.22) yields $\mathbf{S}^{\mu'}$. Differentiating Eq. (4.5) with respect to t, we have

$$\sigma^{\mu'} = E(\varepsilon^{\mu'} - \varepsilon_p^{\mu'}). \tag{4.31}$$

Substitution of $\mathbf{E}^{\mu'}$ and $\mathbf{S}^{\mu'}$ into Eq. (4.31) leads to $\mathbf{E}_p^{\mu'}$.

4.3.3 Termination Conditions for Incremental Steps

At every instant when any stiffness coefficient change discontinuously, an incremental step must be terminated. The conditions for the termination are written as follows:

$$\sigma_{yt} - \sigma^{\mu+1} = 0 \qquad \text{for yielding in tension,} \tag{4.32}$$

$$\sigma_{yc} - \sigma^{\mu+1} = 0 \qquad \text{for yielding in compression,} \tag{4.33}$$

$$\bar{\lambda}_c - \lambda_c^{\mu+1} = 0 \qquad \text{for load reversals} \tag{4.34}$$

where $\bar{\lambda}_c = \psi$ or $-\psi$. In addition, to prevent excessive accumulation of truncation errors, the incremental steps are terminated so that the following condition is satisfied.

$$t^{\mu+1} - t^{\mu} - \Delta\bar{t}_{max} = 0, \tag{4.35}$$

where $\Delta\bar{t}_{max}$ is a specified value. When only the first-order derivatives are taken into consideration, Eqs (4.33)-(4.35) become linear equations of $t^{\mu+1}$. The incremental step $\Delta t = t^{\mu+1} - t^{\mu}$ is determined as the smallest value among the values calculated by Eqs. (4.32)-(4.35).

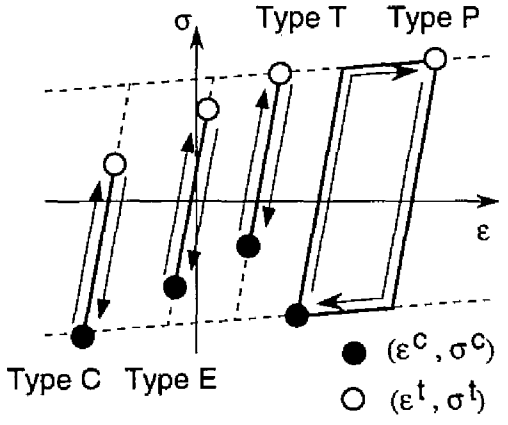

Figure 4.4: Classification of cyclic responses.

4.3.4 Stress-Strain Responses

For later discussion, we examine all the possible types of stress-strain cycles after convergence to steady states. Classification of the responses is shown in Fig. 4.4. The type E is the elastic shakedown state in which no equilibrium state exists on the strain hardening lines. The type T is the elastic shakedown states whose maximum stress reaches the strain hardening line in tension. The type C is the elastic shakedown states whose minimum stress reaches the strain hardening line in compression. The type P is the plastic shakedown state. The superscripts t and c indicate that the state variables for the equilibrium states at which strain take its maximum and minimum values in a cycle, respectively.

4.4 DEVIATION FROM STEADY STATES

4.4.1 Outline of Formulation

Consider deviation from a steady state due to the slight change of the amplitude of cyclic loads. This change is defined by $\Delta\tau = \tau_{h+1} - \tau_h$. The deviation from the steady state at $\tau = \tau_h$ in the period $t^0 \leq t \leq t^\gamma$ is illustrated in Fig. 4.5. To formulate the deviation, the following hypothesis is introduced:

Hypothesis 4.1: All the instants t^μ, the state variables at $t = t^\mu$ and its partial derivatives with respect t are the continuous and piecewisely differentiable functions of τ.

Then, using the Taylor-series expansion, we can write the state variables under the perturbed loading condition defined by $\tau = \tau_{h+1}$ as

$$\mathbf{U}^\mu(\tau_{h+1}) = \mathbf{U}^\mu(\tau_h) + \dot{\mathbf{U}}^\mu(\tau_h)\,(\tau_{h+1} - \tau_h) + \frac{1}{2}\ddot{\mathbf{U}}^\mu(\tau_h)\,(\tau_{h+1} - \tau_h)^2 + \cdots, \qquad (4.36)$$

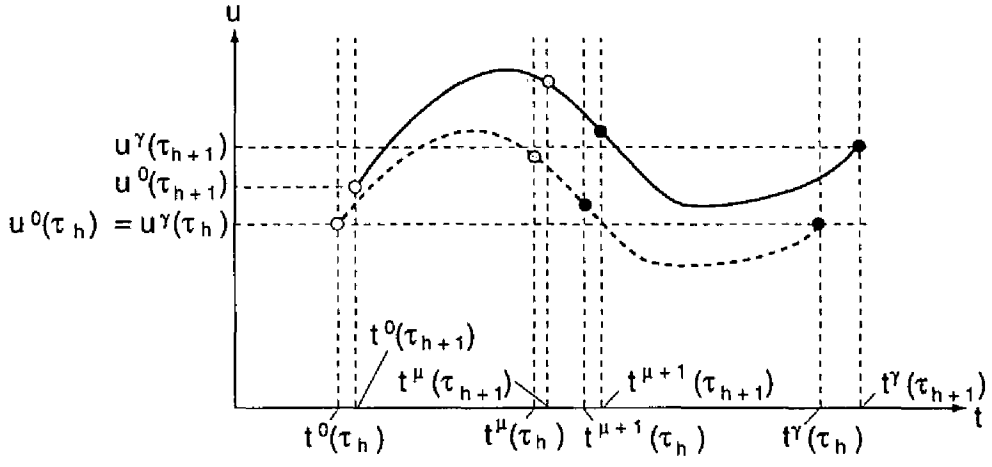

Figure 4.5: Deviation from a steady state.

$$\mathbf{F}^{\mu}(\tau_{h+1}) = \mathbf{F}^{\mu}(\tau_h) + \dot{\mathbf{F}}^{\mu}(\tau_h)(\tau_{h+1}-\tau_h) + \frac{1}{2}\ddot{\mathbf{F}}^{\mu}(\tau_h)(\tau_{h+1}-\tau_h)^2 + \cdots, \tag{4.37}$$

$$\mathbf{E}^{\mu}(\tau_{h+1}) = \mathbf{E}^{\mu}(\tau_h) + \dot{\mathbf{E}}^{\mu}(\tau_h)(\tau_{h+1}-\tau_h) + \frac{1}{2}\ddot{\mathbf{E}}^{\mu}(\tau_h)(\tau_{h+1}-\tau_h)^2 + \cdots, \tag{4.38}$$

$$\mathbf{S}^{\mu}(\tau_{h+1}) = \mathbf{S}^{\mu}(\tau_h) + \dot{\mathbf{S}}^{\mu}(\tau_h)(\tau_{h+1}-\tau_h) + \frac{1}{2}\ddot{\mathbf{S}}^{\mu}(\tau_h)(\tau_{h+1}-\tau_h)^2 + \cdots, \tag{4.39}$$

$$\mathbf{E}_p^{\mu}(\tau_{h+1}) = \mathbf{E}_p^{\mu}(\tau_h) + \dot{\mathbf{E}}_p^{\mu}(\tau_h)(\tau_{h+1}-\tau_h) + \frac{1}{2}\ddot{\mathbf{E}}_p^{\mu}(\tau_h)(\tau_{h+1}-\tau_h)^2 + \cdots, \tag{4.40}$$

where dot indicates the differentiation with respect to τ. For simplicity, our discussion in this paper is restricted to the case where all the terms higher than first order are neglected.

Now our object is to obtain the derivatives with respect to τ. A difficulty arises here because no direct stress rate-strain rate relation such as Eqs. (4.23)-(4.26) is given. The strategies to overcome this difficulty are outlined as follows:

1. To use the stress rate-strain rate relations obtained by differentiating (4.5), which is valid in any equilibrium state, with respect to τ. This idea was proposed by Uetani and Kobayashi [16]. Since plastic strains are included in the stress rate-strain rate relations, as shown in the next subsection, all the derivatives can be expressed as

$$\dot{\mathbf{U}}^{\mu} = \mathbf{H}_u^{\mu}\dot{\mathbf{E}}_p^{\mu} + \mathbf{h}_u^{\mu}, \tag{4.41}$$

$$\dot{\mathbf{F}}^{\mu} = \mathbf{H}_f^{\mu}\dot{\mathbf{E}}_p^{\mu} + \mathbf{h}_f^{\mu}, \tag{4.42}$$

$$\dot{\mathbf{E}}^{\mu} = \mathbf{H}_e^{\mu}\dot{\mathbf{E}}_p^{\mu} + \mathbf{h}_e^{\mu}, \tag{4.43}$$

$$\dot{\mathbf{S}}^{\mu} = \mathbf{H}_s^{\mu}\dot{\mathbf{E}}_p^{\mu} + \mathbf{h}_s^{\mu}, \tag{4.44}$$

   where $\mathbf{H}^{\mu}$ and $\mathbf{h}^{\mu}$ are the constant matrix vector, respectively.

2. To express the plastic strain rates at $t = t^{\mu}$ as

$$\dot{\mathbf{E}}_p^{\mu} = \mathbf{G}^{\mu}\dot{\mathbf{E}}_p^{0} + \mathbf{g}^{\mu}. \tag{4.45}$$

   where $\mathbf{G}^{\mu}$ and $\mathbf{g}^{\mu}$ are the constant matrix and vector, respectively. This relation is derived in the later subsection 4.4.3.

3. To obtain the recurrence equation that relates the plastic strain rates at the two consecutive periodic instants $t = t^0$ and $t = t^{\gamma}$ by substituting $\mu = \gamma$ into Eq. (4.45).

$$\dot{\mathbf{E}}_p^{\gamma} = \mathbf{G}^{\gamma}\dot{\mathbf{E}}_p^{0} + \mathbf{g}^{\gamma}. \tag{4.46}$$

   The plastic strain rate $\dot{\mathbf{E}}_p^0$ is obtained as the limit of the solution of the recurrence equation (4.46) as $I \to \infty$. Substituting $\dot{\mathbf{E}}_p^0$ into Eq. (4.45), we have $\dot{\mathbf{E}}_p^{\mu}$. Substitution of $\dot{\mathbf{E}}_p^{\mu}$ into Eqs. (4.41)-(4.44) yields the first-order derivatives at $t = t^{\mu}$.

4.4.2 Rate Relations at Arbitrary Instants

In this subsection, it is shown that all the first-order derivatives with respect to τ are expressed as Eqs. (4.41)-(4.44), which are the linear equations of $\dot{\mathbf{E}}_p^\mu$. Differentiating (4.1)-(4.4), we have the rate forms of strain-displacement relations as

$$\dot{\varepsilon}^\mu = \frac{\partial\, \varepsilon^\mu}{\partial\, u_i^\mu}\dot{u}_i^\mu. \tag{4.47}$$

The rate forms of equilibrium conditions are written as

$$\dot{f}_i^\mu = AL_0\left(\dot{\sigma}^\mu\frac{\partial\, \varepsilon^\mu}{\partial\, u_i^\mu} + \sigma^\mu\frac{\partial^2\, \varepsilon^\mu}{\partial\, u_i^\mu\, \partial\, u_j^\mu}\dot{u}_j^\mu\right). \tag{4.48}$$

Differentiating Eq. (4.5) yields

$$\dot{\sigma}^\mu = E(\dot{\varepsilon}^\mu - \dot{\varepsilon}_p^\mu). \tag{4.49}$$

Note that this relation is valid even if plastic loading occurs at $t = t^\mu$ and that $\dot{\varepsilon}^\mu$ is deliberately remained as unknowns in this formulation though $\varepsilon_p^{\mu\prime}$ is usually eliminated in the formulation for tracing equilibrium paths. Substitution of Eqs. (4.47) and (4.49) into Eq. (4.48) leads to

$$\begin{aligned}\dot{f}_i^\mu &= AL_0\left(E\frac{\partial\, \varepsilon^\mu}{\partial\, u_i^\mu}\frac{\partial\, \varepsilon^\mu}{\partial\, u_j^\mu} + \sigma^\mu\frac{\partial^2\, \varepsilon^\mu}{\partial\, u_i^\mu\, \partial\, u_j^\mu}\right)\dot{u}_j - AL_0E\frac{\partial\, \varepsilon^\mu}{\partial\, u_i^\mu}\dot{\varepsilon}_p^\mu \\ &= {}_Ek_{ij}^\mu\dot{u}_j^\mu + {}_Eb_i^\mu\dot{\varepsilon}_p^\mu,\end{aligned} \tag{4.50}$$

where ${}_Ek_{ij}^\mu$ is the coefficient of $\dot{u}_j^\mu$ and ${}_Eb_i^\mu$ is the coefficient of $\dot{\varepsilon}_p^\mu$. Assembling the rate equations (4.50) yields the rate relations for the total system

$$\dot{\mathbf{F}}^\mu = {}_E\mathbf{K}^\mu\dot{\mathbf{U}}^\mu + {}_E\mathbf{B}^\mu\dot{\mathbf{E}}_p^\mu, \tag{4.51}$$

where ${}_E\mathbf{K}$ and ${}_E\mathbf{B}$ are the coefficient matrices of $\dot{\mathbf{U}}$ and $\dot{\mathbf{E}}_p$, respectively. By using the boundary conditions and by arranging Eq. (4.51) as shown in Appendix A, we can express $\dot{\mathbf{F}}$ and $\dot{\mathbf{U}}$ as

$$\dot{\mathbf{F}}^\mu = \mathbf{H}_f^\mu\dot{\mathbf{E}}_p^\mu + \mathbf{h}_f^\mu, \tag{4.52}$$

$$\dot{\mathbf{U}}^\mu = \mathbf{H}_u^\mu\dot{\mathbf{E}}_p^\mu + \mathbf{h}_u^\mu, \tag{4.53}$$

in which $\mathbf{H}^\mu$ and $\mathbf{h}^\mu$ denote the constant matrix and constant vector, respectively, and the subscripts f and u indicate the variables corresponding to $\mathbf{F}$ and $\mathbf{U}$. Using the rate forms of the compatibility condition (4.47) and the stress-strain relation (4.49), we have

$$\dot{\mathbf{E}}^\mu = \mathbf{H}_e^\mu\dot{\mathbf{E}}_p^\mu + \mathbf{h}_e^\mu, \tag{4.54}$$

$$\dot{\mathbf{S}}^\mu = \mathbf{H}_s^\mu\dot{\mathbf{E}}_p^\mu + \mathbf{h}_s^\mu, \tag{4.55}$$

where the subscripts e and s indicate that the variables refer to those for $\mathbf{E}$ and $\mathbf{S}$.

4.4.3 Recurrence Relations between Consecutive Periodic Instants

Let us shown that the relation between $\dot{\mathbf{E}}_p^0$ and $\dot{\mathbf{E}}_p^\gamma$ are expressed as the recurrence relation (4.46). This is shown in two stages based on the procedure of the mathematical induction. First, obviously, we have

$$\dot{\mathbf{E}}_p^0 = \mathbf{G}^0\dot{\mathbf{E}}_p^0 + \mathbf{g}^0, \tag{4.56}$$

where $\mathbf{G}^0 = \mathbf{I}$ and $\mathbf{g}^0 = \mathbf{0}$. Next, assume that $\dot{\mathbf{E}}_p^\mu$ is assumed to be expressed as

$$\dot{\mathbf{E}}_p^\mu = \mathbf{G}^\mu\dot{\mathbf{E}}_p^0 + \mathbf{g}^\mu \tag{4.57}$$

and that $\dot{t}^\mu$ is written as

$$\dot{t}^\mu = \mathbf{g}_t^{\mu T}\dot{\mathbf{E}}_p^0 + g_t^\mu \tag{4.58}$$

in which $\mathbf{g}_t^\mu$ and g_t^μ are the constant vector and the constant, respectively, and the superscript T indicates the transpose of the vector. Then our problem is to show that $\dot{\mathbf{E}}_p^{\mu+1}$ is written as

$$\dot{\mathbf{E}}_p^{\mu+1} = \mathbf{G}^{\mu+1}\dot{\mathbf{E}}_p^0 + \mathbf{g}^{\mu+1}. \tag{4.59}$$

The incremental relation between $\mathbf{E}_p^\mu$ and $\mathbf{E}_p^{\mu+1}$ is expressed as

$$\mathbf{E}_p^{\mu+1} = \mathbf{E}_p^\mu + \mathbf{E}_p^{\mu\prime}(t^{\mu+1} - t^\mu), \tag{4.60}$$

where the higher-order terms with respect to t more than first order are neglected. Differentiating Eq. (4.60) with respect to τ, we have

$$\dot{\mathbf{E}}_p^{\mu+1} = \dot{\mathbf{E}}_p^\mu + \dot{\mathbf{E}}_p^{\mu\prime}(t^{\mu+1} - t^\mu) + \mathbf{E}_p^{\mu\prime}(\dot{t}^{\mu+1} - \dot{t}^\mu). \tag{4.61}$$

Here, from the assumptions, $\dot{\mathbf{E}}_p^\mu$ and $\dot{t}^\mu$ in Eq. (4.61) are expressed as the linear equations of $\dot{\mathbf{E}}_p^0$. The variables $t^\mu, t^{\mu+1}$ and $\mathbf{E}_p^{\mu\prime}$ can be regarded as constants since they are the known quantities in the current steady state at $\tau = \tau_h$. Since, as shown in Appendix B, both $\dot{\mathbf{E}}_p^{\mu\prime}$ and $\dot{t}^{\mu+1}$ are expressed as

$$\dot{\mathbf{E}}_p^{\mu\prime} = \mathbf{R}_p^\mu\dot{\mathbf{E}}_p^0 + \mathbf{r}_p^\mu, \tag{4.62}$$

$$\dot{t}^{\mu+1} = \mathbf{g}_t^{\mu+1T}\dot{\mathbf{E}}_p^0 + g_t^{\mu+1}, \tag{4.63}$$

where $\mathbf{R}_p^\mu$ and $\mathbf{r}_p^\mu$ are the constant matrix and the constant vector, respectively. Now we can express $\dot{\mathbf{E}}_p^{\mu+1}$ as the linear equation of $\dot{\mathbf{E}}_p^0$.

Substituting Eqs. (4.58), (4.62) and (4.63) into Eq. (4.61) and comparing it with Eq. (4.59), we have

$$\mathbf{G}^{\mu+1} = \mathbf{G}^{\mu} + \mathbf{R}_p^{\mu}\left(t^{\mu+1} - t^{\mu}\right) + \mathbf{E}_p^{\mu\prime}\left(\mathbf{g}_t^{\mu+1} - \mathbf{g}_t^{\mu}\right)^T, \tag{4.64}$$

$$\mathbf{g}^{\mu+1} = \mathbf{g}^{\mu} + \mathbf{r}_p^{\mu}\left(t^{\mu+1} - t^{\mu}\right) + \mathbf{E}_p^{\mu\prime}\left(g_t^{\mu+1} - g_t^{\mu}\right). \tag{4.65}$$

Repeating the procedure shown in Eqs. (4.64) and (4.65), we obtain the relations

$$\mathbf{G}^{\gamma} = \mathbf{G}^{0} + \sum_{\mu=0}^{\gamma-1}\left[\mathbf{R}_p^{\mu}\left(t^{\mu+1} - t^{\mu}\right) + \mathbf{E}_p^{\mu\prime}\left(\mathbf{g}_t^{\mu+1} - \mathbf{g}_t^{\mu}\right)^T\right], \tag{4.66}$$

$$\mathbf{g}_p^{\gamma} = \mathbf{g}_p^{0} + \sum_{\mu=0}^{\gamma-1}\left[\mathbf{r}_p^{\mu}\left(t^{\mu+1} - t^{\mu}\right) + \mathbf{E}_p^{\mu\prime}\left(g_t^{\mu+1} - g_t^{\mu}\right)\right], \tag{4.67}$$

where $\mathbf{G}^0 = \mathbf{I}$, $\mathbf{g}^0 = \mathbf{0}$, $\mathbf{g}_t^0 = \mathbf{0}$ and $g_t^0 = I(T(\tau_{h+1}) - T(\tau_h))$.

4.4.4 Stress-Strain Responses

According to the types of the stress-strain responses in a steady cycle, the types of those in the deviation from the steady cycle are classified into the four types shown in Fig. 4.6. When the current type is E, the type of the deviation is the type (E), where no plastic deformation occurs in a period. If the current type of the response is T, the type of the disturbance is the type (E) or the type (T). In the type (T), plastic loading occurs only in tension. If the current type of the response is C, the type of the disturbance is the type (C) or (E). In the type (C), plastic loading occurs in compression. When the current type of the response is P, the type of the deviation is the type (P), where plastic deformation occurs in both tension and compression.

When the type in a steady cycle is T or C, the type in the deviation can not be determined uniquely. In addition, if yielding occur in more than one element at the same instant in

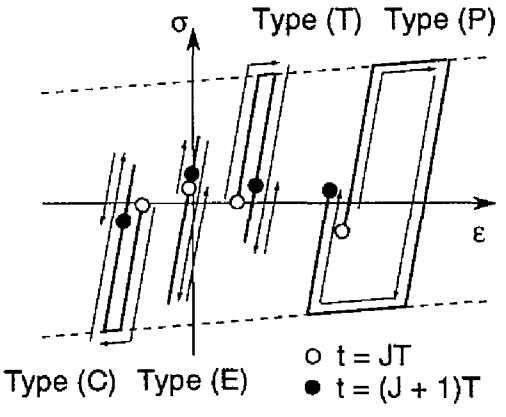

Figure 4.6: Classification of transient responses.

the steady-state response, the order of the instants in the deviation cannot be determined uniquely. Hence if such situation takes place, the types of the response and the order of the instants should be assumed in constructing the recurrence equation (4.46).

4.5 STABILITY OF STEADY STATES

4.5.1 Definition of Stability

Following the definition of stability of solution due to Liapunov [2], the concept of *stability of steady states* is simply stated as "*a steady state is stable if a small change in loading condition leads to a small deviation in the responses*". Note that the small change in the loading condition is given as the level of external loads here, while that is given as initial conditions in the definition by Liapunov.

The rigorous definition of the stability is stated as

Definition 4.1 For an arbitrary positive number ϵ, if there exists a positive number δ such that every solution with $|\Delta\tau| < \delta$ satisfies the inequality $\Delta U(t) < \epsilon$ for all times $t \geq 0$, the steady state is called stable.

Here, $\Delta U(t)$ is the norm defined by

$$\begin{aligned} \Delta U(t) &= \|\mathbf{U}(\tau + \Delta\tau, t) - \mathbf{U}(\tau, t)\| \\ &= \left\{ \sum_{n=1}^{3N} [U_n(\tau + \Delta\tau, t) - U_n(\tau, t)]^2 \right\}^{\frac{1}{2}} \end{aligned} \tag{4.68}$$

where the subscript n indicates the number of the component of $\mathbf{U}$.

4.5.2 Stability Criterion

As shown in the previous section, if the type of the stress-strain responses under the perturbed loading condition is assumed, the relation between the plastic strain rates at periodic instants $t = IT$ and $t = (I+1)T$ are uniquely expressed in the form of recurrence equation Eq. (4.46)

$$\dot{\mathbf{E}}_p^{\gamma} = \mathbf{G}^{\gamma} \dot{\mathbf{E}}_p^{0} + \mathbf{g}.$$

This equation can be partitioned as

$$\begin{Bmatrix} \bar{\dot{\mathbf{E}}}_p^{\gamma} \\ \hline \tilde{\dot{\mathbf{E}}}_p^{\gamma} \end{Bmatrix} = \left[\begin{array}{c|c} \tilde{\mathbf{G}} & \mathbf{0} \\ \hline \mathbf{0} & \mathbf{I} \end{array}\right] \begin{Bmatrix} \bar{\dot{\mathbf{E}}}_p^{0} \\ \hline \tilde{\dot{\mathbf{E}}}_p^{0} \end{Bmatrix} + \begin{Bmatrix} \bar{\mathbf{g}} \\ \hline \tilde{\mathbf{g}} \end{Bmatrix}, \tag{4.69}$$

where $\bar{\dot{\mathbf{E}}}$ indicate the plastic strain rates of the elements in which no plastic deformation occurs in a period, $\tilde{\dot{\mathbf{E}}}$ indicate those of the other elements, and $\tilde{\mathbf{G}}$ is the coefficient matrix of $\tilde{\dot{\mathbf{E}}}_p^0$. The displacement rate $\dot{\mathbf{U}}^0$ is expressed as the linear equation of $\dot{\mathbf{E}}_p^0$ as far as ${}_E\mathbf{K}$ is positive definite as shown in subsection 4.4.2. The stability criterion is therefore written in terms of the eigenvalues of $\tilde{\mathbf{G}}$ as

Theorem 4.1 Suppose that the maximum absolute eigenvalue of $\tilde{\mathbf{G}}$ is less than one for all the possible combinations of the types of the stress-strain response to the incremental change in loading condition. And suppose that all the equilibrium states are stable in the sense of Hill [7]. Then the steady state is stable.

Since the number of the combination are finite, it is theoretically possible to examine all the possible combinations. It must be recognized here that, without this criterion, one has to perform equilibrium path analysis for infinite number of the pattern change in the loading conditions in order to ensure the stability. And it is generally very difficult to examine by using the equilibrium analysis whether or not the transient response converges to a steady state as $I \rightarrow \infty$ because of the accumulation of numerical errors.

However, if the number of elements exhibiting the type T or C becomes large, it seems to virtually impossible to examine all the possible combinations. To obtain more practical stability criterion that can be used in this case, the following two hypotheses are introduced. Let $\tilde{\mathbf{G}}_L$ indicate $\tilde{\mathbf{G}}$ that is constructed in the case where all the elements exhibiting the type T and C exhibit (T) and (C), respectively. Then the hypotheses are given as:

Hypothesis 4.2 The values of the components of $\tilde{\mathbf{G}}$ are independent of the order of the yielding times of the elements exhibiting type (T) or (C).

Hypothesis 4.3 The maximum absolute eigenvalue of $\tilde{\mathbf{G}}_L$ is less than or equal to those of $\tilde{\mathbf{G}}$ constructed for all the possible combinations of the types of the stress-strain response in the perturbed response.

On the basis of Hypotheses 4.2 and 4.3, a more relaxed and practical stability criterion is give by the following theorem.

Theorem 4.2 The steady state is stable if the maximum absolute eigenvalue of $\tilde{\mathbf{G}}_L$ is less than one.

Here, theorems 4.1 and 4.2 states the sufficient conditions for the stability of a steady state.

4.6 STEADY-STATE LIMIT

4.6.1 Outline of Formulation

In this section, a method is presented for finding the steady state limit. For the structures under an idealized cyclic loading program with continuously increasing amplitude shown in Fig. 4.7, the steady-state limit is defined as the critical amplitude beyond which the structures no convergence occurs to any steady state.

In the method, variation of a steady state under the idealized cyclic loading program is traced by repeating the Taylor-series expansions (4.15)-(4.19). The derivatives with respect to τ is obtained using the recurrence equation (4.46). The steady-state limit is found as the critical steady state at which loss of the stability of steady states occur.

4.6.2 Rate Relations for Variation of Steady States

As mentioned in the previous sections, when all the state variables are known in the current steady state at $\tau = \tau_h$, variation of the response is described using the recurrence equation (4.46)

$$\dot{\mathbf{E}}_p^{\gamma} = \mathbf{G}^{\gamma}\dot{\mathbf{E}}_p^{0} + \mathbf{g}.$$

If the current steady state is stable, the limit of the solution of recurrence equation Eq. (4.46) as $I \rightarrow \infty$ can be obtained as the solution of the simultaneous equation

$$\tilde{\dot{\mathbf{E}}}_p^{\gamma} = \tilde{\mathbf{G}}\tilde{\dot{\mathbf{E}}}_p^{0} + \tilde{\mathbf{g}}, \tag{4.70}$$

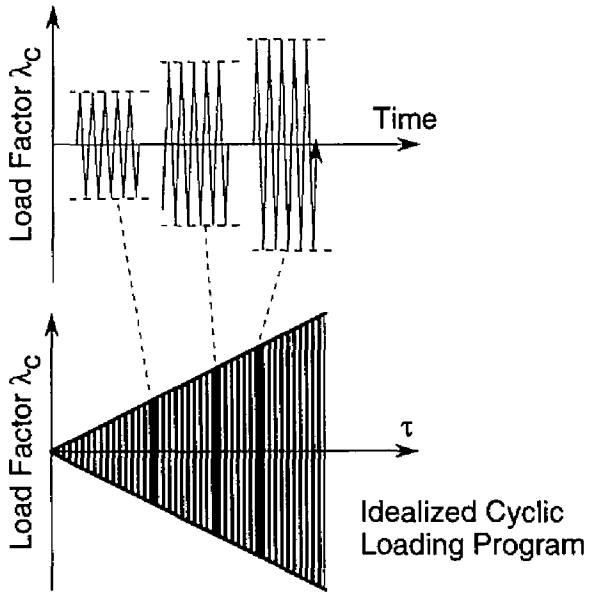

Figure 4.7: The idealized cyclic loading program.

$$\overset{\nabla}{\mathbf{E}}{}_p^{\gamma} = \overset{\nabla}{\mathbf{E}}{}_p^{0}, \tag{4.71}$$

$$\overset{\nabla}{\mathbf{E}}{}_p^{0} = \mathbf{0}. \tag{4.72}$$

Substituting the solution of the simultaneous equations into Eqs. (4.41)-(4.44) and (4.45), we have all the derivatives at $t = t^{\mu}$ with respect to τ.

4.6.3 Consistent Set of Stress-Strain Responses

When an element exhibits type T in the current steady state at $\tau = \tau_h$, the type in the deviation from the steady state is the type (T) or (E). Similar is the case when an element exhibits type C. In constructing the rate relations for variation of a steady state, we assume the type in the deviation for the elements exhibiting the type C and T. On the other hand, direction of the plastic deformation occurred in the transient process between two consecutive steady states must be consistent with the assumed type of the transient response. Therefore, for all the elements exhibiting the type T or the type C behavior, we should choose a set of the stress-strain responses that are consistent with the signs of the resulting strain rates. In addition, when yielding occur in more than one element at the same instant in the current steady state, the order of the instants in the deviation may be different and cannot be determined uniquely. The order is assumed in obtaining the rate relations, and the resulting order should be checked whether they are consistent with the assumptions or not.

To find the consistent set of the stress-strain responses, we employ a trial and error approach. In the trial and error approach, first, we assume the type of the stress-strain responses and the order of instants if necessary. Then, the rate equations are constructed and solved. The consistency is checked between the assumption and the results. This procedure is continued until all the assumptions are consistent with the results.

4.6.4 Termination Conditions for Incremental Steps

When the types of the stress-strain responses in steady states change as shown in Fig. 4.8, different types of the stress-strain responses in deviation should be used in constructing the recurrence equation (4.46). Incremental steps $\Delta\tau$ is therefore determined considering the conditions for the transition of the types of the stress-strain responses in steady states.

The step length $\Delta\tau$ is selected as the smallest positive value among the values calculated from the following conditions (4.73)-(4.79):

$$\sigma_{yt}^{\mu} - \sigma^{\mu}(\tau_{h+1}) = 0, \tag{4.73}$$

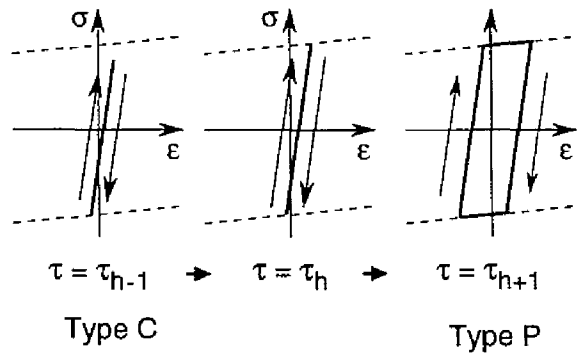

Figure 4.8: An example of variation of a cyclic response.

$$\sigma_{yc}^{\mu} - \sigma^{\mu}(\tau_{h+1}) = 0, \tag{4.74}$$

$$\sigma^{t}(\tau_{h+1}) - \sigma^{c}(\tau_{h+1}) - 2\sigma_y = 0, \tag{4.75}$$

$$\sigma^{\mu}(\tau_{h+1}) - \sigma_{yt}^{\beta}(\tau_{h+1}) = 0, \quad \text{if } \sigma^{\beta} = \sigma_{yc}^{\beta} \text{ at } \tau = \tau_h, \tag{4.76}$$

$$\sigma^{\mu}(\tau_{h+1}) - \sigma_{yc}^{\beta}(\tau_{h+1}) = 0, \quad \text{if } \sigma^{\beta} = \sigma_{yt}^{\beta} \text{ at } \tau = \tau_h, \tag{4.77}$$

where the superscript β indicate the variables for the equilibrium states at which the last unloading occurs before $t = t^{\mu}$. Note that both of the subsequent yield stresses are given by substituting ε_p^{μ} into Eqs. (4.8) and (4.9). In addition, the order of the instants t^{μ} and $t^{\mu+1}$ in a steady state may be different when τ is changed. In this case, the incremental step should be terminated using the condition given by

$$t^{\mu}(\tau_{h+1}) - t^{\mu+1}(\tau_{h+1}) = 0. \tag{4.78}$$

Besides the conditions above, the step length $\Delta\tau$ should be kept small enough to prevent excessive accumulation of truncation errors. Hence the incremental steps are terminated by

$$\Delta\tau - \Delta\bar{\tau}_{max} = 0. \tag{4.79}$$

4.6.5 Steady-State Limit Condition

In the preceding chapters, the steady-state limit has been characterized as the first limit point of the steady-state path. That is, the steady-state limit has been characterized by $\dot{\psi} \leq 0$. On the other hand, in this section, the steady-state limit is found as the steady state at which the loss of the stability of steady states occurs.

4.7 NUMERICAL EXAMPLES

The proposed method is applied to the two-bar and ten-bar trusses shown in Figs. 4.9 and 4.10, respectively. To show the validity of the proposed method, the results of the proposed method is compared to those obtained by the method presented in the previous chapters.

The cross-sectional areas of the the ten-bar truss are as follows: $A_{(1)} = A_{(4)} = A_{(5)} = 11$ cm^2, $A_{(2)} = A_{(3)} = 1.1$ cm^2, $A_{(6)} = A_{(9)} = A_{(10)} = 10$ cm^2, and $A_{(7)} = A_{(8)} = 1$ cm^2, and those of the two-bar truss are $A_{(1)} = A_{(2)} = 10$ cm^2. The ten-bar and two-bar trusses obey a bi-linear kinematic hardening rule with $E = 1.961 \times 10^2$GPa, $E_t = 0.01E$, and $\sigma_y = 2.942 \times 10^2$MPa.

The constant forces and the cyclic forced displacements are denoted by $\lambda_0 \bar{F}_0$ and $\lambda_c \bar{U}_c$, respectively. The constants are set to be $\bar{F}_0 = 9.807 \times 10^3$N and $\bar{U}_c = 1$cm. For the ten-bar truss, λ_0 is set to be $\lambda_0 = 28.27$ and $\lambda_0 = 14.94$. As shown in the last chapter, in the case of $\lambda_0 = 14.94$, strain reversals occur not only at load reversals but at yielding points. The load factor λ_0 is set to be $\lambda_0 = 5.000$ for the two-bar truss.

For the present and previous methods, several constants should be specified. In the present method, we specify the values of $\Delta \bar{t}_{max}$, $\Delta \bar{\tau}_{max}$ and the highest order of the derivatives taken

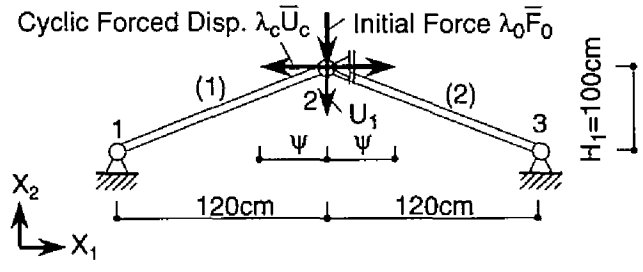

Figure 4.9: The two-bar truss.

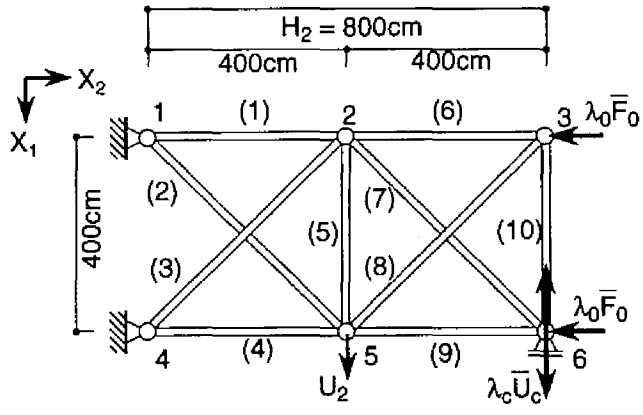

Figure 4.10: The ten-bar truss.

into account with respect to both t and τ. Throughout the analysis, the higher-order terms more than and equal to second order is neglected for both of the derivatives. For the ten-bar truss, these constants are $\Delta\bar{t}_{max} = \Delta\bar{\tau}_{max} = 0.2$ under $\lambda_0 = 28.27$, and $\Delta\bar{t}_{max} = 0.2$ and $\Delta\bar{\tau}_{max} = 0.002$ under $\lambda_0 = 14.94$. And they are $\Delta\bar{t}_{max} = \Delta\bar{\tau}_{max} = 0.001$ for the two-bar truss. On the other hand, in the previous method, $\Delta\bar{\tau}_{max}$ and the highest order of the derivatives taken into consideration with respect to τ is specified. These are set to be identical to those for the present method.

Variation of the maximum absolute eigenvalues of $\tilde{\mathbf{G}}_L$ is shown in Figs. 4.11- 4.13. The steady-state path obtained by the previous and the present method are illustrated in Figs. 4.14-4.16. The solid lines show the steady-state path obtained by the previous method. The white circles indicate the results obtained by the present method. For the ten-bar truss under $\lambda_0 = 28.27$ and $\lambda_0 = 14.94$ and the two-bar truss, the values of the steady-state limit ψ_{ssl} predicted by the present method are $\psi_{ssl} = 2.590$, $\psi_{ssl} = 13.17$ and $\psi_{ssl} = 0.1200$, respectively. Those obtained by the previous method are $\psi_{ssl} = 2.589$, $\psi_{ssl} = 13.16$ and $\psi_{ssl} = 0.1199$. From these figures and values, it may be stated that good agreement is observed between the steady state limits predicted by the previous and the current methods.

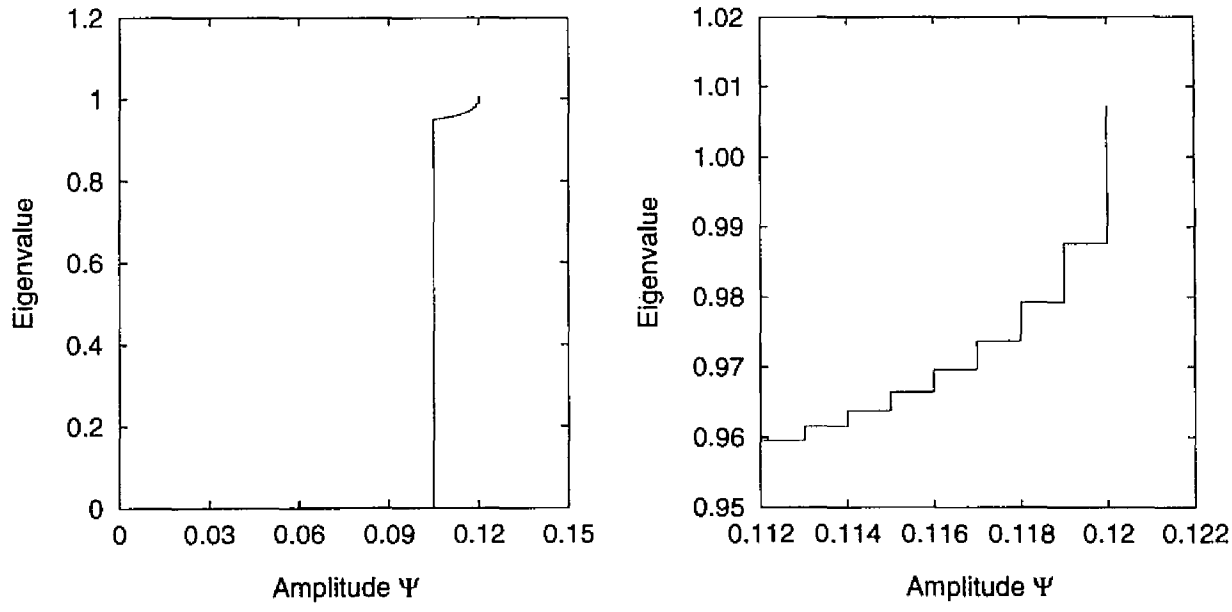

Figure 4.11: Variation of maximum absolute eigenvalue of $\tilde{\mathbf{G}}_L$ for the two-bar truss.

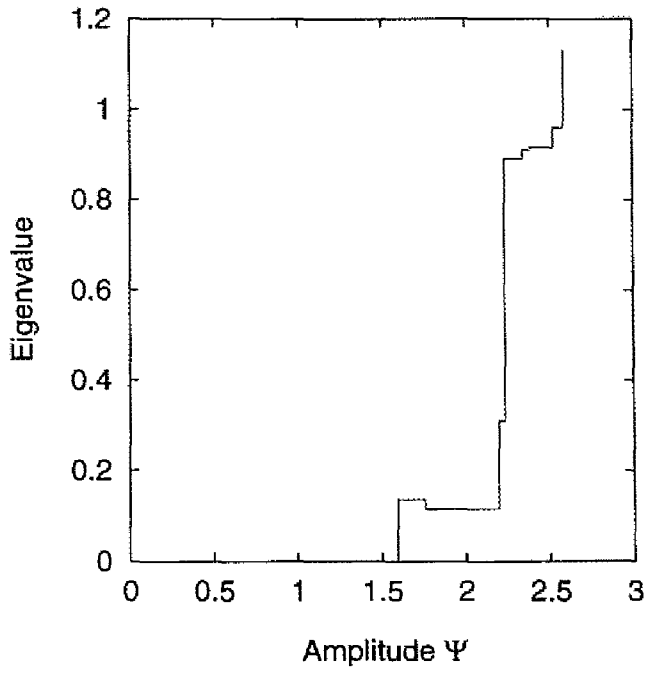

Figure 4.12: Variation of maximum absolute eigenvalue of $\tilde{\mathbf{G}}_L$ for the ten-bar truss under $\lambda_0/\lambda_b = 0.70$.

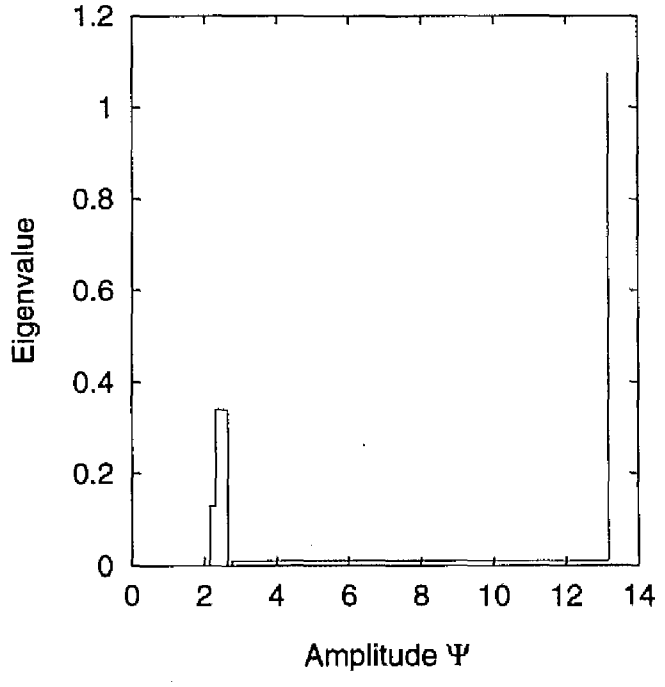

Figure 4.13: Variation of maximum absolute eigenvalue of $\tilde{\mathbf{G}}_L$ for the ten-bar truss under $\lambda_0/\lambda_b = 0.37$.

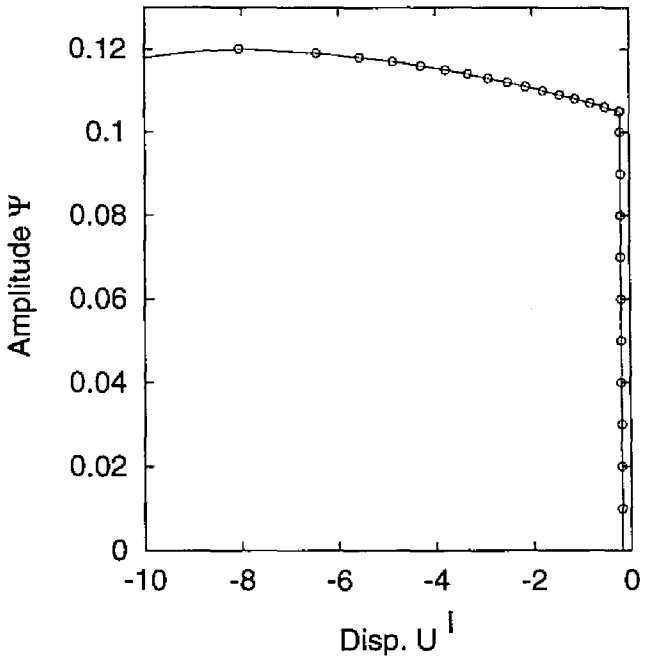

Figure 4.14: Steady-state path for the two-bar truss.

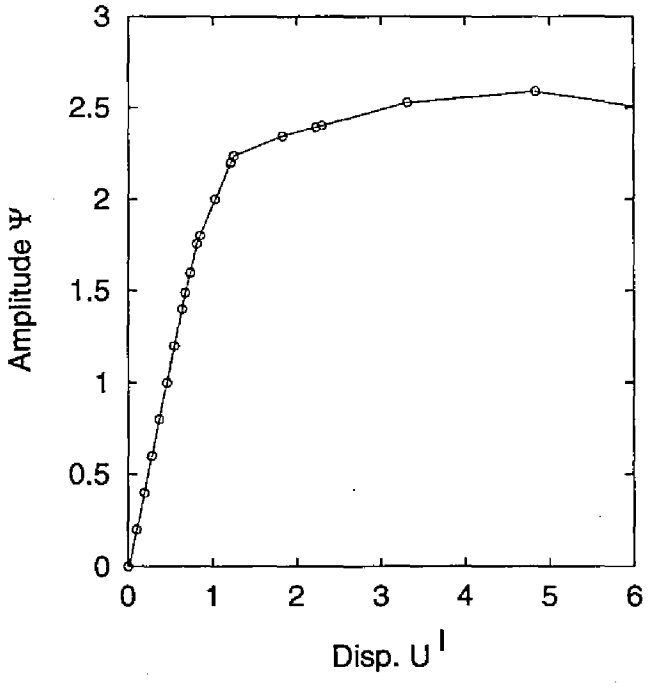

Figure 4.15: Steady-state path for the ten-bar truss under $\lambda_0/\lambda_b = 0.70$.

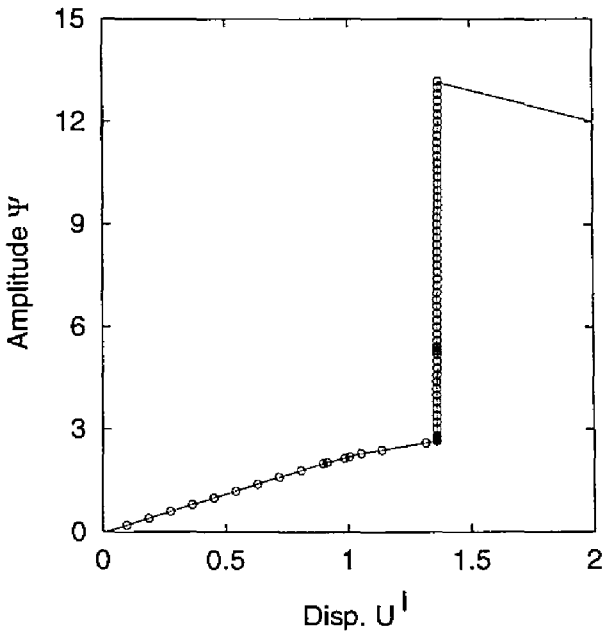

Figure 4.16: Steady-state path for the ten-bar truss under $\lambda_0/\lambda_b = 0.37$.

4.8 CONCLUSIONS

For elastoplastic trusses subjected to quasi-static cyclic loads in the presence of constant loads, a theory has been presented for finding the steady-state limit as the critical steady state, which, roughly speaking, bounds the convergence and divergence of plastic deformations. The following conclusion is made on this research.

1. Deviation from a steady-state response due to change of the amplitude of cyclic loads has been formulated using the recurrence equations that relates the plastic strains at two consecutive periodic instants.
2. The concept of stability of steady states has been introduced to quasi-static problem of elastoplastic structures. A new stability criterion has been derived using the eigenvalue of the coefficient matrix in the recurrence equations. Since this criterion may be difficult to apply the trusses with a number of elements, a more relaxed criterion has been presented by introducing two hypotheses on the combination of stress-strain responses.
3. Using the recurrence equations, a method has been presented for tracing the variation of a steady state under an idealized cyclic loading program with continuously increasing amplitude. The steady-state limit is found as the critical steady state at which the stability of steady state is lost.
4. Through numerical examples, validity of the present method has been presented. Good agreement has been shown between the results obtained by the proposed method and those obtained by the method presented in the previous chapters.

Appendix A. Relations between $\dot{\mathbf{U}}^{\mu}$, $\dot{\mathbf{F}}^{\mu}$ and $\dot{\mathbf{E}}_p^{\mu}$

According to boundary conditions, Eq. (4.51) can be arranged into

$$\left\{\begin{array}{c}\dot{\lambda}_c\bar{\mathbf{F}}\\ \hdashline \dot{\tilde{\mathbf{F}}}\end{array}\right\} = \left[\begin{array}{c:c}\mathbf{K}^{aa} & \mathbf{K}^{ab}\\ \hdashline \mathbf{K}^{ba} & \mathbf{K}^{bb}\end{array}\right]\left\{\begin{array}{c}\dot{\tilde{\mathbf{U}}}\\ \hdashline \dot{\lambda}_c\bar{\mathbf{U}}\end{array}\right\} + \left[\begin{array}{c:c}\mathbf{B}^{aa} & \mathbf{B}^{ab}\\ \hdashline \mathbf{B}^{ba} & \mathbf{B}^{bb}\end{array}\right]\left\{\begin{array}{c}\dot{\mathbf{E}}_p^a\\ \hdashline \dot{\mathbf{E}}_p^b\end{array}\right\} \tag{4.80}$$

where bar and the tilde indicate that the vectors corresponds to the known and unknown vectors, and the subscript a and b are used only for distinguishing the vectors corresponding to the known and unknown vectors. Suppose that $\mathbf{K}_{aa}$ is not singular. Then Eq. (4.80) can be written as

$$\left\{\begin{array}{c}\dot{\tilde{\mathbf{U}}}\\ \hdashline \dot{\lambda}_c\bar{\mathbf{U}}\end{array}\right\} = \left[\begin{array}{c:c}-\mathbf{K}^{aa-1}\mathbf{B}^{aa} & -\mathbf{K}^{aa-1}\mathbf{B}^{ab}\\ \hdashline \mathbf{0} & \mathbf{0}\end{array}\right]\left\{\begin{array}{c}\dot{\mathbf{E}}_p^a\\ \hdashline \dot{\mathbf{E}}_p^b\end{array}\right\} + \dot{\lambda}_c\left\{\begin{array}{c}\mathbf{K}^{aa-1}\bar{\mathbf{F}} - \mathbf{K}^{ab}\bar{\mathbf{U}}\\ \hdashline \bar{\mathbf{U}}\end{array}\right\} \tag{4.81}$$

$$\left\{\begin{array}{c}\dot{\lambda}_c\bar{\mathbf{F}}\\ \hdashline \dot{\tilde{\mathbf{F}}}\end{array}\right\} = \left[\begin{array}{c:c}\mathbf{0} & \mathbf{0}\\ \hdashline -\mathbf{K}^{ba}\mathbf{K}^{aa-1}\mathbf{B}^{aa} + \mathbf{B}^{ba} & -\mathbf{K}^{ba}\mathbf{K}^{aa-1}\mathbf{B}^{ab} + \mathbf{B}^{bb}\end{array}\right]\left\{\begin{array}{c}\dot{\mathbf{E}}_p^a\\ \hdashline \dot{\mathbf{E}}_p^b\end{array}\right\}$$

$$+\dot{\lambda}_c\left\{\begin{array}{c}\bar{\mathbf{F}}\\ \hdashline \mathbf{K}^{ba}\left(\mathbf{K}^{aa-1}\bar{\mathbf{F}} - \mathbf{K}^{ab}\bar{\mathbf{U}}\right) + \mathbf{K}^{bb}\bar{\mathbf{U}}\end{array}\right\}. \tag{4.82}$$

By substituting the specified value of $\dot{\lambda}_c$ into Eqs (4.81) and (4.82), we obtain Eq. (4.53) and Eq. (4.52), respectively.

Appendix B. Relations between $\dot{\mathbf{E}}_p^{\mu'}$, $\dot{t}^{\nu+1}$ and $\dot{\mathbf{E}}_p^0$

First, consider the relation between $\dot{\mathbf{E}}_p^{\mu'}$ and $\dot{\mathbf{E}}_p^0$. Differentiating Eqs. (4.28) and (4.29) with respect to τ and substituting Eq. (4.49) into it, we have

$$\dot{f}_i^{\mu'} = {}_T k_{ij}^{\mu}\dot{u}_i^{\mu'} + {}_T a_{ij}^{\mu}\dot{u}_j^{\mu} + {}_T b_i^{\mu}\dot{\varepsilon}_p^{\mu}. \tag{4.83}$$

where

$${}_T k_{ij}^{\mu} = AL_0\left({}_T C^{\mu}\frac{\partial\,\varepsilon^{\mu}}{\partial\,u_i^{\mu}}\frac{\partial\,\varepsilon^{\mu}}{\partial\,u_j^{\mu}} + \sigma^{\mu}\frac{\partial^2\,\varepsilon^{\mu}}{\partial\,u_i^{\mu}\,\partial\,u_j^{\mu}}\right), \tag{4.84}$$

$${}_T a_{ij}^{\mu} = AL_0 u_k^{\mu'}\left({}_T C^{\mu}\frac{\partial^2\,\varepsilon^{\mu}}{\partial\,u_i^{\mu}\,\partial\,u_j^{\mu}}\frac{\partial\,\varepsilon^{\mu}}{\partial\,u_k} + {}_T C^{\mu}\frac{\partial\,\varepsilon^{\mu}}{\partial\,u_i^{\mu}}\frac{\partial^2\,\varepsilon^{\mu}}{\partial\,u_j^{\mu}\,\partial\,u_k^{\mu}} + E\frac{\partial^2\,\varepsilon^{\mu}}{\partial\,u_i^{\mu}\,\partial\,u_k^{\mu}}\frac{\partial\,\varepsilon^{\mu}}{\partial\,u_j^{\mu}}\right) \tag{4.85}$$

$${}_T b_i^{\mu} = -AL_0 E\frac{\partial^2\,\varepsilon^{\mu}}{\partial\,u_i^{\mu}\,\partial\,u_j^{\mu}}u_j^{\mu'}. \tag{4.86}$$

Assembling Eq. (4.83), we have the equation for the total system

$$\dot{\mathbf{F}}^{\mu'} = {}_T\mathbf{K}^{\mu}\dot{\mathbf{U}}^{\mu'} + {}_T\mathbf{A}^{\mu}\dot{\mathbf{U}}^{\mu} + {}_T\mathbf{B}^{\mu}\dot{\mathbf{E}}_p^{\mu} \tag{4.87}$$

where ${}_T\mathbf{K}$, ${}_T\mathbf{A}$ and ${}_T\mathbf{B}$ are the coefficient matrices of $\dot{\mathbf{U}}^{\mu'}$, $\dot{\mathbf{U}}^{\mu}$ and $\dot{\mathbf{E}}_p^{\mu}$. Substituting Eqs. (4.53) and (4.57) into Eq. (4.87) and arranging it, we obtain

$$\dot{\mathbf{F}}^{\mu'} = \mathbf{R}_f^{\mu}\dot{\mathbf{E}}_p^{0} + \mathbf{r}_f^{\mu}, \tag{4.88}$$

$$\dot{\mathbf{U}}^{\mu'} = \mathbf{R}_u^{\mu}\dot{\mathbf{E}}_p^{0} + \mathbf{r}_u^{\mu}. \tag{4.89}$$

Differentiating Eqs. (4.20), (4.22) and (4.31) with respect to τ, we have

$$\dot{\varepsilon}^{\mu'} = \frac{\partial^2 \varepsilon^{\mu}}{\partial u_i^{\mu} \partial u_j^{\mu}} u_i^{\mu'} \dot{u}_j^{\mu} + \frac{\partial \varepsilon}{\partial u_i} \dot{u}_i^{\mu'}, \tag{4.90}$$

$$\dot{\sigma}^{\mu'} = {}_TC^{\mu}\dot{\varepsilon}^{\mu'}, \tag{4.91}$$

$$\dot{\sigma}^{\mu'} = E(\dot{\varepsilon}^{\mu'} - \dot{\varepsilon}_p^{\mu'}) \tag{4.92}$$

By using these relations, other state variables can be expressed as

$$\dot{\mathbf{E}}^{\mu'} = \mathbf{R}_e^{\mu}\dot{\mathbf{E}}_p^{0} + \mathbf{r}_e^{\mu}, \tag{4.93}$$

$$\dot{\mathbf{S}}^{\mu'} = \mathbf{R}_s^{\mu}\dot{\mathbf{E}}_p^{0} + \mathbf{r}_s^{\mu}, \tag{4.94}$$

$$\dot{\mathbf{E}}_p^{\mu'} = \mathbf{R}_p^{\mu}\dot{\mathbf{E}}_p^{0} + \mathbf{r}_p^{\mu}. \tag{4.95}$$

Next consider the relation between $\dot{t}^{\nu+1}$ and $\dot{\mathbf{E}}_p^{0}$. Differentiation of Eqs. (4.32)-(4.35) yields

$$\dot{\sigma}_{yt} - \dot{\sigma}^{\mu+1} = 0 \qquad \text{for yielding in tension,} \tag{4.96}$$

$$\dot{\sigma}_{yc} - \dot{\sigma}^{\mu+1} = 0 \qquad \text{for yielding in compression,} \tag{4.97}$$

$$\dot{\bar{\lambda}}_c - \dot{\lambda}_c^{\mu+1} = 0 \qquad \text{for load reversals,} \tag{4.98}$$

$$\dot{t}^{\mu+1} - \dot{t}^{\mu} - \Delta\dot{\bar{t}}_{max} = 0, \qquad \text{for truncation errors} \tag{4.99}$$

where

$$\dot{\sigma}_{yt} = \dot{\sigma}_{yc} = \frac{EE_t}{E - E_t}\dot{\varepsilon}_p^{\mu}, \tag{4.100}$$

$$\dot{\sigma}^{\mu+1} = \dot{\sigma}^{\mu} + \dot{\sigma}^{\mu'}\left(t^{\mu+1} - t^{\mu}\right) + \sigma^{\mu'}\left(\dot{t}^{\mu+1} - \dot{t}^{\mu}\right), \tag{4.101}$$

$$\dot{\bar{\lambda}}_c = \pm\dot{\psi}, \tag{4.102}$$

$$\dot{\lambda}_c^{\mu+1} = \dot{\lambda}^{\mu} + \lambda^{\mu'}\left(t^{\mu+1} - t^{\mu}\right) + \lambda^{\mu'}\left(\dot{t}^{\mu+1} - \dot{t}^{\mu}\right), \tag{4.103}$$

$$\Delta\dot{\bar{t}}_{max} = 0. \tag{4.104}$$

From the assumption, $\dot{t}^{\mu}$ is written as the linear equation of $\dot{\mathbf{E}}_p^0$, and $t^{\mu+1}, t^{\mu}$ and all the partial derivatives with respect t are known variables. Hence, by arranging Eqs. (4.96)-(4.99), $\dot{t}^{\nu+1}$ is expressed as

$$\dot{t}^{\mu+1} = \mathbf{g}_t^{\mu+1^T} \dot{\mathbf{E}}_p^0 + g_t^{\mu+1}. \tag{4.105}$$

Nomenclature

The following symbols are used in this chapter:

A initial cross sectional area;

${}_T a_{ij}^{\mu}$ coefficient of $\dot{u}_j^{\mu}$ that relates $\dot{f}_i^{\mu'}$, $\dot{u}_i^{\mu'}$, $\dot{u}_j^{\mu}$ and $\dot{\varepsilon}_p^{\mu}$;

${}_E\mathbf{B}$ coefficient matrix of $\dot{\mathbf{E}}_p$ that relates $\dot{\mathbf{F}}$, $\dot{\mathbf{U}}$ and $\dot{\mathbf{E}}_p$;

${}_E b$ coefficient of $\dot{\varepsilon}_p$ that relates $\dot{f}_j$, $\dot{u}_j$ and $\dot{\varepsilon}_p$;

${}_T b_{ij}^{\mu}$ coefficient of $\dot{\varepsilon}_p^{\mu}$ that relates $\dot{f}_i^{\mu'}$, $\dot{u}_i^{\mu'}$, $\dot{u}_j^{\mu}$ and $\dot{\varepsilon}_p^{\mu}$;

${}_T C$ coefficient of ε';

E Young's modulus;

E_t tangent modulus after yielding;

$\mathbf{E}$ strain vector for total system;

$\mathbf{E}_p$ plastic strain vector for total system;

$\mathbf{F}$ nodal force vector for total system;

$\mathbf{G}^{\mu}$ constant matrix that relates $\dot{\mathbf{E}}_p^{\mu}$ and $\dot{\mathbf{E}}_p^{0}$;

$\mathbf{g}^{\mu}$ constant vector that relates $\dot{\mathbf{E}}_p^{\mu}$ and $\dot{\mathbf{E}}_p^{0}$;

$\mathbf{g}_t^{\mu}$ constant vector that relates $\dot{t}^{\mu}$ and $\dot{\mathbf{E}}_p^{0}$;

g_t^{μ} constant that relates $\dot{t}^{\mu}$ and $\dot{\mathbf{E}}_p^{0}$;

f_i nodal force;

$\mathbf{H}_e^{\mu}$ constant matrix that relates $\dot{\mathbf{E}}^{\mu}$ and $\dot{\mathbf{E}}_p^{\mu}$;

$\mathbf{H}_f^{\mu}$ constant matrix that relates $\dot{\mathbf{F}}^{\mu}$ and $\dot{\mathbf{E}}_p^{\mu}$;

$\mathbf{H}_s^{\mu}$ constant matrix that relates $\dot{\mathbf{S}}^{\mu}$ and $\dot{\mathbf{E}}_p^{\mu}$;

$\mathbf{H}_u^{\mu}$ constant matrix that relates $\dot{\mathbf{U}}^{\mu}$ and $\dot{\mathbf{E}}_p^{\mu}$;

$\mathbf{h}_e^{\mu}$ constant vector that relates $\dot{\mathbf{E}}^{\mu}$ and $\dot{\mathbf{E}}_p^{\mu}$;

$\mathbf{h}_f^{\mu}$ constant vector that relates $\dot{\mathbf{F}}^{\mu}$ and $\dot{\mathbf{E}}_p^{\mu}$;

$\mathbf{h}_s^{\mu}$ constant vector that relates $\dot{\mathbf{S}}^{\mu}$ and $\dot{\mathbf{E}}_p^{\mu}$;

$\mathbf{R}_e^{\mu}$ constant matrix that relates $\dot{\mathbf{E}}^{\mu'}$ and $\dot{\mathbf{E}}_p^{0}$;

$\mathbf{R}_f^{\mu}$ constant matrix that relates $\dot{\mathbf{F}}^{\mu'}$ and $\dot{\mathbf{E}}_p^{0}$;

$\mathbf{R}_s^{\mu}$ constant matrix that relates $\dot{\mathbf{S}}^{\mu'}$ and $\dot{\mathbf{E}}_p^{0}$;

$\mathbf{R}_u^{\mu}$ constant matrix that relates $\dot{\mathbf{U}}^{\mu'}$ and $\dot{\mathbf{E}}_p^{0}$;

$\mathbf{R}_p^{\mu}$ constant matrix that relates $\dot{\mathbf{E}}_p^{\mu'}$ and $\dot{\mathbf{E}}_p^{0}$;

$\mathbf{r}_p^\mu$ constant vector that relates $\dot{\mathbf{E}}_p^{\mu'}$ and $\dot{\mathbf{E}}_p^0$;

$\mathbf{h}_u^\mu$ constant vector that relates $\dot{\mathbf{U}}^\mu$ and $\dot{\mathbf{E}}_p^\mu$;

I number of cycles;

${}_T\mathbf{K}$ tangent stiffness matrix;

${}_E\mathbf{K}$ coefficient matrix of $\dot{\mathbf{U}}$ that relates $\dot{\mathbf{F}}$, $\dot{\mathbf{U}}$ and $\dot{\mathbf{E}}_p$;

${}_Tk_{ij}$ coefficient of u_j';

${}_Ek$ coefficient of $\dot{u}_j$ that relates $\dot{f}_j$, $\dot{u}_j$ and $\dot{\varepsilon}_p$;

L current length;

L_0 initial length;

M number of elements;

N number of nodes;

$\bar{\mathbf{P}}_0$ constant vector for constant loads;

$\bar{\mathbf{P}}_c$ constant vector for cyclic load;

$\mathbf{S}$ stress vector for total system;

T period of cyclic loads;

t equilibrium path parameter;

t^0 $t^0 = IT$;

t^γ $t^0 = (I+1)T$;

t^μ an arbitrary instant between t^0 and t^γ;

t^ν an arbitrary instant between t^0 and t^γ;

$\mathbf{U}$ nodal displacement vector for total system;

U_n nth component of $\mathbf{U}$;

u_i nodal displacement;

x_i current position of nodes;

x_i^0 initial position of nodes;

ε Green-Lagrangian strain;

ε_p plastic strain;

λ_0 load factor for constant load;

λ_b load factor at initial buckling load;

λ_c load factor for cyclic loads;

$\bar{\lambda}_c$ ψ or $-\psi$;

σ second Piola-Kirchhoff stress;

σ_y initial tensile yield stress;

$\bar{\sigma}_y$ $\bar{\sigma}_y = (1 - E_t/E)\sigma_y$;

σ_{yc} subsequent yield stress in compression;

σ_{yt} subsequent yield stress in tension;

τ steady-state path parameter;

τ_h an arbitrary value of τ;

Δt of equilibrium path parameter;

$\Delta \mathbf{U}$ $\mathbf{U}(\tau + \Delta\tau, t) - \mathbf{U}(\tau, t)$;

ΔU norm of $\Delta \mathbf{U}$;

$\Delta \bar{t}_{max}$ maximum allowable value of Δt;

$\Delta\tau$ increment of steady-state path parameter;

$\Delta \bar{\tau}_{max}$ maximum allowable value of $\Delta\tau$;

ψ amplitude of λ_c;

ψ_{ssl} amplitude at steady-state limit;

Superscripts

t variables for the equilibrium states at strain reversals in tension;

c variables for the equilibrium states at strain reversals in compression;

0 variables for the equilibrium states at $t = t^0$;

μ variables for the equilibrium states at $t = t^\mu$;

ν variables for the equilibrium states at $t = t^\nu$;

γ variables for the equilibrium states at $t = t^\gamma$;

Signs

$\dot{(\ )}$ derivatives with respect to τ;

$(\ )'$ derivatives with respect to t.

References

[1] A. M. Liapunov. *The General Problem of the Stability of Motion.* Taylor & Francis, London, 1992. Translated and edited by A. T. Fuller.

[2] P. Z. Bazant and L. Cedolin. *Stability of Structures.* Oxford University Press, New York, 1991.

[3] AIJ. *Collapse Analysis of Structures*, volume 1. Maruzen, 1997. (in Japanese).

[4] W. T. Koiter. *On the Stability of Elastic Equilibrium.* Ph.D dissertation, 1945, Delft, Holland, 1967. English Translation, NASA, TTF-10833.

[5] J. M. T. Thompson. A general theory for the equilibrium and stability of discrete conservative systems. *Zeitschrift fur Angewandte Mathematik und Physik*, 20:794–846, 1969.

[6] J. M. T. Thompson and G. W. Hunt. *A general theory of Elastic Stability.* John Wiley & Sons, New York, 1973.

[7] R. Hill. A general theory of uniqueness and stability in elastic-plastic solids. *Journal of the Mechanics and Physics of Solids*, 6:236–249, 1958.

[8] J. M. T. Thompson and H. B. Stewart. *Nonlinear Dynamics and Chaos.* John Wiley & Sons Ltd., 1986.

[9] J. Guckenheimer and P. Holmes. *Nonlinear Oscillations, Dynamical Systems, and Bifurcations of Vector Fields.* Springer, New York, 1983.

[10] S. Wiggins. *Introduction to Applied Nonlinear Dynamical Systems and Chaos.* Springer, New York, 1990.

[11] W. T. Koiter. General theorems for elastic-plastic structures. In J. N. Sneddon and R. Hill, editors, *Progress in Solid Mechanics*, volume 1, pages 167–221, North Holland, Amsterdam, 1960.

[12] J. A. König. *Shakedown of Elastic-Plastic Structures.* Elsevier, Amsterdam, 1987.

[13] K. Uetani and T. Nakamura. Symmetry limit theory for cantilever beam-columns subjected to cyclic reversed bending. *Journal of the Mechanics and Physics of Solids*, 31(6):449–484, 1983.

[14] K. Uetani. *Symmetry Limit Theory and Steady-State Limit Theory for Elastic-Plastic Beam-Columns Subjected to Repeated Alternating Bending.* PhD thesis, Kyoto University, 1984. (in Japanese).

[15] K. Uetani and T. Nakamura. Steady-state limit theory for cantilever beam-columns subjected to cyclic reversed bending. *Journal of Structural and Construction Engineering, AIJ*, (438):105–115, 1992.

[16] K. Uetani and M. Kobayashi. Steady-state path analysis of continua subjected to alternating plastic deformation (analysis of elastic perfectly plastic solids). In *Summaries, 1991 Meeting of the Architectural Institute of Japan*, pages 267–268, 1991.

[17] Y. Yokoo, T. Nakamura, and K. Uetani. The incremental perturbation method for large displacement analysis of elastic-plastic structures. *International Journal for Numerical Methods in Engineering*, 10:503–525, 1976.

Chapter 5

Concluding Remarks

For elastoplastic trusses subjected to an idealized cyclic loading program with continuously increasing amplitude, two methods have been presented for finding the steady-state limit, which bounds the convergence and divergence of plastic deformations. The former method has been presented in chapters 2 and 3, and the later has been presented in chapter 4. Serious difficulty arises when the previous steady-state limit theory, originally developed for cantilever beam-columns, is applied to trusses. The previous steady-state limit theory was constructed based on the fundamental hypothesis that strain reversals in a steady state occur only at load reversals. But this hypothesis may not be valid in trusses. This difficulty is overcome in the former method by relaxing the hypothesis so that the strain reversals due to yielding are taken into consideration. In the later method, this hypothesis is completely excluded.

Moreover, in chapter 4, the concept of the stability of steady states has been introduced to the quasi-static problem of elastoplastic trusses under cyclic loading. A new stability criterion has been derived. And a more practical criterion has been given by introducing the two hypotheses concerning the combination of the types of stress-strain responses. In the former method presented in chapter 2 and 3, the steady-state limit is characterized as the first limit point of the steady-state path, which represents the variation of steady state under the idealized cyclic loading program. In contrast, the steady-state limit is found as the steady state at which the stability of the steady states is lost in the later method presented in chapter 4. Since the former method yields only steady states, which may be stable or unstable, the characterization of the steady-state limit in the later method is more desirable.

Through numerical examples, validity of the two methods have been demonstrated. Good agreements have been observed between the results obtained by the former method and those obtained by the conventional response analysis if the loading conditions for these analyses are close enough. Verification of the later method has been given by showing the good

agreement between the results obtained by the former and the later methods. It is worth noting that, though this is not a quantitative result, the steady-state limits, defined under an idealized cyclic loading program with continuously increasing amplitude, provide lower bounds for the limiting values of convergence obtained by the response analysis performed under the two typical and realistic cyclic loading programs.

There is a trade-off between the proposed two methods in tracing the steady-state path. In the former method, no equilibrium path is needed to be traced. This is an advantage. But, the size of simultaneous equations might be very large when the number of the elements exhibiting plastic shakedown becomes large. This is a disadvantage. On the other hand, the drawback of the later method is that one must perform equilibrium analysis, though only for one cycle. The advantage of the later method is that the size of simultaneous equations is generally much smaller than that in the former method. Hence, if the number of the elements exhibiting plastic shakedown is not so large, the former method is more suitable than the later method. Otherwise, the later method may be better. It should be noted that these drawbacks are not inherent and may be overcome by making effort on the numerical efficiency.

Throughout this thesis, only trusses are treated as the simplest finite dimensional structure. But once the backbone procedure is developed for a simplified model, then it is expected to provide a guideline for developing the procedures for practically acceptable models. The methods and theories presented in this thesis can be easily extended to the arbitrarily shaped structures whose behavior is described by uni-axial stress-strain relations. The later method is expected to be directly applicable to three dimensional continua with almost no restriction. Furthermore, the later method appears to be suitable for taking into account dynamic effects.

This conclusion ends with the topics of our future research:

1. To develop more efficient method based on the present methods.
2. To exclude the hypothesis on the combination of the types of stress-strain cyclic response. This is expected to lead to a uniqueness criterion of variation of a steady state.
3. To derive the stability criterion of a steady-state response taking dynamic effects into account.